HAL open science

Swelling and dissolution mechanisms of cellulose fibres

Nicolas Le Moigne

To cite this version:

Nicolas Le Moigne. Swelling and dissolution mechanisms of cellulose fibres. Mechanics [physics.med-ph]. École Nationale Supérieure des Mines de Paris, 2008. English. NNT : 2008ENMP1581 . tel-00353429

HAL Id: tel-00353429

https://pastel.hal.science/tel-00353429

Submitted on 15 Jan 2009

HAL is a multi-disciplinary open access archive for the deposit and dissemination of scientific research documents, whether they are published or not. The documents may come from teaching and research institutions in France or abroad, or from public or private research centers.

L'archive ouverte pluridisciplinaire **HAL**, est destinée au dépôt et à la diffusion de documents scientifiques de niveau recherche, publiés ou non, émanant des établissements d'enseignement et de recherche français ou étrangers, des laboratoires publics ou privés.

Ecole Doctorale 364 : Sciences Fondamentales et Appliquées

N° attribué par la bibliothèque

|__|__|__|__|__|__|__|__|__|__|

T H E S E

pour obtenir le grade de
Docteur de l'Ecole Nationale Supérieure des Mines de Paris
Spécialité «Science et Génie des Matériaux»

présentée et soutenue publiquement par

M. Nicolas Le Moigne

le 9 Décembre 2008

MECANISMES DE GONFLEMENT ET DE DISSOLUTION DES FIBRES DE CELLULOSE

SWELLING AND DISSOLUTION MECHANISMS OF CELLULOSE FIBRES

Directeur de thèse : Patrick Navard

Jury :

M. Pedro Fardim	Rapporteur
M. Jürgen Puls	Rapporteur
M. Herman Höfte	Examinateur
M. Patrick Navard	Examinateur
M. Jürgen Engelhardt	Membre invité
Mme Kristina Jardeby	Membre invité
M. Michel Pierre	Membre invité
M. Christoph Schrempf	Membre invité

À Hélène et Lucas,

Contents

Introduction francophone 3

Chapter I: State of the Art – Review on cellulose biosynthesis, structure and dissolution mechanisms

Introduction 9
1.1 Biosynthesis of cellulose fibres 10
1.2 Structure of cellulose fibres 15
1.3 Swelling and dissolution mechanisms of cellulose fibres 32

Chapter II: Gradient in dissolution capacity of successively deposited cell wall layers in cotton fibres. 43

Chapter III: Restricted dissolution capacity of native and regenerated cellulose fibres under uniaxial elongational stress. 55

Chapter IV: Dissolution mechanisms of wood cellulose fibres in NaOH-water. 67

Chapter V: Structural changes and alkaline solubility of wood cellulose fibres after enzymatic peeling treatment. 91

Chapter VI: Contraction and rotation of natural and regenerated cellulose fibres during swelling and dissolution. 109

Chapter VII: Kinetics of dissolution of cellulose and cellulose derivatives under shear. 121

Conclusions 131

Articles and Communications 135

Remerciements

Résumé du travail de thèse

Contexte de l'étude

À la différence des réserves minérales et fossiles qui furent formées il y a plusieurs millions d'années, les polysaccharides, comme la cellulose et l'amidon, représentent une ressource quasi inépuisable de matériaux naturels qui se renouvelle année après année. Parmi la grande variété de polysaccharides synthétisés dans la nature, la cellulose constitue le polymère naturel le plus abondant. On la trouve en composé majoritaire au sein des fibres dans les plantes, les algues et les champignons mais elle est aussi synthétisée par certains organismes tels que les cyanobactéries.

La plupart des polymères de grande diffusion sont synthétisés à partir des ressources pétrolières. Du fait de la limitation des stocks et des nouvelles normes environnementales, la recherche s'est concentrée ces dernières années sur la valorisation de matériaux polymères produits par la nature de façon pérenne, comme la cellulose. Cependant, leur usage et leur transformation présentent plusieurs contraintes principalement liées à leurs structures morphologiques et chimiques très spécifiques. Bien qu'utilisée depuis des siècles dans l'industrie textile et la papeterie, la cellulose fait toujours l'objet de nombreuses études scientifiques et techniques visant à améliorer, diversifier et simplifier son utilisation. Dans la majorité des cas, la cellulose ne peut être utilisée sous sa forme fibrillaire naturelle, excepté pour les applications en fibres de renforcement ou textile (cas du coton, du lin, du chanvre…). Elle ne peut pas non plus être fondue comme la plupart des polymères semi cristallins et sa transformation doit donc être précédée d'une étape de dissolution ou de dérivation. Cependant, sa structure complexe n'offre pas une grande accessibilité aux réactifs et de nombreuses études ont été menées afin de mieux comprendre comment démanteler ou modifier cette structure pour améliorer son accessibilité tout en préservant au maximum les propriétés originelles du matériau. Bien qu'améliorant la dissolution, les prétraitements chimiques, physiques ou enzymatiques utilisés aujourd'hui entraînent le plus souvent une forte dégradation de la structure qui a pour principale conséquence une forte diminution des propriétés des produits transformés (fibres textiles, éponges, films…) et ne sont pas toujours aussi performant que l'industrie le souhaite.

En dépit d'une bonne connaissance et d'une bonne maîtrise de la dissolution et de la dérivation d'un point de vue chimique, les prétraitements dits d' « activation » sont optimisés de façon relativement empirique. Le but de nos travaux est d'identifier les principaux paramètres impliqués dans la dissolution de la cellulose afin d'« activer » la cellulose de façon plus efficace afin d'enlever ou de modifier seulement ce qui est nécessaire. Notre approche scientifique est basée sur les nombreuses connaissances accumulées sur la biosynthèse et la structure des fibres de cellulose et d'étudier leurs mécanismes de gonflement et de dissolution dans différentes conditions (qualité du solvant, type de fibres, tension…) afin d'analyser leur capacité de dissolution aux différentes échelles structurales.

Principaux résultats obtenus

L'état de l'art nous a permis de décrire les mécanismes de biosynthèse et la composition et la structure des trois principales échelles structurales des fibres de cellulose, c'est à dire moléculaire, agrégée et macrostructurale, et de leurs principaux constituants, la cellulose, les hémicelluloses, les protéines, les pectines, la lignine (Chapitre I). Lors de cette étude bibliographique, nous avons pu constater que malgré l'étendue des connaissances, la dynamique complète de synthèse et de déposition de la cellulose sur les parois des fibres ainsi que le rôle que jouent les différents composés non cellulosiques dans la structuration des parois ne sont pas totalement élucidés. Les études existantes sur les mécanismes de gonflement et de dissolution des fibres de cellulose montrent une forte influence de la qualité du solvant et de la morphologie originelle des fibres. Le comportement des différentes échelles structurales en terme de gonflement et de dissolution n'est quant à lui pas clairement établi.

Nos travaux se sont concentrés sur l'étude du gonflement et de la dissolution des fibres de cellulose en faisant varier la qualité du solvant (*N*-methylmorpholine-*N*-oxide avec différentes quantités d'eau et solutions aqueuses de NaOH à 8%), les conditions de dissolution, comme la tension, et l'origine des fibres (coton, bois, fibres régénérées ou dérivées). Les mécanismes de gonflement et de dissolution ont été étudiés par des observations microscopiques à haute résolution. Une séparation sélective des fractions solubles et insolubles a été réalisée par centrifugation. La distribution de masse molaire, la cristallinité, la composition en sucre, l'allomorphie et la quantité de chaque fraction ont été analysées. A partir de ces résultats, nous avons pu mieux décrire les mécanismes de gonflement et de dissolution des fibres de cellulose et ainsi identifier les principaux paramètres gouvernant la dissolution.

Notre apport principal est de montrer que la capacité de dissolution de la cellulose doit être considérée aux différentes échelles structurales des fibres :

De l'échelle macrostructurale à l'échelle agrégée :

Nous avons montré qu'il existe un gradient de dissolution au sein des fibres de coton entre les trois principales parois (primaire, secondaire S1, secondaire S2) déposées successivement au cours de la biosynthèse. Les parois les plus anciennement déposées (parois primaire et S1) sont les plus difficiles à dissoudre (Chapitre II), laissant supposer que la grande quantité de matériaux non cellulosiques présents dans ces parois constitue une gêne à la dissolution. Nous avons ensuite démontré de façon claire qu'outre les classiques raisons thermodynamiques contrôlant la dissolution d'un polymère, la suppression des parois primaire et S1 par pelage enzymatique (Chapitre V) ainsi que la déstructuration des parois par explosion à la vapeur, hydrolyse en milieu acide ou par traitement enzymatique (chapitre IV et V) permettent d'améliorer la dissolution des fibres de cellulose. Un facteur très important et totalement nouveau est le fait que les mouvements de rotation et de contraction des fibres et la convection du solvant autour des fibres doivent aussi être favorisés au cours de la dissolution (chapitre VI et VII). Cependant, certaines fractions restent insolubles et leur capacité de dissolution doit être analysée à une échelle plus fine de la structure. L'un des résultats importants est la présence de quantités plus élevées d'hémicelluloses dans les fractions insolubles par rapport aux fractions solubles suggérant que la cellulose provenant des fractions insolubles est peut être plus intimement incorporée dans la matrice d'hémicelluloses (Chapitre IV).

De l'échelle agrégée à l'échelle moléculaire :

Nous avons montré qu'une fraction importante de chaînes de cellulose, similaires en longueur, peuvent appartenir soit à la fraction soluble soit à la fraction insoluble, prouvant que la masse molaire n'est pas un facteur discriminant pour la dissolution de la cellulose (Chapitre IV). Ce résultat est à mettre en relation avec l'environnement chimique des chaînes de cellulose qui est plus riche en hémicelluloses dans les fractions insolubles. De plus, un phénomène intéressant a été mis en évidence en faisant varier les conditions de tension durant la dissolution. Nous avons en effet montré que la capacité de dissolution des fibres de cellulose est limitée si elles sont soumises à une contrainte d'élongation axiale (Chapitre III).

Ce résultat suggère que l'accessibilité du solvant aux chaînes de cellulose n'est pas le seul paramètre influent et que la dissolution est fortement dépendante de la possibilité de mobilité conformationelle des chaînes. De tels mouvements nécessitent, dans le cas des fibres de cellulose, une mobilité à grande échelle des chaînes impliquant que leurs extrémités soient libres. Lorsque le réseau de liaisons hydrogènes présent au sein des fibres de cellulose est mise en tension de façon macroscopique, la mobilité conformationelle moléculaire est réduite ce qui limite la capacité de dissolution des fibres.

Principaux paramètres gouvernant la dissolution :

Nos résultats suggèrent donc que plusieurs paramètres moléculaires et structuraux ainsi que des paramètres procédés doivent être bien contrôlés afin d'améliorer la dissolution des fibres de cellulose :

(i) Les paramètres de procédés : nous avons montré que la convection du solvant et la possibilité de mouvements des fibres dans le solvant permettent d'éviter la formation d'une couche très visqueuse diminuant fortement l'efficacité du solvant,

(ii) Les paramètres structuraux : la suppression des parois externes, la déstructuration des parois internes et la suppression sélectives des hémicelluloses sont des paramètres important améliorant la dissolution,

(iii) Les paramètres moléculaires : l'amélioration de la mobilité conformationelle des chaînes est un paramètre important.

Les traitements d'activation préalables à la dissolution doivent donc être orientés vers une déstructuration plus sélective des fibres et une suppression des hémicelluloses qui semblent jouer un rôle important sur la solubilité. Dans ce sens, les traitements enzymatiques sont de bons candidats car leur action est locale et peut être très spécifique en comparaison aux méthodes classiques d'explosion à la vapeur, de broyage ou de dérivation qui entraînent une dégradation globale des chaînes de cellulose. Cependant, l'un des points bloquants est de pouvoir permettre aux enzymes de pénétrer au sein de la structure complexe des fibres afin de supprimer des composants de façon sélective. L'activation doit aussi permettre de favoriser la mobilité moléculaire en cassant le réseau de liaisons hydrogène, en limitant sa reformation et

en démantelant de façon efficace le réseau hémicellulosique. Ces actions pourraient être contrôlés avant ou au cours la dissolution.

En dépit des connaissances avancées dans les domaines de la modification chimique et de la dissolution des fibres de cellulose, le gonflement et la dissolution de la cellulose restent encore aujourd'hui un domaine scientifique complexe qui n'a pas livré tous ses secrets. Une avancée significative pourrait être réalisée par une meilleure compréhension des mécanismes de biosynthèse. En effet, ceci permettrait de mieux contrôler ou modifier les ressources naturelles de cellulose pour les intégrer plus largement dans le monde industriel.

Chapter I

State of the art – Review on cellulose biosynthesis, structure and dissolution mechanisms.

Introduction

As the most important skeletal component in plants, cellulose is an almost inexhaustible polymeric raw material. Mineral and fossil reserves were deposited and formed over billions of years and are, therefore, limited in stock. On the other hand, polysaccharides, especially cellulose and starch, are reproduced in abundance year after year by means of solar energy.

Most of current polymeric materials are synthesized from limited petrochemical resources. Due to the lack of availability of the source materials and the new environmental requirements, recent research has focused on the development of new materials which can be produced from naturally occurring polymers, such as cellulose. However, a limitation to their use is the difficulty involved in their processing and fabrication because of their specific structure. Although hugely used in the textile and paper industry, the challenge that faced generations of scientists and industries is to find a cheap, simple and non polluting dissolving process. In fact, in most cases (except for cotton and bacterial cellulose), cellulose cannot be used in its natural form; it has to be dissolved or derivatized. One of the crucial aspects in cellulose processing is the capacity of the fibres to be "accessible" to reagents in order to undergo subsequent transformation stages. The lack of accessibility of cellulose is related to its complex structure when it comes from cell walls, and many studies have been conducted to understand in what way the structure could be dismantled or modified to enhance the dissolution with a preservation of the original solid state of cellulose. However, aside improving the dissolution, these treatments, called "activation", are always accompanied of strong degradations of the solid state leading to a lowering of the product properties.

Despite a good industrial "know how" to dissolve and derivatize cellulose, the swelling and dissolution mechanisms that leads to the solution state are not fully elucidated. The knowledge of the biosynthetic processes and the structure of cellulose fibre are necessary to better describe the dissolution. On the other hand, an extensive understanding of cellulose swelling and dissolution should give new information on the cellulose structure and the biosynthesis and open the way to design better activation treatments, solvents or reagents.

The present state of the art deals with firstly a short review on cellulose biosynthesis, secondly a description of the particular three structure levels of cellulose fibres and finally a review of several studies focused on swelling and dissolution mechanisms of cellulose fibres.

1.1. Biosynthesis of cellulose fibres

Plant cell walls are complex polysaccharides composites mostly made of cellulose microfibrils but also composed of matrix materials as hemicelluloses, pectins, proteins and lignin. Cellulose has mainly an architectural function and provides strength to plants while the others components help the building of the cell wall and control the cell environment. The synthesis of these different constituents occurs in the cell and is mainly governed by two apparatus the Cellulose Synthase Complex which produces cellulose and the Golgi which produces the matrix polysaccharides [1].

1.1.1. The plant cell

The plant cell is composed of four main entities the cell wall, the cytoplasm delimitated by the plasma membrane, the nucleus which contains the DNA and the organelles as the mitochondria, the Golgi apparatus or the chloroplasts (Figure 1). The chlorophyll molecules present in the chloroplasts are able to convert solar energy (photons), CO_2 and water (present in the vacuole) into glucose molecules, O_2 and water through the photosynthesis mechanism. One part of these glucose molecules is then stored in the cell wall in the form of macromolecules as cellulose, hemicelluloses and pectins while the other part is used in the mitochondria to produce useable energy, called ATP. Chloroplasts are also able to produce their own ATP. The ATP molecules are consumed by many enzymes and cellular processes including biosynthetic reactions, mobility and cell division. A constant amount of about 8000 available ATP molecules is present in each cell [2].

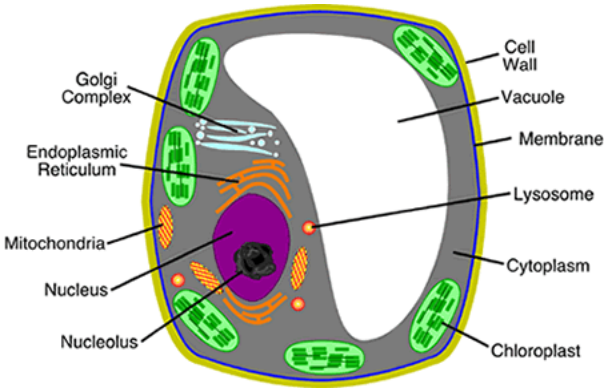

Figure 1. Schematic representation of the plant cell with the main entities involved in the biosynthesis [from http://www.biologycorner.com/bio1/cell.html, 2008].

The glucose molecules made for storage are used by the cell in an activated form called UDP-glucose (Uridine diphosphate glucose). The UDP-glucose is the substrate for the cellulose synthesis by the Cellulose Synthase Complex present in the plasma membrane. Others sugars as NDP-sugars are used in the Golgi apparatus to produce the others matrix components as hemicelluloses and pectins [1].

1.1.2. The Cellulose Synthase Complex and the Golgi

Despite an earlier assumption of its existence by Preston in 1964 [3], first evidence of the Cellulose Synthase Complex (CSC) were provided by Brown and Montezinos in 1976 [4] and afterwards by Mueller and Brown in 1980 [5]. By means of freeze fracture and microscopy, they were able to observe and identify the CSC, firstly called "rosette TCs", in corn root cells as a complex of six particles associated with cellulose microfibrils. However, it was Kimura *et al.* [6] who finally gave the confirmation of the presence of cellulose synthases in the CSC structure. In higher plants and certain green alga, the CSC is a rosette of about 25 to 30 nm consisting of six subunits each composed of six CESA proteins [1] (see Figure 2).

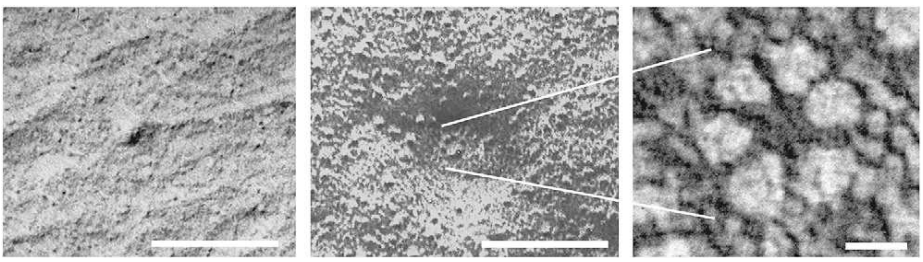

Figure 2. Electron micrographs of plant cell walls from freeze fracture preparations showing a CSC, (left) exoplasmatic face of the plasma membrane, (middle) CSC in the depression form by the plasma membrane (scale bars are both 100 nm), (right) CSC at a higher magnification (scale bar 10 nm) with the six subunits of the rosette. (Illustration taken from [7])

The CSC is thus a complex of 36 CESA proteins each able to produce one cellulose chain. As shown in Figure 3a and b, the UDP-glucose substrate is used by the CESA proteins to produce β-1,4-glucan chains that coalesce as cellulose microfibrils [1] by means of Van der Waals forces and hydrogen bonds [8, 9] (see also chapter 1.2.2). Numerous CESA proteins exist depending of the plant sources and a different set of CESA occur in the primary and secondary walls [1, 10, 11] (see chapter 1.2.3 for details on wall structure).

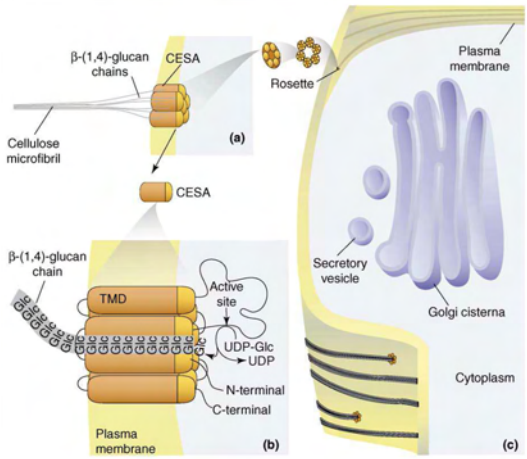

Figure 3. Synthesis of cellulose and matrix polysaccharides in the CSC and the Golgi (illustration taken from [1]). (a, b) rosette in higher plants are composed of 36 CESA proteins able to produce glucan chains by using UDP-glucose as a substrate, (c) the matrix polysaccharides synthesized in the Golgi are delivered by the secretory vesicle to the inner cell wall surface.

As previously mentioned the rosette structure of the CSC occurs mostly in higher plants. However, several CSC structure can be found as diagonal rows of particles in *Vaucheria hamata* and linear CSC in Acetobacter [12] (Figure 4). These CSC structural variations have a strong influence on the microfibrils size. Typical microfibrils consist of 36 to 90 glucan chains in land plants and some green algae [13] while few microfibrils can contain up to 1400 glucan chains in certain green algae as *Valonia macrophysa*.

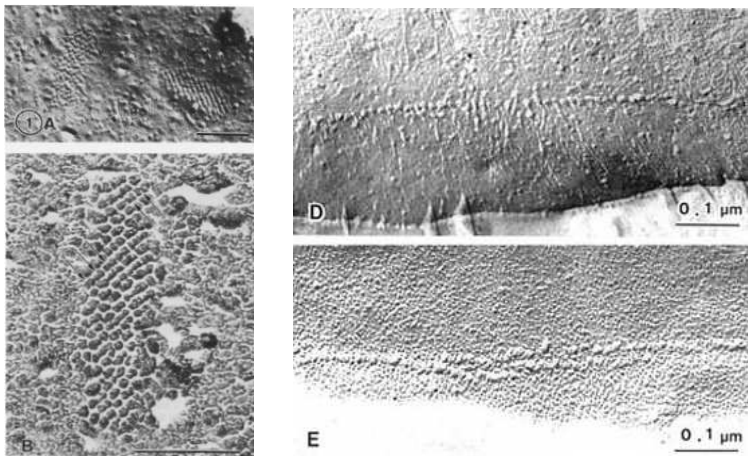

Figure 4. CSCs in *Vaucheria hamata* (left, labelled A and B) and Linear CSCs in Acetobacter (right, labelled D and E). (Illustrations taken from [12])

The formation of the cell wall is engineered by the numerous CSCs present in the plasma membrane which produce and deposit cellulose microfibrils on the cell surface. To achieve

this, the CSCs are thought to be intimately linked and guided by microtubules and to move along the plasma membrane while they deposit the cellulose microfibrils (Figure 5). A meaningful evidence of this movement was given recently by Paredez *et al.* [14]. In fact, they were able to obtain an *in vivo* visualization of the cellulose deposition by fluorescently labelling the CESA.

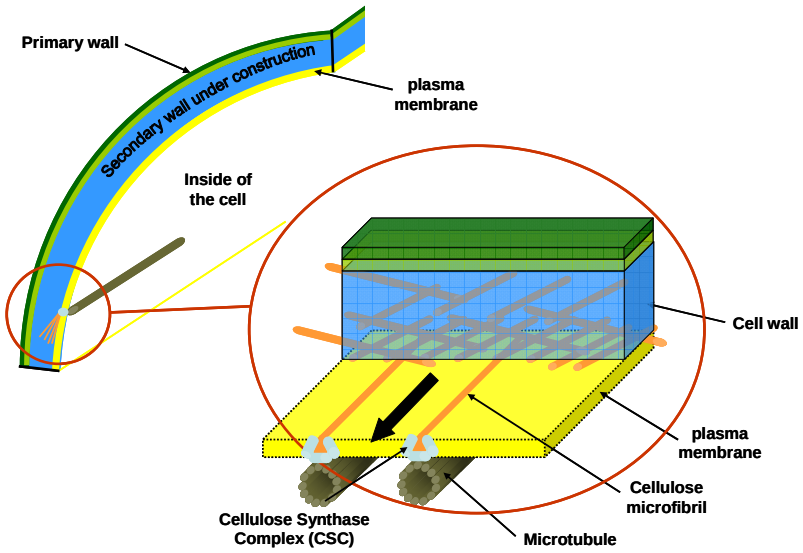

Figure 5. Building of the cell wall. The CSCs localized in the plasma membrane synthesize and depose the cellulose microfibrils along the cell wall. Several distinct cell wall layers are produced by this mechanism.

The movement of the CSC is supposed to be induced by the polymerization and the crystallisation of the glucan chains. A recent modelling approach of this mechanism has been developed by Diotallevi and Mulder [7]. They modelled how the CSCs move by means of the cellulose polymerization as a motor (Figure 6). In this model, they identify the polymerization and the crystallisation as the combined driving forces, and the chains stiffness and the membrane elasticity as force transducers. Their first analytical results were in agreement with the recently reported speed value of the CSC [14] (5.8×10^{-9} m/s). The modelling tools are indeed promising in the description and understanding of cell wall deposition.

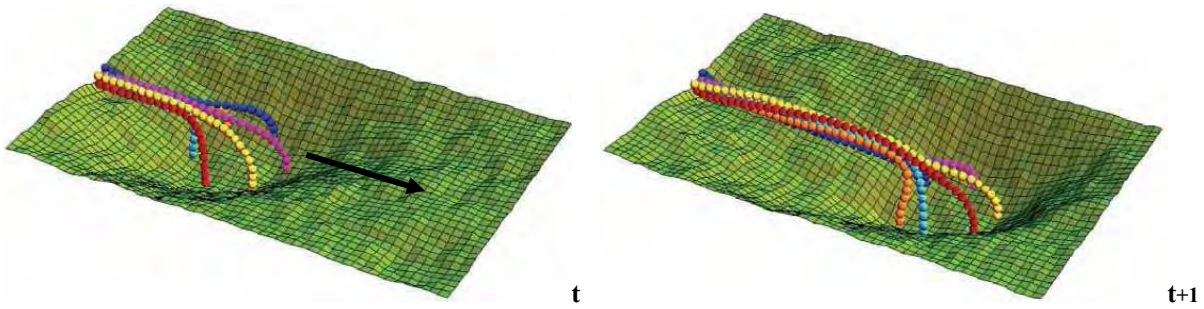

Figure 6. Two snapshots (**t, t+1**) of the movement of one CSC along the plasma membrane involved by the polymerization and the crystallization of the cellulose chains [7]. Each filament represents six cellulose chains.

As was stressed by Emons *et al.* [15], the intimate relationship between microtubules and CSC are not fully understood yet. In fact, they pointed out that highly structured arrays can be observed without a parallelism between microtubules and cellulose microfibrils showing that CSC can also move in ordered patterns in the absence of underlying microtubules. On this basis, a geometrical approach to microfibrils deposition was proposed by Emons and Mulder [16] (see also chapter 1.2.2).

The parallel production of matrix polysaccharides by the Golgi is also subjected to several questions. It is known that the Golgi apparatus synthesizes matrix polysaccharides as hemicelluloses and pectins by means of CSL proteins which use NDP-sugar as a substrate [1]. The polysaccharides are then delivered to the inner cell wall surface by secretory vesicle (Figure 3c). However, much less is known about the topology of the CSL proteins and the way they use the NDP-sugar to produce the polysaccharides.

Finally, after completion of the cell wall deposition, the cell dies and leaves behind a well organized and complex polysaccharide structure, i.e. the cellulose fibre.

1.2. Structure of cellulose fibres

In the preceding chapter, we have seen briefly how the plant cell is able to produce different components by means of the CSCs and the Golgi. These biosynthetic processes lead to the building of a cellulose fibre and end with the death of the cell. In this chapter, we will describe how cellulose is organized together with all the non-cellulosic components considering the different levels of the fibre structure. The structure of cellulose fibres is usually described at three levels [17,18] :

(i) The molecular level (Å), described by the chemical constitution, the steric conformation, the molecular mass distribution, the hydroxyl groups, the intramolecular interactions, etc… of the cellulose macromolecule.
(ii) The aggregated level (nm), described by the aggregation of the cellulose macromolecules into elementary crystals, fibrils and microfibrils (intermolecular interactions, crystal lattices, degree of order, etc).
(iii) The macrostructural level (nm to µm), described by the organization of the microfibrils and macrofibrils into layers and walls (existence of distinct cell wall layers in native cellulose fibres or of skin-core structures in regenerated cellulose fibres, presence of different non-cellulosic components, voids and pores, etc).

1.2.1. Molecular level

There is a rather good knowledge of the chemical constitution, the steric conformation, the molecular mass, the position and function of the three functional hydroxyl groups and their intra- and intermolecular interactions.

a) Chemical structure

The cellulose chemical formula is $C_6H_{10}O_5$. The widely accepted macromolecular structure of cellulose is given in Figure 7. The glucose base units are linked together by β-1,4 glycosidic bonds formed between the carbon atoms C-1 and C-4 of adjacent glucose units.

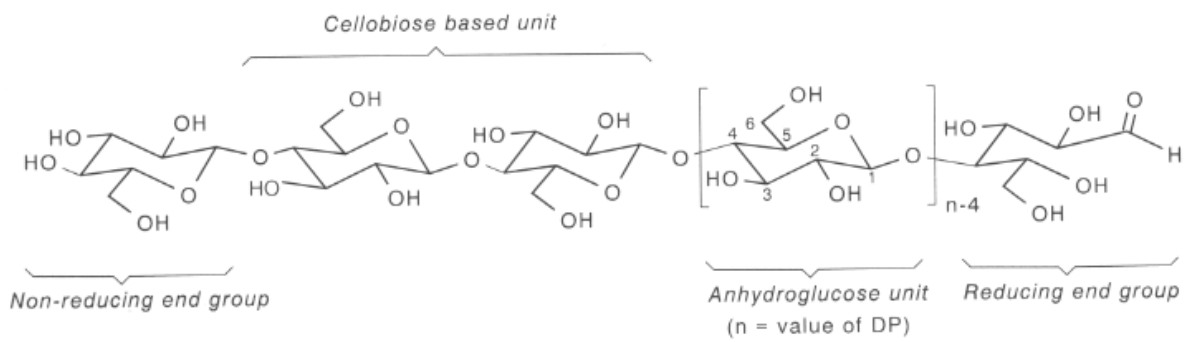

Figure 7. Molecular structure of cellulose. (Illustration taken from [18])

Terminal hydroxyl groups are present at both ends of the cellulose chain molecule. The C-1 hydroxyl group has a reducing activity while the C-4 hydroxyl group at the other end of the chain is non-reducing. Three reactive hydroxyl groups are also present in each of the anhydroglucose (AGU) base unit at C-2, C-3 and C-6 positions.

There are two possible conformations of the AGU depending on the relative position of the hydroxyls with respect to the plane of the pyranose ring [19] (consisting of five carbons and one oxygen). In the axial conformation ($^1C_4$-chair) the hydroxyls are placed alternately above and below the ring plane and in the equatorial conformation ($^4C_1$-chair) they are positioned in the ring plane with the hydrogen atoms in a vertical position. AGU in the cellulose chain generally adopt the thermodynamically more stable $^4C_1$-chair conformation [17]. The possible AGU conformations and the steric conformation formula of the cellulose molecule are shown in Figure 8.

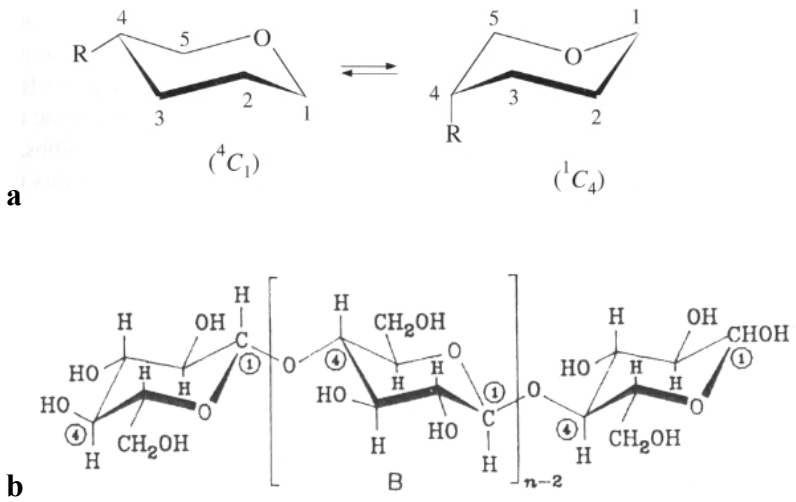

Figure 8. Possible conformations of the AGU (a) and conformation of the cellulose molecules (b). (Illustration taken from [17, 19])

b) Chain length and molecular mass distribution

An AGU ($C_6H_{10}O_5$) has a molecular mass of 162 g/mol. The average molecular mass of a cellulose substrate has an average degree of polymerization (DP) equals to n × 162.

Native cellulose has DP varying upon the cellulose source. It can be higher than 10,000 for cotton. Depending on the severity of cooking and pre-treatment, cellulose used in dissolving wood pulps has an average DP of 600 to 1200 and 100 to 200 for cellulose powders [18] (e.g. microcrystalline cellulose prepared by acidic hydrolysis). Cellulose chains are polydisperse and the molecular mass distribution strongly depends on sources as shown in Figure 9.

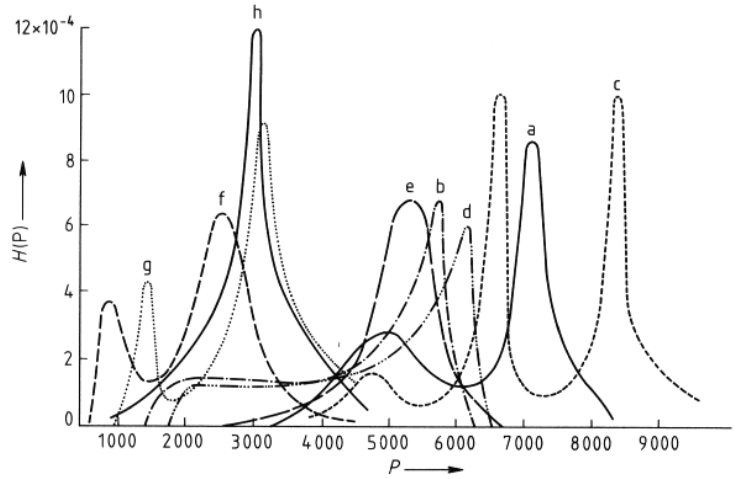

Figure 9. Chain length distribution of various celluloses sources (P is the degree of polymerisation): a) Cotton; b) Other cotton specie; c) China grass ; d) Flax ; e) Ramie; f) Balsam ; g) White fir ; h) Birch. (Illustration taken from [20])

c) Intramolecular hydrogen bonding

The three hydroxyls group of the AGU are able to interact and form hydrogen bonds by means of intra and inter molecular interactions. The strength of these hydrogen bonds is around 25 kJ/mol (Van der Waals forces 0.15 kJ/mol; O-H covalent bond 460 kJ/mol) [17].

From infrared spectroscopy, X-ray diffraction and nuclear magnetic resonance (NMR) investigations, it was shown that intramolecular hydrogen bonds are formed between O-3-H and O-5' of the adjacent glucose unit [21]. Thereafter, Blackwell *et al.* [22] assumed the existence of a second intramolecular hydrogen bond between O-2-H and O-6'. The two possible intramolecular hydrogen bonds are shown in Figure 10.

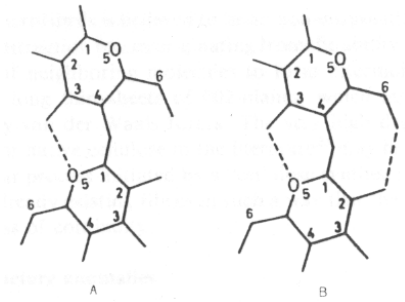

Figure 10. Intramolecular hydrogen-bonding according to (A) Liang and Marchessault [21] and (B) Blackwell *et al.* [22]. (Illustration taken from [17])

Intramolecular hydrogen bonding is responsible for the stiffness of the cellulose molecule. The chair conformation of the pyranose ring and the β-glucosidic linkage also favour the linear nature and the stiffness of the chain [17].

1.2.2. Aggregated Level

When synthesised in the plasma membrane, cellulose chains have a high tendency to align and aggregate in larger entities, i.e. elementary fibrils then microfibrils and macrofibrils, due to the regular build-up of the cellulose molecule, the stiffness of the chain and especially their high hydrogen bonding capacity.

a) Fibrillar structure

As was discussed in chapter 1.1.2, in higher plants, cellulose is synthesized in the plasma membrane by a ring of six complexes of six hexagonally arranged cellulose synthase enzymes (CESAs): the cellulose synthase complex (CSC) also called “rosette”. In such a reactor, six adjacent β-1,4-glucan chains produced by each of the six CESAs complexes are extruded and probably start associating by Van der Walls forces then form hydrogen bonds [8, 9], thus building the first basic fibrillar unit called “elementary fibril”. Larger and larger associations are then built up to the formation of the complete wall structure.

As shown in Figure 11, the elementary fibrils constituted of six glucan chains, aggregate in microfibrils having typical cross sections of 3,5 to 10 nm and consisting of 36 to 90 glucan chains in land plants and some green algae [13], i.e. six or more elementary fibrils. However, microfibrils can contain until 1400 glucan chains in certain green algae as *Valonia macrophysa*. In fact, the dimension of the microfibrils is highly dependant of the CSC structure [13] and the latter can undergo strong variation depending on the plant and algae

species (see chapter 1.1.2). The aggregation of the elementary fibrils in microfibrils forms crystalline units called "elementary crystallites". The size of these crystals is typically 5-6 nm in diameter for bacterial cellulose and 4-5 nm for cotton [23]. Their length is 10-20 nm for regenerated cellulose fibres and longer for cotton and other natural cellulosic fibres [17]. Thereafter, the microfibrils organized in macrofibrils to form the cell wall.

It has to be noticed that there is some confusion in the literature concerning the description of the different aggregated entities, i.e. the elementary fibrils, the microfibrils and the macrofibrils. Often, the microfibrils are considered as the smallest morphological unit [24] instead of the elementary fibril (aggregate of six glucan chains). Considering the fact that microfibrils undergo large dimension variations due to the varied existing structure of the CSC, we will consider the elementary fibril as the smaller basic cellulose unit synthesized. Larger entities as micro and macrofibrils are thus only aggregates of this elementary entity.

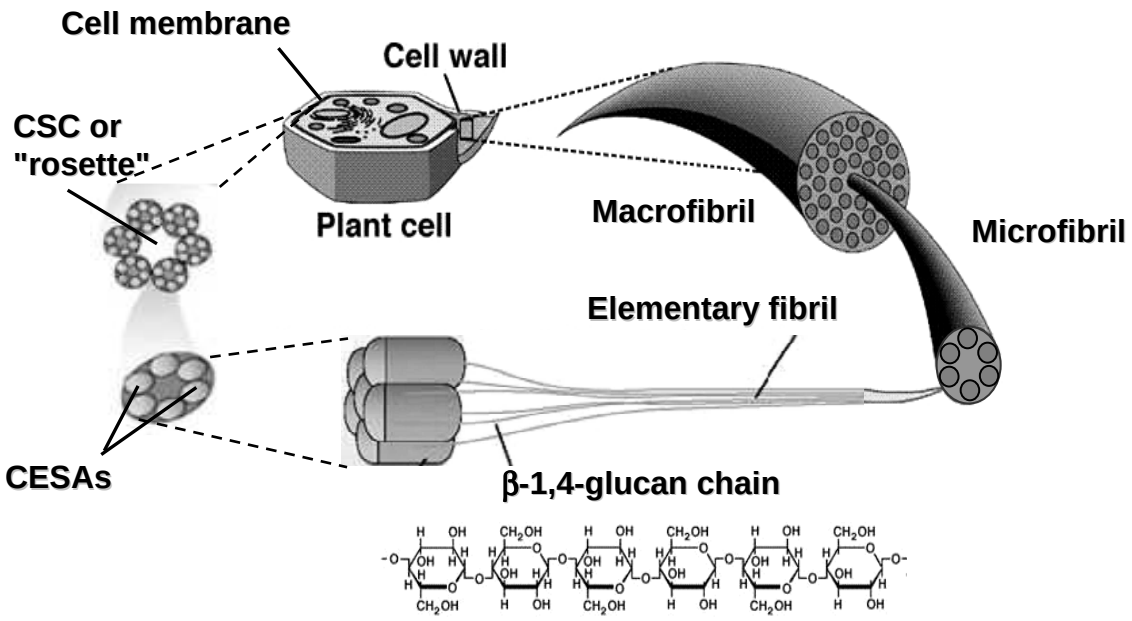

Figure 11. Elementary cellulose fibrils synthesis and the different levels of organisation in the cell wall of plant. (Scheme reconstructed with illustrations taken from [1, 25])

Many hypotheses have been suggested for the internal build-up of the fibrillar structure over the years. The model accepted today was proposed by Hearle in 1958 and supported by recent WAXS and ^{13}C CP-MAS NMR results [18]. This model assumes low ordered ("amorphous") and highly ordered ("crystalline") regions arranged in a fringed fibrillar fashion. As can be seen on Figure 12, elementary fibrils aggregate in elementary crystallites and form microfibrils and macrofibrils. Several imperfections occur in this structure as the

less ordered regions in the microfibrils, the interstice between the microfibrils and the larger voids between the microfibrils and the macrofibrils [17]. The cohesion of these different entities is ensured by an hydrogen bond network.

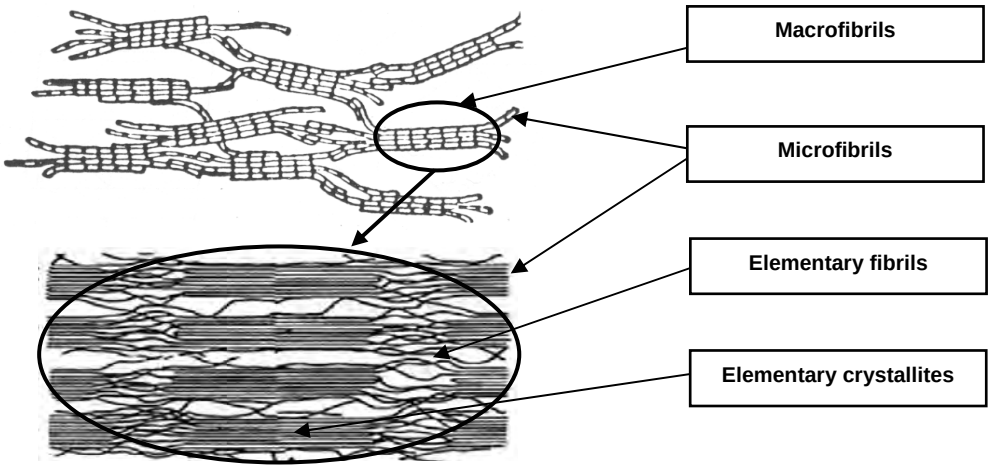

Figure 12. Representation of the fringed fibrillar model of the fibre structure. (Scheme reconstructed with illustrations taken from [17])

However, considering several studies on "amorphous" cellulose, O'Sullivan [23] suggested that "amorphous" cellulose probably still possess a degree of order. This hypothesis is in accordance with the fact that CSC produces chains that all keep a parallel straight conformation up to coagulating on the cell wall because of their stiffness, their high hydrogen bonding capacity [17, 18] and also topological constraints due to the proximity of the many chains exiting from the CSC orifices [5, 7, 26, 27].

b) <u>Cellulose polymorphs</u>

Cellulose can adopt different crystalline forms – it is a polymorphic material. Native crystalline cellulose is called "cellulose I" and is composed of two main forms I_α and I_β [28]. Higher plant, e.g wood and cotton, are principally made with I_β form. I_α is more present in primitive organism like bacteria. I_α phase has a triclinic P-1 structure with one cellulose chain per unit cell and I_β presents a monoclinic unit cell with two chains per unit (space group P-2_1) [29]. I_α is metastable and can be transformed by annealing into the thermodynamically more stable I_β phase [18].

I_α cellulose have a unit cell with width parameters (a= 6.74 Å, b= 5.93 Å, c= 10.36 Å, γ-angle= 81°) shorter than those of the I_β form (a= 7.85 Å, b= 8.27 Å, c=10.38 Å, γ-angle= 96.3°) [30]. As shown on Figure 13, both forms adopt a packing arrangement, in which the molecules are organized in a parallel manner.

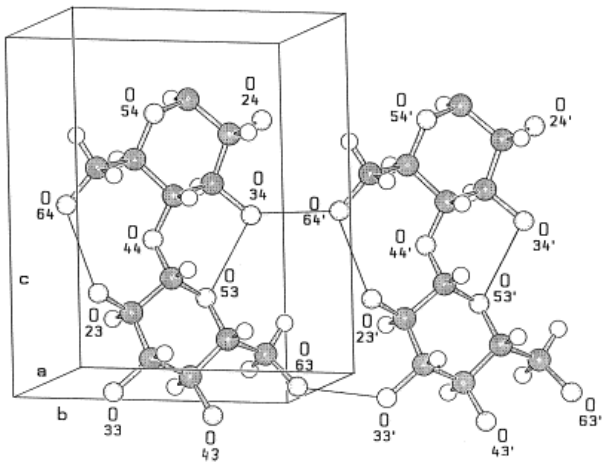

Figure 13. Representation of the model of cellulose I_β [31], intrasheet (100) through the center of the unit cell. (Illustration taken from [30])

Cellulose can also adopt other polymorphic crystal structures. When native celluloses are treated at room temperature with strong alkaline solutions, or when native cellulose is precipitated from a dissolved state, such as the Lyocell process, cellulose adopts a modified crystal structure giving a specific X-ray diffraction pattern (see Figure 15). This modification is known as cellulose II (sometimes called "hydratecellulose", "mercerized cellulose", "regenerated cellulose" [17]) and is the most important form from an industrial point of view. The crystal lattice structure of this polymorph has a monoclinic unit cell $P2_1$ – like cellulose-I – with axis dimensions of 8.1 Å for the a-axis, 9.05 Å for the b-axis, 10.31 Å for the c-axis, and 117.1° for the γ-angle [30]. Cellulose II unit has an antiparallel arrangement of the chains with two cellulose molecules rotated by 180° around their axis that form a 2/1 helix (Figure 14). The reasons that lead to the irreversible transition from cellulose I and cellulose II without an intermediate stage of dispersion of the cellulose molecules is not yet well understood [32]. It has to be noticed that cellulose II can be produced by Nature by a mutant strain of *Gluconacetobacter xylinum* [24].

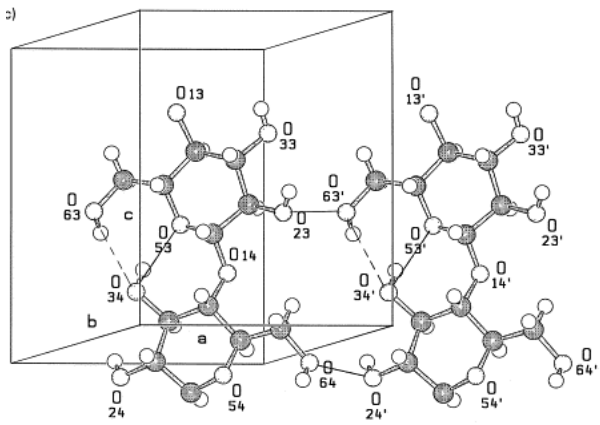

Figure 14. Representation of the model of cellulose II [33] intrasheet (010) through the center of the unit cell. (Illustration taken from [30])

Besides cellulose I and II modifications, two other polymorphs lattice structures of much less practical importance are known, called cellulose III and cellulose IV. Cellulose III is formed by the treatment of native cellulose fibres with liquid ammonia and has a parallel chain arrangement [30]. Cellulose IV can be obtained from cellulose III sources by a treatment in hot glycerol baths under stretch [24]. The chain arrangement of the form IV_2 of this polymorph is antiparallel as in cellulose II [30]. The existence of these two modifications is supported by some distinct differences in the X-ray diffraction pattern and in the RMN^{13}C spectra (see Figure 15).

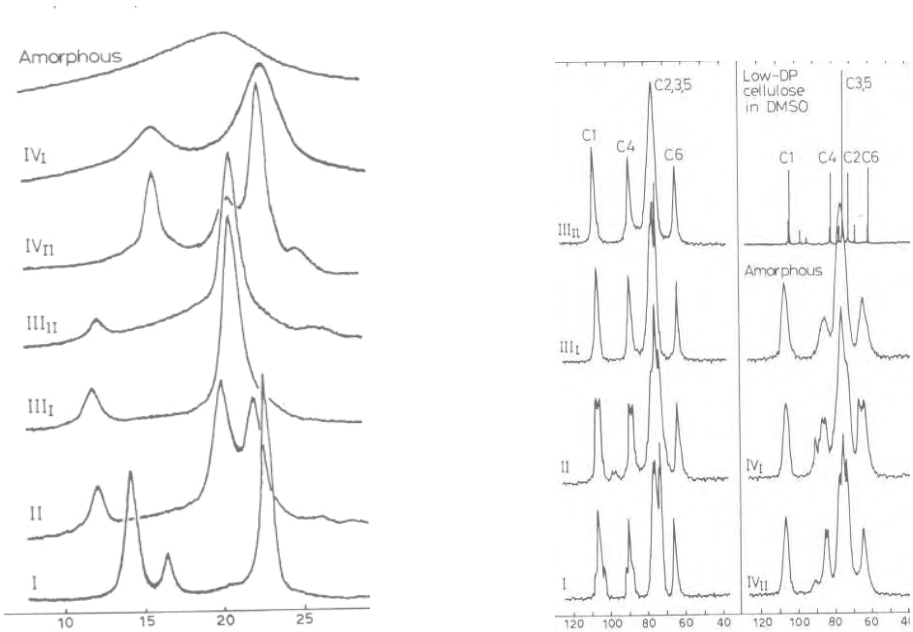

Figure 15. X-ray diffraction pattern (left) and RMN Spectra (right) for the different polymorphs of cellulose. (Illustration taken from [34])

c) Intermolecular hydrogen bonding

As was shown in chapter 1.2.1, cellulose molecules could have one or two intramolecular hydrogen bond. This leaves the possibility for an interlinkage by another intermolecular hydrogen bond between the hydroxyl O-3-H and the hydroxyl O-6 of the neighboring chain (Figure 16). The packing of the cellulose chains in cellulose I is thus very dense and the hydroxyls inside the crystals are not easily accessible.

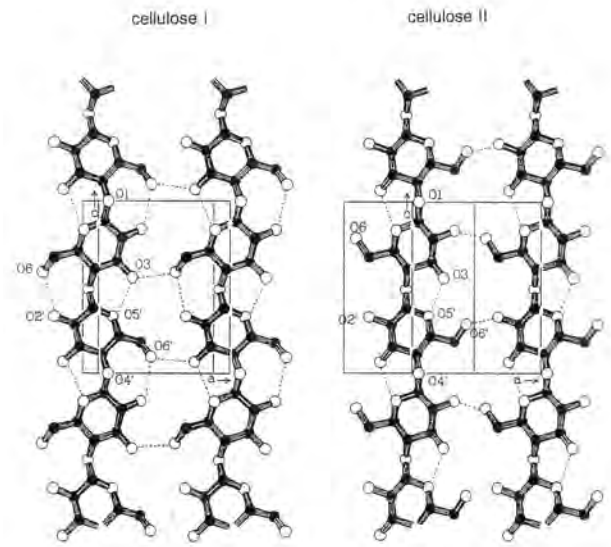

Figure 16. Intermolecular (and intramolecular) hydrogen bond patterns of cellulose I and cellulose II. (Illustration taken from [18]).

In cellulose II, the position of the hydroxyls favours the formation of intermolecular hydrogen bonds (Figure 16). The intramolecular bonds are similar to cellulose I. Consequently, cellulose II is more densely packed and the cellulose molecules are strongly linked with an average bond length shorter than in cellulose I.

1.2.3. Macrostructural Level

a) Cell wall structure of native celluloses fibres

Cellulose microfibrils and macrofibrils are the basic fibrillar elements of the cell wall building. During the period of cell growth, the fibres possess only a very thin cell wall, named

"primary wall", which envelops the protoplasm. After completion of the growth in length, the thickness of the cell wall increases by the deposition of cellulose microfibrils in a second relatively thick layer, the "secondary wall", on the inner side of the primary wall. At the end of the biosynthesis, the plant cell die and the central channel of the cell is more or less narrowed depending of the maturity of the fibre.

The cell wall morphology is composed of cellulose layers differing in their fibrillar texture, as shown schematically in Figure 17 for a cotton hair (or fibre as it is often called) and a wood fibre. These two materials consist of cellulose layers with different thickness and microfibrils orientations.

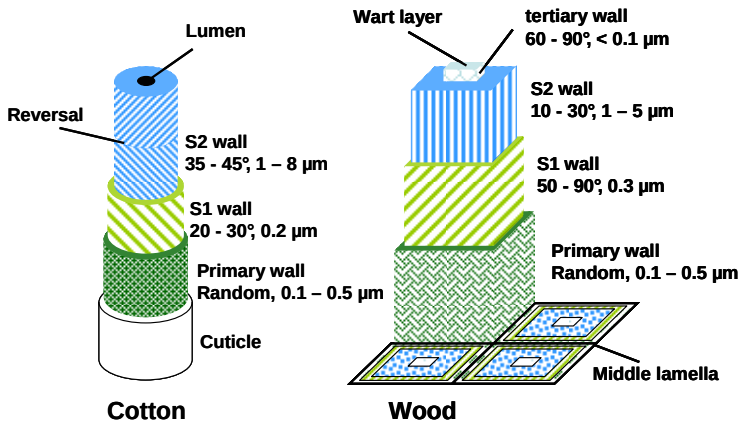

Figure 17. Schematic drawing of the macrostructural morphology of a cotton fibre (A) and a wood fibre (B) with : cuticle (rich in pectins and waxes), lumen, middle lamella (mainly lignin), primary wall, reversal of the fibril spiral, S1-secondary wall, S2-secondary wall (main body), tertiary wall, wart layer. For each wall, the thickness and the microfibrils orientation are drawn according to [17, 18, 35, 36].

In the outer cell layer, i.e. the primary wall (P), the microfibrils are almost randomly positioned over a thickness of 500 nm. The secondary wall (S) consists of two layers S1 and S2. In the case of cotton, the thickness of the S1 layer is about 200 nm, and for a wood fibre, it is 300 nm. The microfibrils are parallel and densely packed in a flat S-helix with variable angles function of the nature of fibres (50 to 70° for wood fibres and 20 to 30° for cotton fibres). The S2 layer is several µm-thick depending of the maturity of the fibre and contains most of the cellulose mass [17, 18, 37] (see table 1). The microfibrils from cotton are well aligned with periodical reversal in a so-called S-Z fashion and orientated around 35-45° to the fibre axis. For other natural sources like wood, flax, hemp… the microfibrils are positioned in an extended helix at a high degree of orientation towards the fibre axis (10 to 30° for wood fibres, see also Table 1).

Fibre	Cellulose content (wt.%)	Spiral angle (°)	Cross-sectional area $A \times 10^{-2}$ (mm^2)	Cell-length L (mm)	L/D-ratio (D is the cell diameter (–)
Jute	61	8.0	0.12	2.3	110
Flax	71	10.0	0.12	20.0	1687
Hemp	78	6.2	0.06	23.0	960
Ramie	83	7.5	0.03	154.0	3500
Sisal	67	20.0	1.10	2.2	100
Coir	43	45.0	1.20	3.3	35

Table 1. Variation of the cellulose content and the spiral angle for some plant cell walls in the S2 layer. (Illustration taken from [37])

The last layer deposited closest to the fibre lumen, called tertiary layer (T) in the case of wood fibres and S3 layer in the case of cotton, is not always present and is very thin (< 100 nm). Its microfibrils are aligned in a flat helix forming a small angle with the cross-sectional axis (60 to 90° for wood fibres).

b) Cell wall components of native cellulose fibres and fine structure of the walls

The primary wall is the most complex part of the cell wall and contains many components. Cellulose (15-30%) and hemicelluloses (25% ; Xyloglucan, Xylan and glucomannan) are present as in the secondary wall but the primary wall may also contains pectins (30% ; Homogalacturonan, RG type I, RG type II [1]), proteins (20% ; strongly glycosyled HRPG, slightly glycosyled PRP, not glycosyled GRP, AGP [38]), lignin and phenolic acids (feluric, coumaric) [39]. The cellulose microfibrils are randomly positioned and linked to hemicelluloses by hydrogen bonds that help the positioning of the microfibrils. A gelled matrix is formed by pectins associated with Ca^{2+} ions. It determines the porosity and the pH of the wall. Proteins, as Hydroxyprolin Rich Glyco Proteins (HRGPs) so-called expansins or extensins, and enzymes, as endoglucanases, help the elongation of the primary wall, repositioning the cellulose microfibrils by disrupting the hydrogen interactions with hemicelluloses [40] (see Figure 18). At the end of the elongation stage, structural proteins form a secondary network by covalent and hydrogen interactions and block the plasticity of the primary wall [39, 41]. In addition, proteins are supposed to be crosslinked to pectins and also phenolic acids by forming protein-phenolic-protein interactions [42]. In general, the different components present in the primary wall undergo strong interactions as revealed by dynamic FT-IR spectroscopy [43]. The complex structure of the primary wall is shown in Figures 18 and 19.

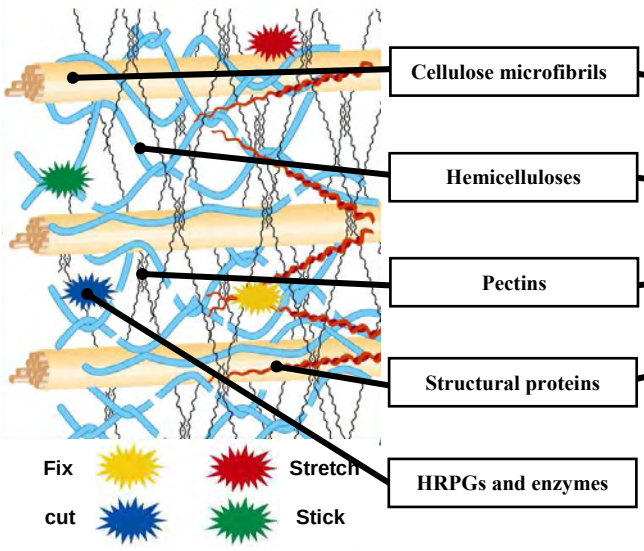

Figure 18. Role of the proteins and enzymes during the elongation stage. (Illustration taken from [44])

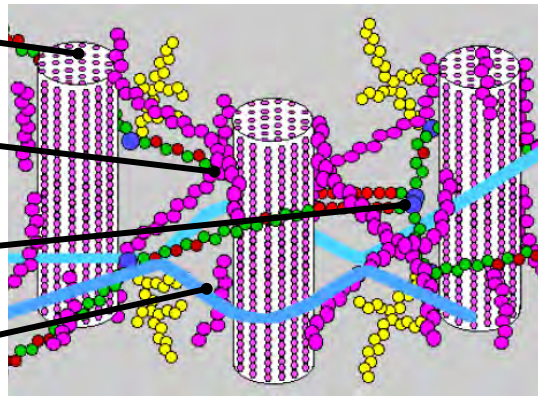

Figure 19. Complexity of the primary wall at the end of the elongation stage. (Illustration taken from [41])

In addition to this complex structure, the arrangement of the cellulose microfibrils is not homogeneous across the thickness of the primary wall (Figure 20). During their synthesis by the protoplasm (in red), microfibrils are ordered in a regular manner (Stage A, zone 1). During the elongation, microfibrils are orientated and are pushed back towards outside (Stages B and C) [41]. The oldest zones are thinned in consequence of the elongation (Stage C, zone 1).

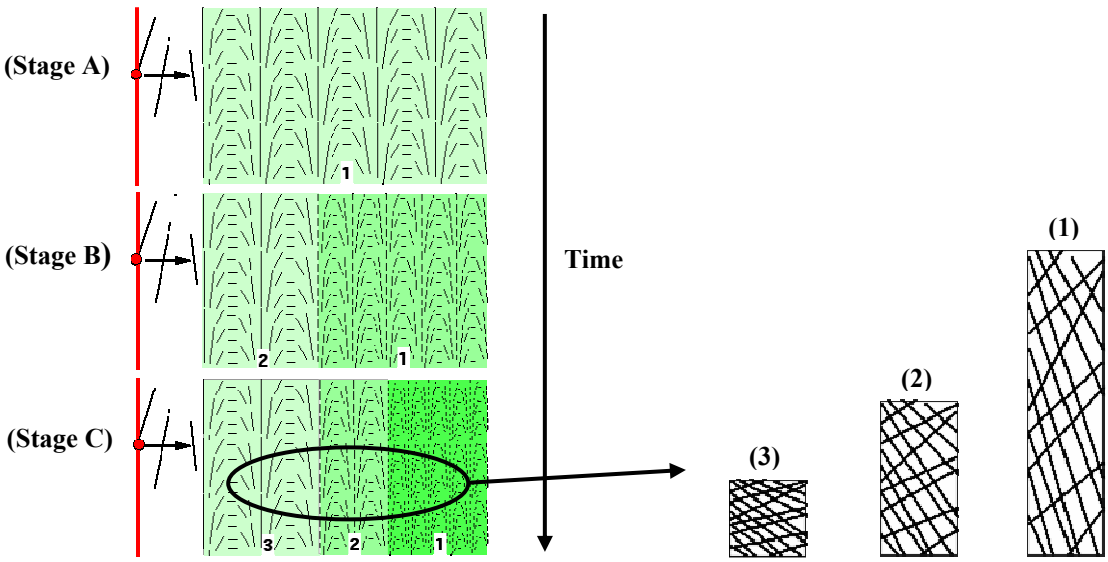

Figure 20. Orientation of the cellulose microfibrils during the elongation stage. (Illustrations taken from [41])

The secondary wall is mostly composed of cellulose (50-85%), hemicelluloses (0-25%) and lignin (0-25%) depending to plant species. In the case of cotton fibres, the secondary wall contains almost only cellulose (around 99%). Components are linked together by hydrogen bonds (cellulose-hemicelluloses) and crosslink in the case of lignin-cellulose or lignin-hemicelluloses. Several authors assume that the hemicelluloses and lignin are dispersed in layers between the cellulose microfibrils [23, 36, 45]. The cellulose microfibrils are arranged helically as discussed in the preceding chapter on cell wall structure.

c) Geometrical model for cell wall formation

As was shown in chapter 1.1.2, new tools as computer modelling are now used to describe the synthesis and the morphology of cellulose fibre. Mulder and Emons [16] build a geometrical model to explain how the CSCs, the distance between cellulose microfibrils being deposited and the cell geometry, determine wall texture. In this model they have proposed that the default mechanism, which determines the orientation of cellulose microfibrils as they are deposited in the absence of other influences, has geometrical origin. The first results showed that several known cell wall textures can be reproduced: axial, helical, helicoidal and crossed wall texture as shown in Figure 21.

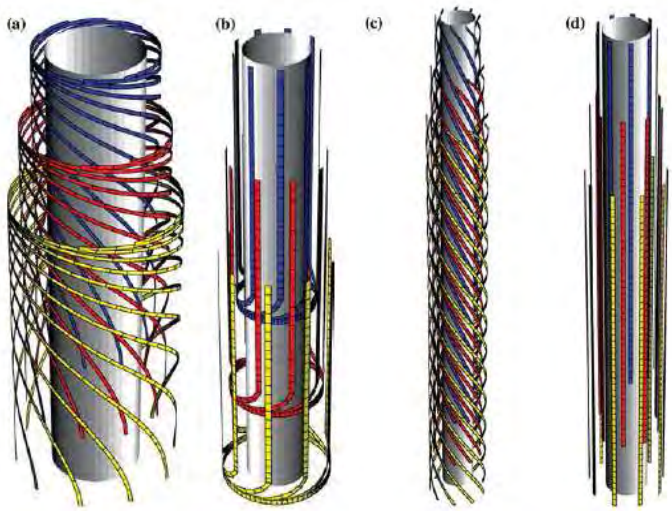

Figure 21. Different cell wall textures as predicted by the geometrical model of Mulder *et al.* [16]. (a) helicoidal texture, (b) crossed polylamellate texture, (c) helical texture, (d) purely axial texture.

d) Pore structure

In addition to the fibrillar morphology of the fibre cell wall, there is a system of pores, capillaries, voids, and interstices [18]. There is a wide distribution of the pores in terms of size and shape. A total pore volume and an average pore size are thus not enough to give a complete and precise description of the pore system. Some data on pores of various cellulose samples measured by two techniques are given in table 2 and 3.

Sample	Volume of pores (%)	Inner surface of pores (m^2/g)	Parameter of average pore size (nm)
Cotton linters	1.7–1.8	5.3–6.0	11.6–13.1
Sulfite dissolving pulp	0.7–1.5	1.7–3.2	10.1–25.4
Sulfate pulp[a]	1.2	3.7	13.1
Cellulose powder[b]	1.4	5.2	10.4
Cellulose powder mercerized	1.7	15.8	4.4
Cellulose powder enzyme-treated	2.5	6.2	15.9

[a] Prehydrolyzed.
[b] Prepared from spruce sulfite pulp by partial hydrolysis and mechanical disintegration.

Table 2. Data on pores of cellulose samples calculated by SAXS measurements. (Illustration taken from [18])

Sample	Covered Pore size (nm)	Pore volume (cm^3/g)	Porosity[a] (%)
Cotton	>800	0.087	–
	>150	0.045	6.6
Spruce sulfite pulp	8000–400000	0.072	17.3
Viscose rayon	1100–150	0.073	–
	>15	0.018	–
Viscose staple fiber	8000–400000	0.018	6.6

[a] The term porosity denotes the total percentage of pores including the large ones (>1000 nm)

Table 3. Void characteristics in native cellulose (cotton, spruce…) and regenerated (viscose rayon, viscose staple) measured by mercury porosimetry. (Illustration taken from [18])

The total pore volume and pore size distribution are very sensitive to pre-treatments. Mercerization leads to a decrease in pore diameter and an enhancement of micropore surface while enzyme treatments enlarge the existing pores [46]. Acid hydrolysis enhances the pore system by removing amorphous cellulose from the surface and revealing the macrofibrillar structure of cellulose fibres [47] (see Figure 22).

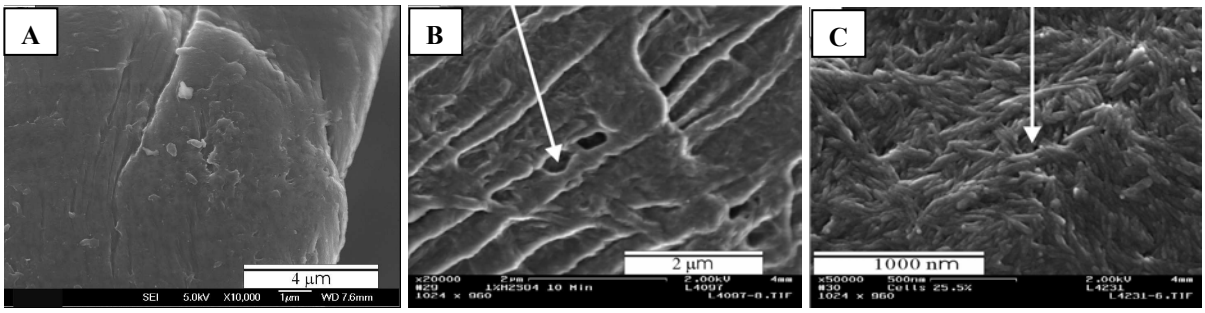

Figure 22. (A) Untreated cotton linters, (B) Cotton linters after 1.0% cellulose was hydrolyzed, (C) Cotton linters after 11.8% cellulose was hydrolyzed, the macrofibrillar structure is revealed. (Illustration taken from [47])

Drying results in an irreversible reduction of the pore volume due to the closing of the smallest pore, a mechanism called hornification (see Figure 23).

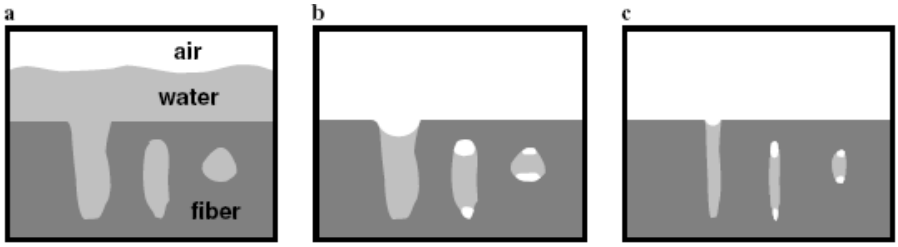

Figure 23. "Conceptual model of pore closure". When water is evaporated (a > b > c), the pores collapse due to the capillary forces with the high surface tension of water (illustration taken from [48]). Formation of hydrogen bonds block the pore and prevent its re-opening.

Due to the pore and void system, the surface area of cellulose fibres exceeds by far the geometrical outer surface of the fibre. The inner surface area is considered as a key parameter with regard to accessibility and reactivity in dissolution and derivatization processes [18].

e) Particular twisting and kidney shape of cotton fibres

Several twists can be observed along the cotton fibre (Figure 24 a and 24 b) and the cross-sections reveal a "kidney" or "bean" shape (Figure 24 c). At the end of the biosynthesis, before boll opening, the lumen is filled with a liquid containing the cell nucleus and the protoplasm. The twists and the "kidney" shape of the dried fibre are due to the removal of this liquid, also called dehydration or desiccation [49, 50].

Althought the spiral reversal S-Z changes only 1 to 3 times per mm, the number of twists in cotton fibres is higher (between 3.9 and 6.5 per mm). However, the lateral alignment of the fibrillar reversals in the concentric cellulose layers and the ultimate twists in the dried fibres are related. Basra *et al.* [50] explain that the probability for reversals in the cellulose layers to coincide laterally increases with fibre maturity and increasing secondary wall thickness. When a sufficient number of reversals coincides, stress leads to twist formation. The twist is thus the region where reversals overlap among concentric layers. When cotton fibres are placed under wet conditions, an untwisting occurs in function of the quality of the swelling agent [35].

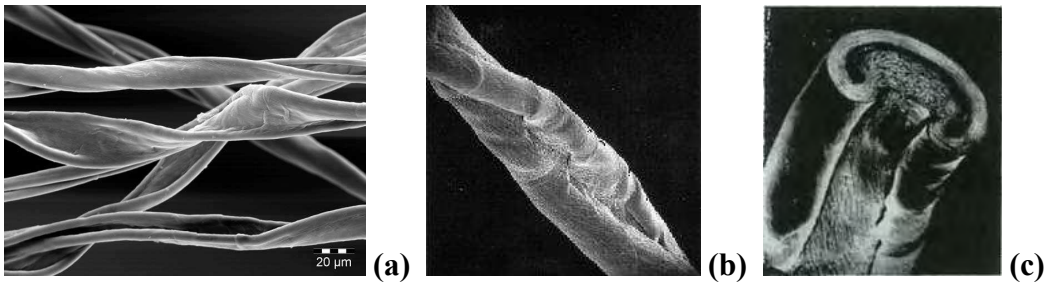

Figure 24. Twists (a, b) and kidney shape (c) in cotton fibres. (Illustrations taken from [49, 51, 52])

The kidney shape is more or less pronounced in function of the fibre maturity. For a high maturity fibre, the shape is almost ellipsoidal due the thickness of the secondary wall. The influence of maturity can be seen in Figure 25. The blue circle shows a cotton fibre cross-section with a thick and well-developed wall. This is a mature cotton fibre. The red circle shows a fibre cross-section with a thin and poorly developed wall. This is an immature cotton fibre.

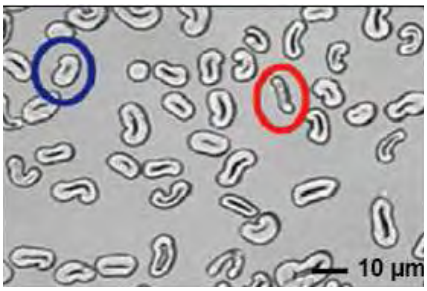

Figure 25. Cross-sections of mature (blue circle) and immature (red circle) cotton fibres. (Illustration taken from [53]).

The dehydration involves mechanical strains and resulting deformations along the fibre. Several authors postulate the existence of a bilateral structure due to an asymmetry in the distributions of stresses which occur during the dehydration of cotton. In fact, fibres undergo an important shape modification from a swollen cell tube to a fibre [49, 54]. Observation of ultrathin sections shows that the density of chain packing is not homogeneous in the secondary wall (Figure 26).

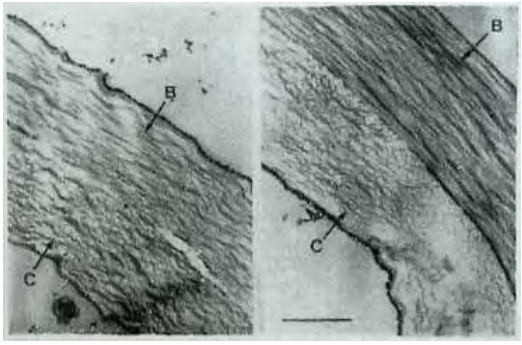

Figure 26. Ultrathin sections of cotton fibres perpendicular to fibre axis showing the fine structure of different zones of the secondary wall (illustration taken from [49]). Zone A, B, C correspond to the different zones as defined in Figure 27.

In the cross sections of mature fibres, different zones were thus distinguished as regard to the organization of their fine structure as shown in Figure 27. They were also thought to differ in their accessibility to reagents and their behaviour during swelling [49].

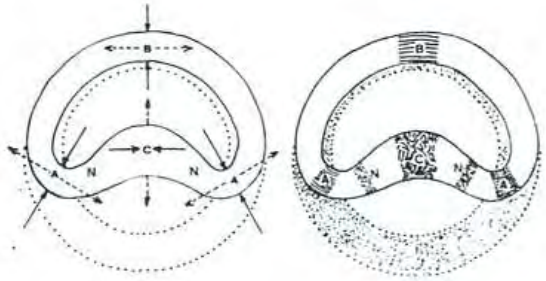

Figure 27. (left) Relations between mechanical strains (full arrows) and deformations (dotted arrows) produced by collapsing of the cotton fibre during initial drying, (right) model showing the changes in packing density and orientation of the fibrillar membranes in a cotton fibre.(Illustration taken from [49])

Conclusions

Many studies have been performed to understand the cellulose structure at all its morphological levels, and the whole structure and organization are now well understood. New methods such as computer modelling are helping to better describe cellulose structure and synthesis. However, several key issues like the full dynamics of cell wall deposition and the role of the various non-cellulosic components in the structuration of the cell wall are mostly unknown. Several aspects are still under question, like the understanding of the formation of the hydrogen bonding network and the transition between cellulose I and cellulose II. The origins of the accessibility and reactivity of cellulose are closely linked to these different aspects.

Primary and secondary walls reveal large differences in their structural organization in terms of components and arrangement of cellulose microfibrils which should have a strong impact on the swelling and dissolution mechanisms of cellulose fibres.

Wood and cotton fibres are rather different in their microfibrils organization, in the presence of lignin in wood and in the absence of hemicelluloses in the secondary wall of cotton. Taking this into consideration, the walls of wood and cotton should show different swelling and dissolution behaviours in a solvent.

1.3. Swelling and dissolution mechanisms of cellulose fibres

Due to their complex and multi-scale structure, the mechanisms of swelling and dissolution of cellulose fibres are not homogeneous. As will be shown, several proposals have been made for explaining the non homogeneous swelling and dissolution of cellulose fibres and cellulose derivatives. This phenomenon has to be related with the fibre source but also with the solvent quality.

1.3.1. Heterogeneous mechanisms of swelling and dissolution of cellulose fibres and cellulose derivatives

The most spectacular effect of the heterogeneous swelling and dissolution of cellulose fibre is the ballooning phenomenon. The swelling can take place in some selected zones along the fibres. This localised swelling gives the impression of having "balloons" growing as shown on Figure 28. This heterogeneous ballooning swelling has been observed long ago, first by Nägeli in 1864 [55], then by Pennetier in 1883 [56], Fleming and Thaysen in 1919 [57], Marsh *et al*. in 1941[58], Hock in 1950 [59] or Rollins and Tripp in 1952 [60, 61] (Numerous other studies are also reported in reference [35]).

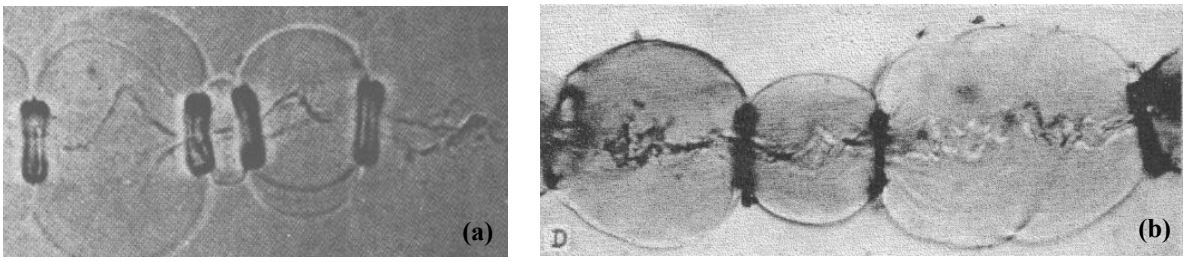

Figure 28. (a) Cellulose fibre swollen by alkali and carbon bisulfite, (b) Ballon formation in raw cotton. (Illustrations taken from [58, 59] respectively)

In 1954, Ott *et al.* [62] proposed an explanation of this phenomenon. It must be noted that similar explanations were suggested in all the preceding references. For a wide range of cellulose fibres, the microfibrils of the secondary wall are aligned in a helical manner with respect to the long axis of the fibre. Ott *et al.* deduces that the swelling is greater transversely than lengthwise (as it is generally for fibres where the orientation of the cellulose chains is mainly in the fibre direction). Consequently, they proposed that "when raw cotton fibres are placed in certain swelling agent, the radial expansion of the cellulose in the secondary wall

causes the primary wall to burst. As the expanding swollen cellulose pushes its way through these tears in the primary wall, the latter rolls up in such a way as to form collars, rings or spirals which restrict the uniform expansion of the fibre and forms balloons". Ott *et al.* have also reported that an irregular swelling can be visible with fibre without the primary wall (removed by alkaline digestion) due to the S1 wall which restricts lateral expansion.

All the authors assume that the ballooning phenomenon has structural origins, i.e. linked to morphological variations between the different walls. However, the explanation cited above assumes that cellulose is in a swollen state in each of the balloons, which remains to be demonstrated. In addition, no data exist on the respective roles of the primary and secondary wall layers in this process. Finally, the different stages that lead to the ballooning phenomenon have not been well described. In paper I of our study, we will describe by means of high resolution observations the state of the cellulose inside the balloons and the swelling and dissolution mechanisms of the different walls.

The main regions implied in the ballooning have been described in details by Cuissinat and Navard [63, 64]. As shown on Figure 29, three zones have been identified: the membrane, the inside of the balloons and the unswollen sections. However, the exact origin of these three zones was not reported.

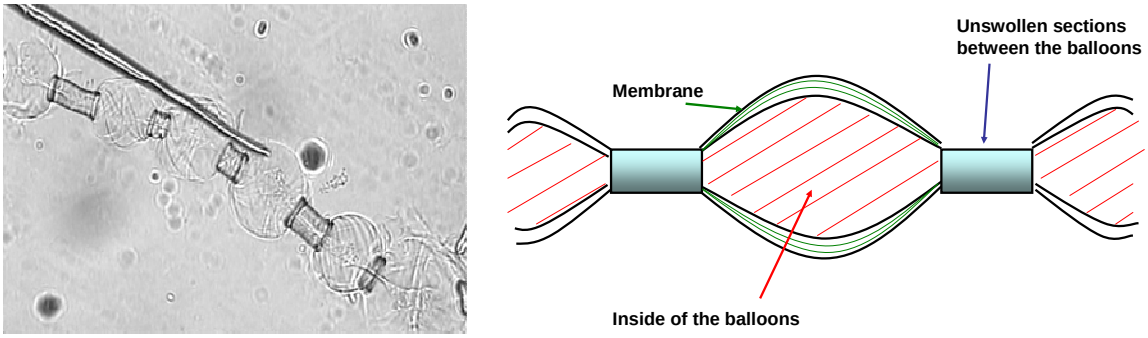

Figure 29. Identification of the three zones of a wood fibre swollen by ballooning in water- 8% NaOH. (Adapted from [63, 64])

Stawitz and Kage [65] have also reported heterogeneous swelling and dissolution in carboxymethyl cellulose (CMC) fibres. The mechanisms of swelling are described on Figure 30. Fibres are swelling by ballooning with a helical structure around the balloons (1 to 3). The breakage of the helical structure and the unswollen sections between the balloons leads to a high homogeneous swelling (4 to 6). The highly swollen sections are then tear into thin sections and finally into fragments (7 to 10). In paper II of our study, we will see that the

model of Stawitz and Kage for CMC is also valid for all wood based fibres in NaOH-water systems. By selecting well defined samples and solvent, we were able to describe in more details in what way the observed features are swelling and dissolving and the exact origins of these phenomena.

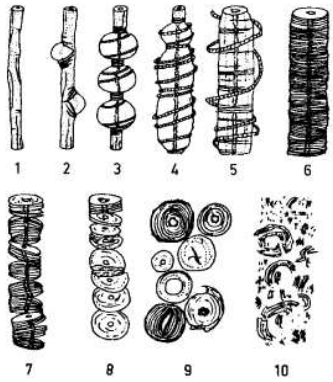

Figure 30. The swelling of Carboxymethyl cellulose (CMC). (Illustration taken from [65])

1.3.2. Influence of the solvent quality on swelling and dissolution mechanisms of cellulose fibres

Chanzy *et al.* [66] have investigated the swelling and dissolution of various cellulose fibres, both native and regenerated, in *N*-methylmorpholine *N*-oxide (NMMO) with different amounts of water. Three domains of "water concentration" were found to be important. When the amount of water was low (NMMO- 16% water), cellulose fibres, such as ramie, cotton and wood were dissolving rapidly by fragmentation without significant swelling. At higher water concentration (e.g., NMMO- 18-20% water), the ramie fibres exhibited a heterogeneous swelling: a ballooning phenomenon was observed in localized places. In the case of wood and cotton fibres, the ballooning was well defined and the difference of swelling with ramie fibre was attributed to a difference of organization of the cellulose microfibrils within the various species. After the removal of the swelling agent, they observed that the initial ramie fibres were converted into an unoriented cellulose II crystalline structure. Chanzy *et al.* called this region "irreversible swelling". With more water (e.g., NMMO- 20% and more), ramie fibres were sometimes both having cellulose I and II after the removal of the swelling agent but most of the time the cellulose I structure of the cellulose crystals was conserved.

The regions of dissolution, irreversible and reversible swelling of cellulose in the NMMO-water solvents as defined by Chanzy *et al.* are schematically represented in Figure 31. Region

A corresponds to the dissolution of the ramie fibres by fragmentation without swelling. Region B and C corresponds the irreversible swelling and reversible swelling ,respectively. When water amounts were below 28% (D), no visible changes were observed which thus corresponds to a region of non activity.

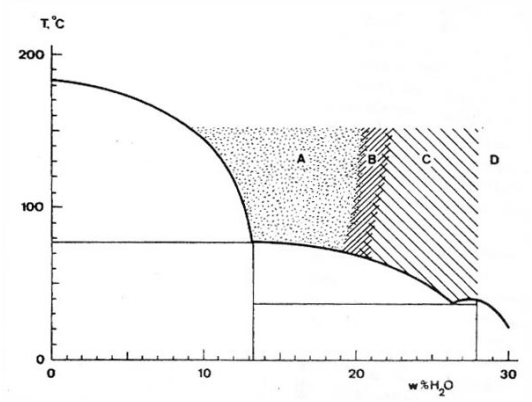

Figure 31. Partial phase diagram [66] of the system NMMO-water on native cellulose fibres showing the various regions of dissolution : (A) by fragmentation without swelling, (B) irreversible swelling, (C) reversible swelling, (D) non activity.

The designation "reversible or irreversible swelling" corresponds to the cellulose organisation within the cellulose crystals but not to structural and morphological modifications that cannot be recovered after the swelling experiments. In the irreversible zone (B), only cellulose II was present after the removal of the swelling agent by washing with water and subsequent drying and cellulose I structure cannot be seen. In the reversible zone (C), the swelling experiments do not lead to a cellulose II lattice and the cellulose I crystal organisation is conserved after washing and drying.

The most important result in this study is that by changing the water amount from 16% to 20 % w/w, an important change from the dissolution by fragmentation of cellulose to reversible swelling was observed. In addition, pronounced differences were found in the crystalline structures of the fibres in function of the amount of water.

Based on the preceding study, Cuissinat and Navard [63, 64] performed observations by optical microscopy of free floating fibres between two glass plates for a wide range of solvent quality. They have identified four main dissolution modes for wood and cotton fibres in function of the quality of the solvent, in NMMO:

Mode 1: Fast dissolution by fragmentation (under 17% water).

Mode 2: Swelling by ballooning and dissolution (from 18 to 24 % water).

Mode 3: Swelling by ballooning and no complete dissolution (from 25 to 30 % water).

Mode 4: Low homogeneous swelling and no dissolution (above 35 % water).

These different dissolution mechanisms are summarized in Figure 32. These mechanisms have been also observed with ionic liquids solvent [67] and for a wide range of plant fibres [68] and some cellulose derivatives if the derivatization occurred without dissolution [69]. From all these studies, it is shown that the key parameter in the dissolution mechanisms is the morphological structure. If the original wall structure of the native fibre is preserved, the dissolution mechanisms are similar for wood, cotton, other plant fibres and some cellulose derivatives, the solvent quality driving the type of mechanism that will occur for a given fibre type.

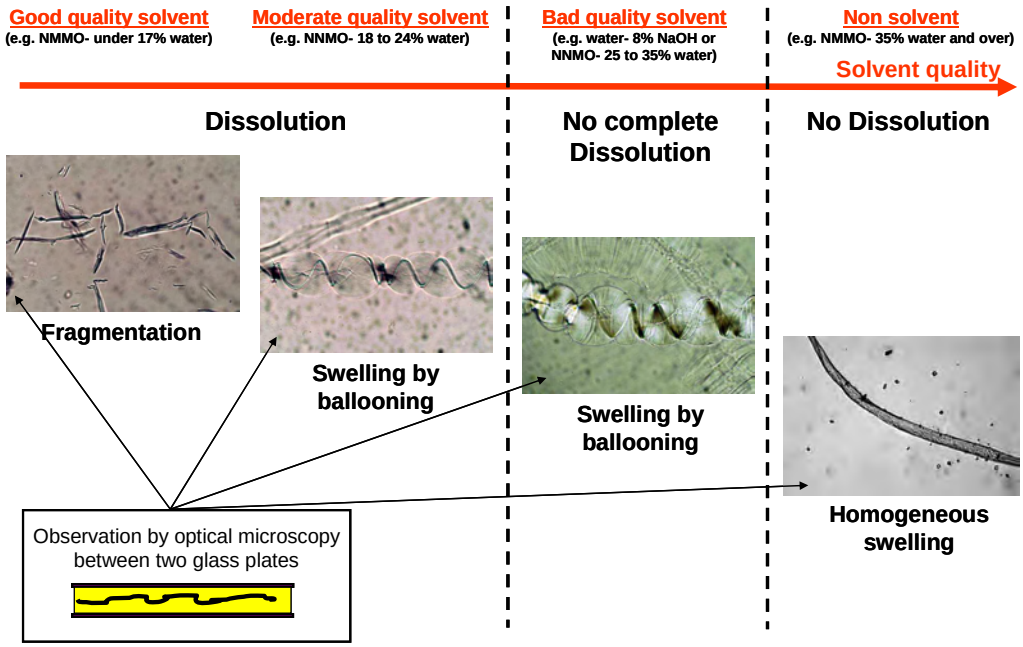

Figure 32. Swelling and dissolution mechanisms of wood and cotton fibres in function of the solvent quality. (Adapted from [63, 64])

Conclusions

The swelling and dissolution mechanisms of cellulose fibre are strongly influenced by the solvent quality but the exact origins of such phenomena are not well understood. The roles of the different levels of the cellulose structure are not well established. By controlling the quality of the solvent, the dissolution conditions (as the tension) and the fibre sources, it will be shown that it is possible to reveal the characteristic mechanisms of the swelling and dissolution at the different length scales of the cellulose structure from the macromolecule to the walls of the fibre. This will be demonstrated in the next parts of this dissertation.

References

[1] Lerouxel, O.; Cavalier, D. M.; Liepman, A. H.; Keegstra, K. Biosynthesis of plant cell wall polysaccharides – a complex process. *Curr. Opin. Plant Biol.* 2006, 9, 1–10.

[2] Zaffran, J. *Initiation à la biologie végétale*. ed. Ellipses, Paris, 1998.

[3] Preston, R. D. *Formation of Wood in Forest Trees*. ed. Zimmerman M.H., Academic Press, New York, 1964, 169–188.

[4] Brown Jr, R. M.; Montezinos, D. Cellulose microfibrils: visualization of biosynthetic and orienting complexes in association with the plasma membrane. *Proceedings of the National Academy of Sciences of the USA*, 1976, 73, 143–147.

[5] Mueller, S. C.; Brown Jr, R. M. Evidence for an intramembrane component associated with a cellulose microfibril synthesizing complex in higher plants. *J. Cell Biol.*, 1980, 84, 315–326.

[6] Kimura, S.; Laosinchai, W.; Itoh, T.; Cui, X.; Linder, C. R.; Brown Jr, R. M. Immunogold labeling of rosette terminal cellulose-synthesizing complexes in the vascular plant *Vigna angularis*. *Plant Cell*, 1999, 11, 2075–2085.

[7] Diotallevi, F.; Mulder, B. The cellulose synthase complex: a polymerization driven supramolecular motor. *Biophys. J.*, 2007, 92, 2666–2673.

[8] Cousins, S. K.; Brown Jr, R. M. Cellulose I microfibril assembly: computational molecular mechanics energy analysis favours bonding by Van de Waals forces as the initial step in crytallization. *Polymer*, 1995, 36, 3885–3888.

[9] Cousins, S. K.; Brown Jr, R. M. X-ray diffraction and ultrastructural analyses of dye-altered celluloses support Van der Walls forces as the initial step in cellulose crystallization. *Polymer*, 1997, 38, 897–902.

[10] Robert, S.; Mouille, G.; Höfte, H. The mechanism and regulation of cellulose synthesis in primary walls: lessons from cellulose deficient Arabidopsis mutants. *Cellulose*, 2004, 11, 351–364.

[11] Taylor, N.G.; Gardiner J.C.; Whiteman, R.; Turner, S.R. Cellulose synthesis in the Arabidopsis secondary cell wall. *Cellulose*, 2004, 11, 329–338.

[12] Diotallevi, F. *The physics of cellulose biosynthesis - Polymerization and self-organization from plants to bacteria*, Ph.D. Thesis, FOM Institute for Atomic and Molecular Physics, Wageningen University, Amsterdam, 2007, 136 p.

http://www.amolf.nl/publications/theses/diotallevi/diotallevi.html

[13] Saxena, I. M.; Brown Jr, R. M. Cellulose biosynthesis: Current views and evolving concepts. *Ann. Bot.*, 2005; 96, 9–21.

[14] Paredez, A. R.; Somerville, C. R.; Ehrhardt, D. W. Visualization of cellulose synthase demonstrates functional association with microtubules. *Science*, 2006, 312, 1491–1495.

[15] Emons, A. M. C.; Höfte, H.; Mulder, B. M. Microtubules and cellulose microfibrils: how intimate is their relationship? *Trends Plant Sci.*, 2007, 12, 279–281.

[16] Mulder, B.; Schel, J.; Emons, A. M. How the geometrical model for plant cell wall formation enables the production of a random texture. *Cellulose*, 2004, 11, 395–401.

[17] Krässig, H. A. *Cellulose - Structure, Accessibility and Reactivity*. Polymer Monographs 11, ed. Huglin M.B., Gordon and Breach Science Publishers, Amsterdam, 1993.

[18] Klemm, D.; Philipp, B.; Heinze, T.; Heinze, U.; Wagenknecht, W. *Comprehensive Cellulose Chemistry.* Vol. 1, Wiley-VCH, Weinheim, 1998.

[19] David, S. *Chimie moléculaire et supramoléculaire des sucres - Introduction chimique aux glycosciences*. InterÉditions et CNRS Editions, Paris, 1995.

[20] Rieckmann, Th. *Laboratory: Decomposition of Cellulose (Pyrolysis)*. Department of Plant Design and Chemical Engineering
http://www.av.fh-koeln.de/professoren/rieckmann/chemischeprozesstechnik/lab_pyrolysis/pyrolysis.html, 2006.

[21] Liang, C. Y.; Marchessault, R.H. Infrared spectra of crystalline polyssacharides. II. Native celluloses in the region from 640 to 1700 cm^{-1}. *J. Polym. Sci.*, 1959, 39, 269–278.

[22] Blackwell, J.; Kolpak, F. J.; Gardner, K. H. Structures of native and regenerated celluloses. *ACS Symp. Ser.*, 1977, 48, 42–55.

[23] O'Sullivan, A. C. Cellulose: the structure slowly unravels. *Cellulose*, 1997, 4, 173–207.

[24] Klemm, D.; Schmauder, H. P.; Heinze, T. In *Biopolymers - Polysaccharides II*. vol. 6, ed. Steinbüchel A., Wiley-VCH, Weinheim, 2002, 275–320.

[25] Moore, R.; Clark, D.; Vodopich, D. *Introduction to Botany*, University of Arkansas, http://www.ualr.edu/botany, 2007.

[26] Emons, A. M. C. Plasma-membrane rosettes in root hairs of equisetum hyemale. *Planta*, 1985, 163, 350–359.

[27] Bowling, A.; Brown Jr, R. M. *A new view of cellulose synthase*. http://www.botany.utexas.edu/lab/research_basic/bowling/default.htm, 2005.

[28] Atalla, R.H.; Vanderhart, D.L. Native cellulose: A composite of two distinct crystalline forms. *Science*, 1984, 223, 283–285.

[29] Gardner K. H.; Blackwell, J**.** The structure of native cellulose. *Biopolymers*, 1974, 13, 1975–2001.

[30] Zugenmaier, P. Conformation and packing of various crystalline cellulose fibers. *Prog. Polym. Sci.*, 2001, 26, 1341–1417.

[31] Finkenstadt, V.L.; Millane, R.P. Crystal structure of valonia cellulose Iβ. *Macromolecules*, 1998, 31, 3776–3778.

[32] Klemm, D.; Heublein, B.; Fink, H. P.; Bohn, A. Cellulose: fascinating biopolymers and sustainable raw material. *Angew. Chem. Int. Edit.,* 2005, 44, 3358–3393.

[33] Langan, P.; Nishiyama, Y.; Chanzy, H. X-ray structure of mercerized cellulose II at 1 Å resolution. *Biomacromolecules*, 2001, 2, 410–416.

[34] Isogai, A. In *Cellulosic polymers, blends and composites, Allomorphs of cellulose and other polysaccharides.* ed. Gilbert R. D., Hanser publishers, New York, 1996, 1–24.

[35] Warwicker, J. O.; Jeffries, R.; Colbran, R. L.; Robinson R. N. *A Review of the Literature on the Effect of Caustic Soda and Other Swelling Agents on the Fine Structure of Cotton*. Shirley Institute Pamphlet 93, St Ann's Press, England, 1966.

[36] Fahlén, J. *The cell wall ultrastructure of wood fibres: Effects of the chemical pulp fibre line*. Ph.D. Thesis, Fibre and Polymer Technology, KTH Royal Institute of Technology Stockholm, 2005, 70 p, http://www.diva-portal.org/kth/theses/abstract.xsql?dbid=129

[37] Bledzki A.K., Gassan J., Composites reinforced with cellulose based fibres, *Prog. Polym. Sci.*, 1999, 24, 221–274.

[38] Jamet, E.; Canut, H.; Boudart, G.; Pont-Lezica, R. F. Cell wall proteins: a new insight through proteomics. *Trends Plant Sci.*, 2006, 11, 33–39.

[39] *La paroi cellulaire*. Université de la Méditerranée, département de biologie, http://biologie.univ-mrs.fr/upload/p210/4_la_paroi.pdf, 2008.

[40] Yuan, S.; Wu, Y.; Cosgrove, D. J. A fungal endoglucanase with plant cell wall extension activity. *Plant Physiol.*, 2001, 127, 324–333.

[41] Prat, R.; Mosiniak, M.; Roland, J. C. *La paroi primaire de la cellule végétale*. Université Pierre & Marie Curie, http://www.snv.jussieu.fr/bmedia/paroi/index.htm, 2008.

[42] Qi, X.; Behrens, B. X.; West, P. R.; Mort, A. J. Solubilization and partial characterization of extensin fragments from cell walls of cotton suspension cultures - Evidence for a covalent cross-Link between extensin and pectin. *Plant Physiol.*, 1995, 108, 1691–1701.

[43] Stevanic, J. S.; Salmén, L. Characterizing wood polymers in the primary cell wall of Norway spruce (*Picea abies* (L.) Karst.) using dynamic FT-IR spectroscopy. *Cellulose*, 2008, 15, 285–295.

[44] Boudet, A.-M. *L'amélioration des plantes, base de l'agriculture*. Rapport de communication, Institut Fédératif de Recherche "Signalisation Cellulaire et Biotechnologie Végétale" (IFR 40), Toulouse, 2002.

[45] Fengel, D. Ideas on the ultrastructural organization of the cell wall components. *J. Polym. Sci.: part C*, 1971, 9, 383–392.

[46] Fink, H.-P.; Philipp, B.; Zschunke, C., Hayn, M. Structural changes of LOPD cellulose in the original and mercerized state during enzymatic hydrolysis. *Acta Polym.*, 1992, 43, 270–274.

[47] Zhao, H.; Kwak, J. H.; Zhang, Z. C.; Brown, H. M.; Arey, B. W.; Holladay, J. E. Studying cellulose fiber structure by SEM, XRD, NMR and acid hydrolysis. *Carbohydr. Polym.*, 2007, 68, 235–241.

[48] Park, S.; Venditti, R. A.; Jameel, H.; Pawlak, J. J. Changes in pore size distribution during the drying of cellulose fibres as measured by differential scanning calorimetry. *Carbohydr. Polym.*, 2006, 66, 97–103.

[49] Kassenbeck, P. Bilateral structure of cotton fibers as revealed by enzymatic degradation. *Text. Res. J.*, 1970, 40, 330–334.

[50] Basra, A. S. *Cotton Fibers: Developmental Biology, Quality Improvement and Textile Processing*, ed. Basra A. S., Food Products Press/Haworth Press, New York, 1999.

[51] *Natural fibres synthetic fibres, Cotton*. Swicofil AG Textile Services, http://www.swicofil.com/products/001cotton.html, 2008.

[52] International Forum for Cotton Promotion (IFCP), Cotton Promotion Bulletin, 16, http://cottonpromotion.org/image/features/bremen/cotton_fibre_650x488/, 2008.

[53] Naylor, G., *Fineness & Maturity Testing: a renaissance in cotton testing*. Commonwealth Scientific and Industrial Research Organisation (CSIRO), Textile and Fibre Technology, http://www.tft.csiro.au/, 2007.

[54] Möck, U. Determination of the bilateral structure of cotton by Electron Beam Micro-Analysis. *Melliand Textilber.*, 1973, 2, 769–771.

[55] Nägeli, C. Über den inneren Bau der vegetabilischen Zellmembranen, *Sitzber. Bay. Akad. Wiss. München*, 1864, 1, 282–323, 2, 114–171.

[56] Pennetier, G. Note micrographique sur les altérations du cotton, *Bull. Soc. Ind. Rouen*, 1883, 11, 235–237.

[57] Flemming, N.; Thaysen, A. C. On the deterioration of cotton on wet storage. *Biochem. J.*, 1919, 14, 25–29, 1921, 14, 407–415.

[58] Marsh, J. T. *The growth and structure of cotton, Mercerising*. Chapman & Hall Ltd, London, 1941.

[59] Hock, C. W. Degradation of cellulose as revealed microscopically. *Text. Res. J.*, 1950, 20, 141–151.

[60] Tripp, V. W.; Rollins, M. L. Morphology and chemical composition of certain components of cotton fiber cell wall. *Anal. Chem.*, 1952, 24, 1721–1728.

[61] Rollins, M. L.; Tripp, V. W. Optical and electron microscopic studies of cotton fiber structure. *Text. Res. J.*, 1954, 24, 345–357.

[62] Ott, E.; Spurlin, H. M.; Grafflin, M. W. *Cellulose and cellulose derivatives (Part 1)*, Interscience Publisher, New York, 1954.

[63] Cuissinat, C.; Navard P. Swelling and dissolution of cellulose, Part I: free floating cotton and wood fibres in *N*-methylmorpholine-*N*-oxide – water mixtures. *Macromol. Symp.*, 2006, 244, 1–18.

[64] Cuissinat, C.; Navard P. Swelling and dissolution of cellulose, Part II: free floating cotton and wood fibres in NaOH water-additives systems. *Macromol. Symp.*, 2006, 244, 19–30.

[65] Stawitz, J.; Kage, M.P. Über die quellungsstadien der wasserlöslichen celluloseäther und die übermolekulare struktur der cellulose. *Das Papier*, 1959, 13, 567–572.

[66] Chanzy, H.; Noe, P.; Paillet, M.; Smith, P. Swelling and dissolution of cellulose in amine oxide / water systems. *J. Appl. Polym. Sci.*, 1983, 37, 239–259.

[67] Cuissinat, C.; Navard, P.; Heinze, T. Swelling and dissolution of cellulose, Part IV: Free floating cotton and wood fibres in ionic liquids. *Carbohydr. Polym.*, 2008, 72, 590–596.

[68] Cuissinat, C.; Navard, P. Swelling and dissolution of cellulose, Part III: Plant fibres in aqueous systems. *Cellulose*, 2008, 15, 67–74.

[69] Cuissinat, C.; Navard, P.; Heinze, T. Swelling and dissolution of cellulose, Part V: Cellulose derivatives fibres in aqueous systems and ionic liquids. *Cellulose*, 2008, 15, 75–80.

Chapter II

Gradient in dissolution capacity of successively deposited cell wall layers in cotton fibres.

Gradient in dissolution capacity of successively deposited cell wall layers in cotton fibres

Abstract The dissolution of cotton fibres has been studied at different development stages before and after the onset of secondary wall deposition in solvents of varying quality. We show that the dissolution of the primary wall is inefficient even in good solvents. In moderately good solvents, the inside of the secondary wall dissolves by fragmentation, whereas the outside of the secondary wall swells. These data demonstrate the existence of a centripetal radial gradient in the dissolution capacity within the fibre, which must be related to age-dependent structural variation in the cell wall layers.

Introduction

Cellulose is the most important skeletal component in plants. For many industrial applications, cellulose must be dissolved. When placed in a swelling agent or a solvent, natural cellulose fibres show a non homogeneous swelling. The most spectacular effect of this non homogeneous swelling is the ballooning phenomenon where swelling takes place in some selected zones along the fibres (Figure 1). This heterogeneous swelling has been observed and discussed long ago by Nägeli in 1864 [1], Pennetier in 1883 [2], Fleming and Thaysen in 1919 [3], Marsh et al in 1941 [4], Hock in 1950 [5] or Tripp and Rollins in 1952.[6,7] One explanation for this phenomenon is that the swelling of the cellulose present in the secondary wall is causing the primary wall to extend and burst. According to this view, the expanding swollen cellulose pushes its way through the tears in the primary wall, the latter rolls up in such a way as to form collars, rings or spirals which restrict the uniform expansion of the fibre and forms balloons as described by Ott.[8] This explanation assumes that cellulose is in a swollen state in each of the balloons, which remains to be demonstrated. In addition, no data exist on the respective roles of the primary and secondary wall layers in this process. Finally, the different stages that lead to the ballooning phenomenon have not been well described.

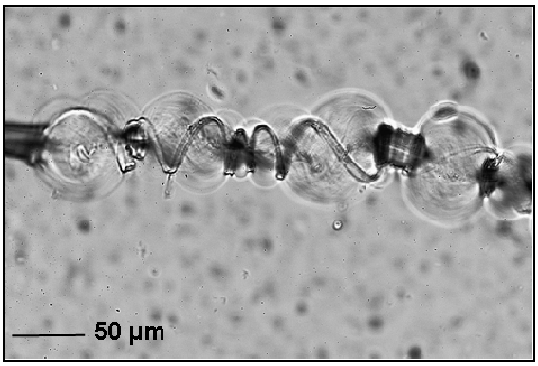

Figure 1. *Gossypium hirsutum* cotton fibre swollen by ballooning in *N*-methylmorpholine-*N*-oxide with 20 % of water w/w.

Further studies of Chanzy and *al* in 1983 [9] and Cuissinat and Navard in 2006 [10] have shown that the dissolution mechanism is strongly dependent on the solvent quality. Cuissinat and Navard performed observations by optical microscopy of free floating fibres between two glass plates for a wide range of solvent quality (as an example *N*-methylmorpholine-*N*-oxide, NMMO, with various amounts of water w/w). They identified four main dissolution modes for wood and cotton fibres as a function of the quality of the solvent (the quality of the solvent decreases from mode 1 to mode 4):

Mode 1: Fast dissolution by fragmentation, occuring in good solvent (e.g. in NMMO with less than 17% of water, 90°C)
Mode 2: Swelling by ballooning and full dissolution, occuring in moderately good solvent (e.g. in NMMO with 19 to 24 % water, 90°C)
Mode 3: Swelling by ballooning and no complete dissolution, occuring in bad solvent (e.g. in NMMO with 25 to 35 % water, 90°C)
Mode 4: Low homogeneous swelling and no dissolution, occuring in very bad solvent (e.g. in NMMO with more than 35 % water, 90°C)

These mechanisms also have been observed with NaOH-water with or without additives [11], ionic liquids [12] and other solvents [13] for a wide range of plant fibres [14] and some cellulose derivatives that had been prepared without dissolution.[15] From all these studies, it is shown that the key parameter in the dissolution mechanism is the morphology of the fibre. Indeed, as long as the original wall structure of the native fibre is preserved, the dissolution mechanisms are similar for wood, cotton, other plant fibres and some cellulose derivatives.

The cotton fruit is a capsule (commonly called cotton boll) composed of 4 or 5 carpel, each of them bearing about 10 seeds. Each cotton fibre is produced by the outgrowth of a single epidermal cell of the seed coat. A cotton fibre is a single cell, mainly made of cellulose microfibrils arranged in concentric walls. Fibre development can be divided in five main growth stages, initiation, elongation, transition, development and maturation.[16]

- The initiation stage corresponds to the differentiation of epidermal cells into fibre cells and takes place around 2 or 3 days preanthesis.
- The elongation stage corresponds to the synthesis of the primary wall and takes place between 1 and 15 days postanthesis (DPA)
- The transition stage corresponds to the end of the primary wall synthesis and to the beginning of the secondary wall deposition (S1 wall) and takes place between 15 and 25 DPA. At this stage, secondary wall deposition is initiated while the cell is still elongating.
- The development stage corresponds to the massive deposition (without elongation) of cellulose forming the main body of the secondary wall (S2 wall) and takes place between 25 and 50 DPA.
- After about 50 days the cotton bolls is mature and it opens. After opening, the cotton fibres dry out. This stage is called maturation.

The focus of this paper is to study the swelling and dissolution mechanisms of cotton fibres in order to clearly identify and separate the behaviour of the primary and the secondary walls in different solvents. To this end, cotton fibres were collected at successive growth stages, from 7 DPA to maturity and their dissolution mechanisms were studied in very good, good and moderately good solvents.

Materials and methods

Cotton production. Cotton*, Gossypium hirsutum, plants* were grown in a greenhouse of the Cell Biology laboratory at the INRA research centre in Versailles. Unopened cotton bolls were collected on plants at various growth stages (counted as DPA or days postanthesis) and immediately sent to Cemef in Sophia Antipolis to be studied.

Solvent preparation. The solvent mixtures were based on NMMO provided by Sigma-Aldrich and various amount of distilled water were added (w/w), i.e. 20% of water corresponds to 0.2 g of water with 0.8 g of NMMO. The monohydrated form of NMMO-water mixtures contains 13.3% water. As was shown by Chanzy *et al.* [9] and Cuissinat and Navard [10], the quality of the NMMO-water solvent decreases with the increase of water content (for 13.3% of water very good solvent, for 16% of water good solvent and for 20% of water moderately good solvent). All the swelling and dissolution experiments were carried out at 368 K to avoid the crystallisation of the NMMO-water system.

Fibre extraction and observation. Cotton fibres were carefully extracted from their bolls (see figures 2 and 3) at various growth stages, isolated from the seeds and slightly dried with a blotting paper. The swelling and dissolution treatments were immediately performed in NMMO with 13.3, 16 and 20% of distilled water, w/w (noted NMMO- 13.3, 16 or 20% water).

Figure 2. Cotton bolls at elongation stage (1) 7 DPA, (2) 11 DPA, (3) 14 DPA.

Figure 3. Cotton bolls at transition stage. (1) 20 DPA, (2) 23 DPA ; development stage, (3) 26 DPA, (4) 29 DPA, (5) 30 DPA, (6) just before opening and (7) mature fibres.

Samples were observed between two glass plates by optical microscopy in transmission mode with a Metallux 3 (Leitz) equipped with a Linkam TMS 91 hot stage at 368 K. The solvent contained in a pipette was injected by capillarity between the two glass plates.

Results and discussion

A. Elongation stage fibres

Cotton fibres taken at elongation stage were studied under the optical microscope. To facilitate the isolation of the fibres, which are wet and adhering one to another and only about 100 µm long, they were dried on a blotting paper and separated in small clusters. The dissolution of these fibres turned out to be impossible in both good and moderately good solvents. In NMMO- 16 and 20% water, the reaction is very slow and leads to a uniform gel like material with no measurable swelling. The elongation stage fibres dissolve only in the very good solvent NMMO monohydrate (13.3% of water). The reaction leads to a uniform gel like material. A subsequent regeneration in water shows that this material was partially dissolved.

These results show that the primary wall of cotton fibres is very resistant to dissolution in solvents that, as will be seen below, are dissolving the secondary wall. Another important observation is that the ballooning phenomenon is not present with these fibres as shown in Figure 4. This is fully in agreement with the common explanation which attributes the balloons to the swelling of the secondary wall causing the extension and the bursting of the primary wall. Without secondary wall, there are no balloons (note that mature fibres without primary walls are also not showing balloons [3, 6, 13]).

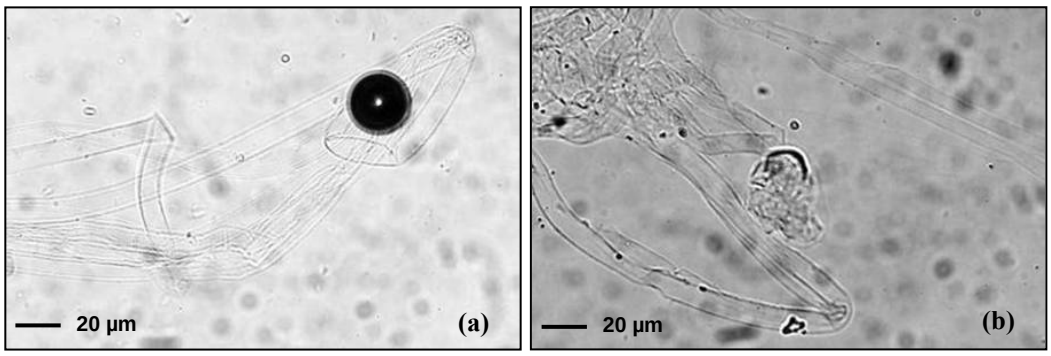

Figure 4. Swelling and dissolution mechanisms of cotton fibres at the elongation stage. (a) in NMMO- 16% water ; (b) in NMMO- 20% water. No ballooning phenomenon is observed.

B. Transition stage fibres

At this stage a small number of balloons can be observed as shown in Figure 5a. These balloons are much smaller (swelling around 100-200 %) than those observed for mature

cotton fibres (swelling around 350-500 %). Balloons may appear in areas of the fibre with more pronounced secondary thickening as suggested by the increased contrast (Figure 5b).

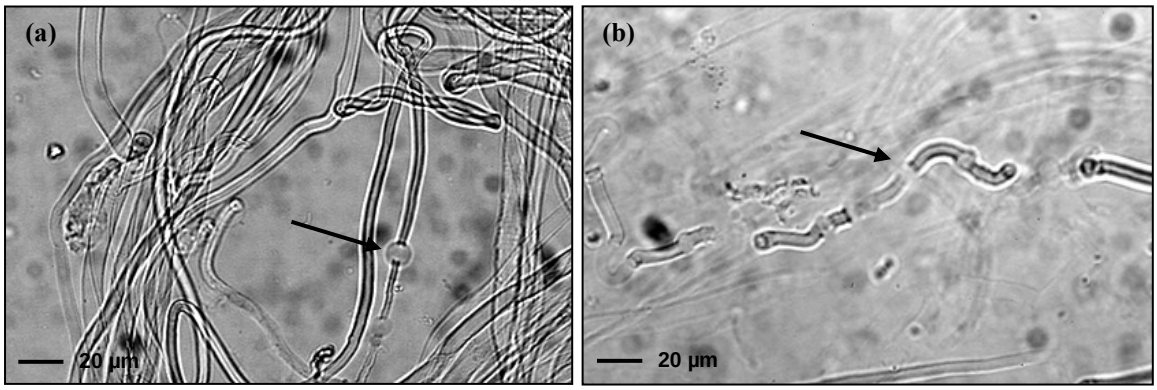

Figure 5. Swelling and dissolution of cotton fibres at transition stage in NMMO- 16 and 20% water ; (a) First balloons appear at the transition stage, (b) outer layer around the inside part that is undergoing ballooning (black arrows).

This result shows that the balloons are indeed linked to the existence of a secondary wall layer under the primary wall. During the transition stage, the rate of cellulose deposition increases up to 100-fold [15] compared to the elongation stage. It is presumably the swelling of this cellulose located in the S1 wall that causes the extension and the bursting of the primary wall, leading to the ballooning aspect. In the good and moderately good solvent (NMMO- 16 and 20 %), the S1 wall cellulose was not dissolving efficiently.

In conclusion, the good and moderately good solvents did not dissolve the primary wall and poorly dissolved S1 wall cellulose.

C. Development and mature stage fibres

- *NMMO-16 % water*

In this good solvent, the fibres dissolved starting from the inside by fragmentation (Figure 6a). Interestingly, the remaining fragments were solid (most probably very crystalline) rod-like pieces, elongated in the fibre direction (Figure 7). This shows that the weak areas, most probably corresponding to less crystalline parts, were also oriented in the fibre direction. It should be interesting to investigate how this heterogeneity in crystallinity arises during the deposition of the cell wall.

The rod-like fragments formed inside the fibre at the beginning of the dissolution process

penetrated the undissolved outer layer of the fibre (Figure 6a). The dissolution process occured without ballooning (mode 1) and the fragments eventually dissolved totally. The outer layer dissolved more slowly. It should be noticed that this outer layer was not always visible.

- *NMMO-20 % water*

In this moderately good solvent, the ballooning phenomenon also occurred. However, balloons were much larger (swelling around 350-500 %) than those observed during the transition stage (swelling around 100-200 %). The ballooning phenomenon is thus directly linked to the existence of the secondary wall. Balloons, formed by the extending secondary S1 wall, break through the outer layer (Figure 6b). The outer layer rolls up and forms helices and unswollen sections as shown in Figure 1.

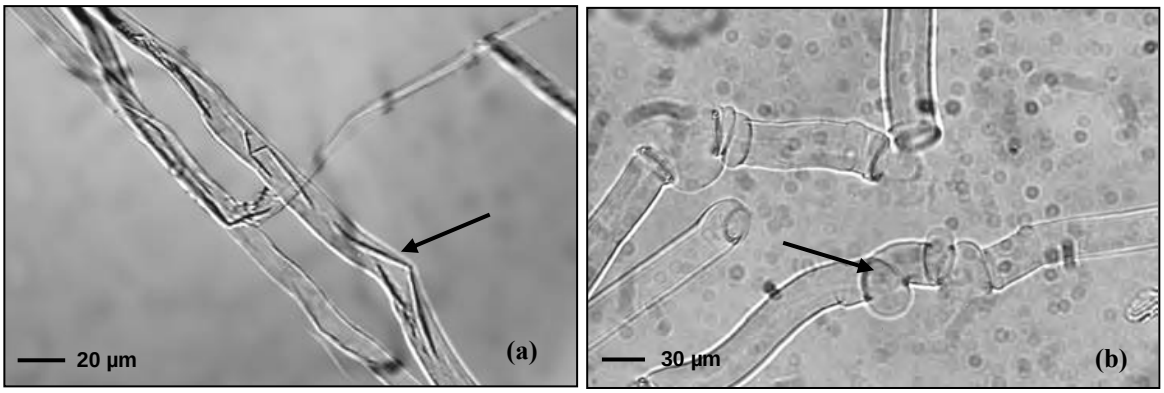

Figure 6. Swelling and dissolution of cotton fibres at development stage ; (a) Dissolution by fragmentation in NMMO- 16 % water ; (b) Swelling by ballooning in NMMO- 20% water (black arrows).

With the appearance of the S2 wall, an important phenomenon is observed. The inside of the balloons dissolves by fragmentation. A fraction of the cellulose chains inside of the balloons is dissolving and balloons are growing due to the intake of solvent (osmotic pressure). Eventually (Figure 7a and b), all visible fragments are fully dissolved. The inside of the balloons is thus a cellulose solution. The fragmentation is the result of the dissolution of the inner part of the fibre. This event is similar to the fragmentation that is occurring in good and very good solvents as NMMO- 16 % water.

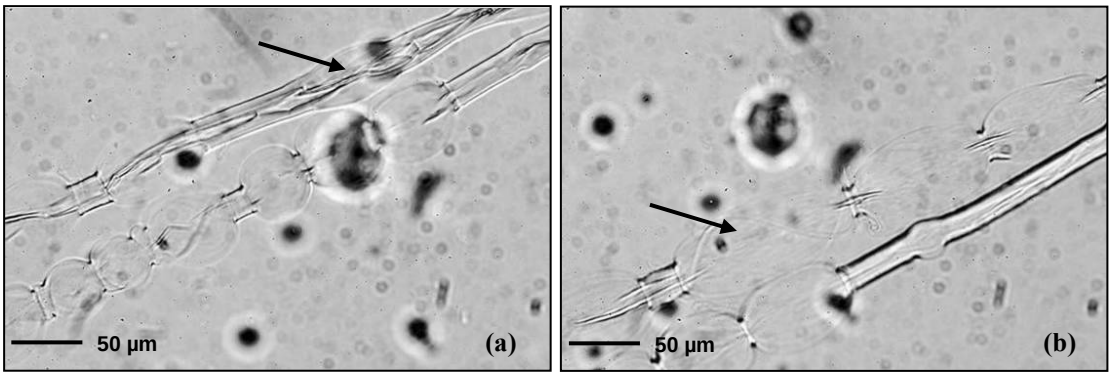

Figure 7. Mature cotton fibre in NMMO-20 % water. Fragments inside the balloons are dissolving and balloons are growing (black arrows). Time is progressing from picture (a) till picture (b).

At this stage of the dissolution, the fibre was composed of two main zones, balloons (highly expanded zones that broke through the primary wall) and unswollen sections. In the balloon, two zones could be distinguished, the inside corresponding to the dissolved cellulose (obtained by the fragmentation mechanism) and the surface of the balloon, composed of a part of the secondary wall that is not dissolved. We showed by using fibres in their transition stage that the dissolution of the S1 wall is very slow, going through a swollen gel phase before dissolving. The balloons in the mature fibres therefore must correspond to the dissolved S2 wall inside the swollen S1 wall. This swollen S1 wall is what we previously referred to as "the membrane" [10-15]. This part is a swollen gel that will dissolve slowly. After the total dissolution of the balloons, the unswollen sections and remainings of the primary wall (Figure 8) will also dissolve. The sequence of dissolution is thus the following: first the inside of the fibre (S2 wall) by fragmentation, then the S1 wall, then the unswollen sections and remainings of the primary wall.

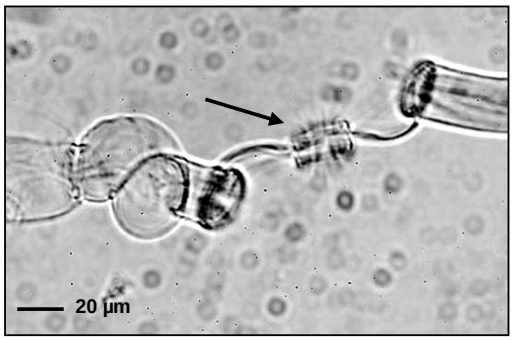

Figure 8. Swelling and dissolution of a cotton fibre in NMMO- 20 % water. The S2 wall dissolves first, followed by the membrane of the balloons (S1). The thick helices (remains of the primary wall) and the unswollen sections (black arrow) dissolve later.

Conclusions

These dissolution experiments on cotton fibres at different growth stages show that there is a gradient of dissolution capacity from the inside to the outside of the fibre.

1- For fibres with enough cellulose inside the secondary wall, the inside of the fibre is the easiest part to dissolve. The dissolution mechanism is fragmentation where weak parts of the wall are quickly dissolved, leaving rod-like fragments floating, which completely dissolve later. The fact that the dissolution kinetics of crystalline parts is slower than that of the amorphous parts backs the hypothesis that the rod-like fragments are highly crystalline. The finding that these fragments are oriented along the fibre direction while the deposition of the cellulose chains occurs at 35-45° might provide meaningful information on the mechanism of cellulose synthesis and deposition in cotton fibres. The availability of tools for the *in vivo* visualisation of cellulose synthase complexes and the cytoskeleton [17] should facilitate the elucidation of this question.

2- Ballooning appears in fibres having a secondary wall, at least being at the transition stage. Balloons are formed by the expansion of the secondary wall due to the dissolution. It must be surrounded by a membrane (otherwise there would be no balloon). The membrane is clearly formed by the swollen S1 layer of the secondary wall, formed during the transition stage, which is more difficult to dissolve than the S2 layer. Why this layer is more difficult to dissolve is not known, but it must be related to differences in composition and/or architecture.

3- When the secondary wall is swelling by ballooning, the primary wall breaks in localized places and rolls up to form helices and surround fibre sections that cannot be swollen (called unswollen sections [10-15]). The primary wall does not dissolve easily, and even sometimes does not dissolve at all as it is occurring in bad solvents like NaOH-water, where only the inside of the fibre can dissolve.[11]

The mechanisms of swelling and dissolution are schematically represented on Figure 9 in function of the solvent quality.

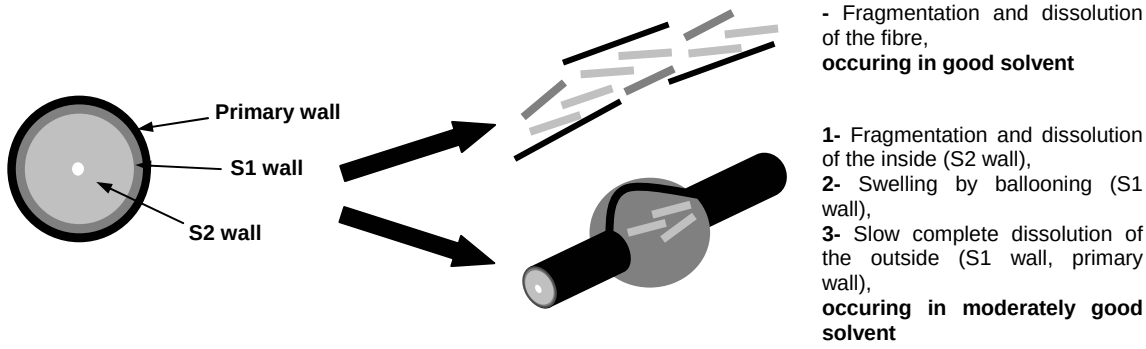

Figure 9. Schematic representation of the S2, S1 and primary wall behaviour in good (e.g. NMMO- 16% water) and moderately good solvent (e.g. NMMO- 20% water).

The study of well characterized cotton fibres in terms of growth stage have shown that most recent deposited cell wall layers (S2 wall) are most easily dissolved. Since the degree of polymerization and the crystallinity increase during the fibre development [16,18], the dissolution capacity depends, in a first instance, not on thermodynamic (molar mass) or kinetic (crystalline or amorphous) parameters, but on the composition and the architecture of the fibre walls. The absence of noncellulosic polysaccharide networks in younger wall layers may explain their higher dissolution capacity. Considering that the same mechanisms have been observed for wood-based fibres, the same conclusion about the influence of the composition of the cell wall layers on the dissolution should also hold for these fibres.

References

(1) Nägeli, C. *Sitzber Bay. Akad. Wiss. Munchen* **1864**, 1, 282, 2, 114.

(2) Pennetier, G. *Bull. Soc. Ind. Rouen* **1883**, 11, 235.

(3) Flemming, N.; Thaysen, A. C. *Biochem. J.* **1919**, 14, 1, 25.

(4) Marsh, J. T. In *The growth and structure of cotton, Mercerising*, Chapman & Hall Ltd, London, 1941

(5) Hock, C. W. *Text. Res. J.* **1950**, 20, 3, 141.

(6) Tripp, V. W.; Rollins, M. L. *Anal. Chem.* **1952**, 24, 11, 1721.

(7) Rollins, M. L.; Tripp, V. W. *Text. Res. J.* **1954**, 24, 345.

(8) Ott, E.; Spurlin, H. M.; Grafflin, M. W. In ,*Cellulose and cellulose derivatives (Part 1)*, Interscience Publisher, New York, 1954.

(9) Chanzy, H.; Noe, P.; Paillet, M.; Smith, P. *J. Appl. Polym. Sci.* **1983**, 37, 239.

(10) Cuissinat, C.; Navard, P. *Macromol. Symp.* **2006**, 244, 1, 1.

(11) Cuissinat, C.; Navard, P. *Macromol. Symp.* **2006**, 244, 1, 19.

(12) C. Cuissinat, T. Heinze, P. Navard, *Carbohydr. Polymer* **2008**, 72, 590.

(13) Cuissinat, C. Thèse Science et Génie des Matériaux de l'Ecole des Mines de Paris, 2006.

(14) Cuissinat, C.; Navard, P. *Cellulose*, **2008**, 15, 67.

(15) Cuissinat, C.; Heinze, T.; Navard, P. *Cellulose*, **2008,** 15, 75.

(16) Basra, A. S. In *Cotton Fibers : Developmental Biology, Quality Improvement and Textile Processing*, Food Products Press, Haworth Press, Inc., New york, 1999.

(17) Paredez, A. R.; Somerville, C. R.; Ehrhardt, D. W. *Science* **2006**, 312, 1491.

(18) Marx-Figini, M. *Nature* **1966**, 210, 754.

Chapter III

Restricted dissolution capacity of native and regenerated cellulose fibres under uniaxial elongational stress.

Restricted dissolution capacity of native and regenerated cellulose fibres under uniaxial elongational stress

Abstract Cellulose is a major future source of materials and biofuel but its extraction, chemical or enzymatic treatments are difficult, polluting and inefficient tasks due to a lack of cellulose chain accessibility supposedly due to pore structure, tight hydrogen bond arrays, presence of resistant materials like lignin or crystallinity. We are investigating if conformational movements are also contributing to reactivity, in addition to cellulose chain accessibility. We found that dissolution is mainly controlled by the possibility for cellulose chains to perform conformational movements that are requiring chain ends to be free. Studying cellulose fibres under uniaxial tension, we show that accessibility of cellulose to reagents is not the only requirement for reactivity. Tension is preventing cellulose to dissolve in chemicals that would dissolve the same cellulose fibre tension-free. This is not due to the native cell wall structure since regenerated cellulose fibres behave in the same way. The lack of dissolution capability of native cellulose under tension is due to the hampering of local conformational movements due to the impossibility for the chain to perform axial movements. The availability of performing local conformational movements is a main component of cellulose activation. This finding opens the way to design better treatments, solvents or reagents.

Introduction

These last fifteen years, huge progress have been made in the understanding of the mechanisms leading to the production of cellulose inside a vascular plant cell nucleus and in the way cellulose chains are assembled by the cellulose synthase complex (CSC) through the plasma membrane.[1,2] However, not much is known about how the chains produced by one CSC are cooperatively arranging themselves to crystallise as microfibrils. One of the ways to answer these questions is to understand the physical and chemical requirements needed to dismantle the wall structure, a process of huge economical and technological importance. It is well known that cellulose in cell walls is not “very accessible”,[3] an empirical statement reflecting the difficulty to extract or treat cellulose. To overcome this accessibility problem, cell walls are usually swollen in various chemicals and/or under different thermodynamic conditions (like steam explosion) before cellulose can be extracted or treated. Classical

evoked reasons for non-accessibility or difficulties to be treated are like limited pore accessibility, high chain length, high crystallinity, presence of hydrogen bonds or influence of other molecules like hemicelluloses or lignin.[4] It has been suggested that these reasons are not giving the full story and that other "long range" interactions should be hypothesised, without being able to identify the nature of these interactions.[5]

During the course of a study on cellulose dissolution, we found incidentally that imposing a small uniaxial tension on cellulose fibres can have a dramatic effect, preventing dissolution in chemicals that are otherwise solvating the same tension-free cellulose. This astonishing finding can be a tool to understand how cellulose chains are arranged in the cell wall and on the mechanisms hidden under the "accessibility" requirement always advocated for treating and transforming cellulose.

Native cotton hairs and regenerated Lyocell cellulose fibres were swollen and dissolved with and without tension in N-methylmorpholine N-oxide (NMMO)-water solutions. Cotton hairs have a very complex native wall structure with varying molecular orientation angle (from 20 to 45° to the fibre axis) depending of the considered layer.[3,6] Regenerated Lyocell fibres have a much simpler, well oriented morphology.[7] NMMO-water mixtures are solvents or swelling agents depending of water content (at 90°C, the mixture is a solvent when the water content is above 13% and below about 25%, depending on the physical characteristics and provenance of the cellulose used. The behaviour of cotton hairs in NMMO-water mixtures has been reported to depend on water concentration: fast dissolution by fragmentation under 17% water, large swelling by ballooning, then dissolution between 19 to 23.5 % water, large swelling by ballooning, but no complete dissolution between 25 to 30 % water, homogeneous swelling and no dissolution between 35 to 40 % water, and very low swelling above 40 % water.[8]

In order to slow down dissolution and to avoid a fast disintegration of the fibres, we will use in this study the intermediate case where the water concentration in the NMMO-water solvent is such as being able to dissolve regenerated fibres after a large swelling and cellulose cotton hairs after the production of balloons. The set-up used to place fibres under axial tension has two side effects. It is preventing the fibre to rotate when swelling and it is not allowing chemicals to penetrate into the lumen by the end of the fibre.

Experimental Part

Materials and solvents. One cotton fibre, *Gossypium barbadense*, provided by INRA (France) and one Lyocell regenerated fibre, Tencel®, provided by Lenzing AG (Austria) were used. The mean diameters of cotton and regenerated fibres were 15 µm and 11 µm respectively. The swelling and dissolution treatments were performed in mixtures of *N*-methylmorpholine *N*-oxide (NMMO) and water at 90°C. The water content was varied from 20 to 23% w/w (between 20 and 23 % of water, the NMMO - water mixture is a moderately good solvent for cellulose[8,9]).

Experimental Protocol. The experiments were performed by mixing the cotton and regenerated fibres and the solvent in a container made of two glass plates separated with double-sided tape. The solvent, previously heated at 90°C and contained in a pipette, was introduced by capillary forces between the two plates (Figure 1a). No agitation was applied to the mixture. To understand the influence of the fibre tension and the accessibility to the lumen on the swelling and dissolution, four configurations of experiments were tested (Figure 1b). Since the dimension of the fibres and the experimental assembly does not allow measuring the initial tension applied to the fibres, the four configurations were defined as follows: (i) the fibre was fixed without tension, (ii) the fibre was fixed under low tension, very loosely so that the contraction upon swelling leads to a low tension of the fibre, (iii) for higher tension experiments, the fibres were put under tension between the two points of silicone grease, (iv) an access to the lumen was tested with fibres free at one end.

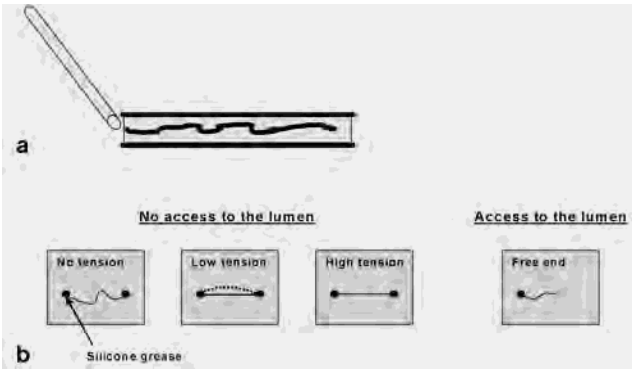

Figure 1. Experimental protocol and assembly. (a), The solvent is injected by capillarity between the two glass plates. (b), Four configurations of experiments: no tension, under low tension (the fibre loosely attached reaches a low tension state due to the contraction during swelling) and under high tension with no access to the lumen ; and free end with an access to the lumen.

Observations method. The swelling and dissolution of cotton and regenerated fibres were observed by optical microscopy with a Metallux 3 (Leitz) equipped with a Linkam TMS 91 hot stage. The samples were investigated in transmission mode, at 90°C. To obtain high resolution pictures, the microscope was equipped with a high resolution numerical reflex camera (3000*2000 pixels) CANON D100 (Figure 2) and a high resolution 3-CCD camera (1360*1024 pixels) JVC KY-F75U (Figure 3). An enhancement of the contrast and the exposure was performed with the Photoshop® software to obtain a better visualization of the fibres.

Results and discussion

Swelling and dissolution without axial tension.

NMMO-water mixtures with water concentrations between 20 to 23 % are slowly dissolving cotton hairs through a ballooning mechanism. During swelling, cotton hairs undergo a large rotation and an axial contraction increasing with swelling (diameter of the swollen hair over the initial mean diameter). The breaking of the primary wall involved by the swelling and the dissolution of the inside of the fibre lead to successive highly swollen regions (the location of balloons) in between regions of the hair which are keeping about the original hair diameter (unswollen regions). Balloons are formed by a membrane, surrounded by helices from the primary wall, and composed of older deposited secondary wall layers (S1 layer) enclosing dissolved cellulose from S2 layer. The sequence of dissolution is the following: first the inside of the fibre (S2 layer) by fragmentation, then the S1 wall, then the unswollen regions and remaining of the primary wall.[9] For the cotton hairs used, balloons reach a maximum swelling of 430% in NMMO-water 20 to 23 % (Figure 2a). Regenerated fibres swells and then dissolves in NMMO-water mixtures with water concentration at 20% (Figure 3a). They are also contracting upon swelling, but they are not rotating. The maximum swelling can reach 850% and the swollen fibre aspect is very translucent. The fact that the regenerated fibres show higher swelling as compared to cotton hairs is explained by the longitudinal orientation of their cellulose chains which do not impede the radial swelling.

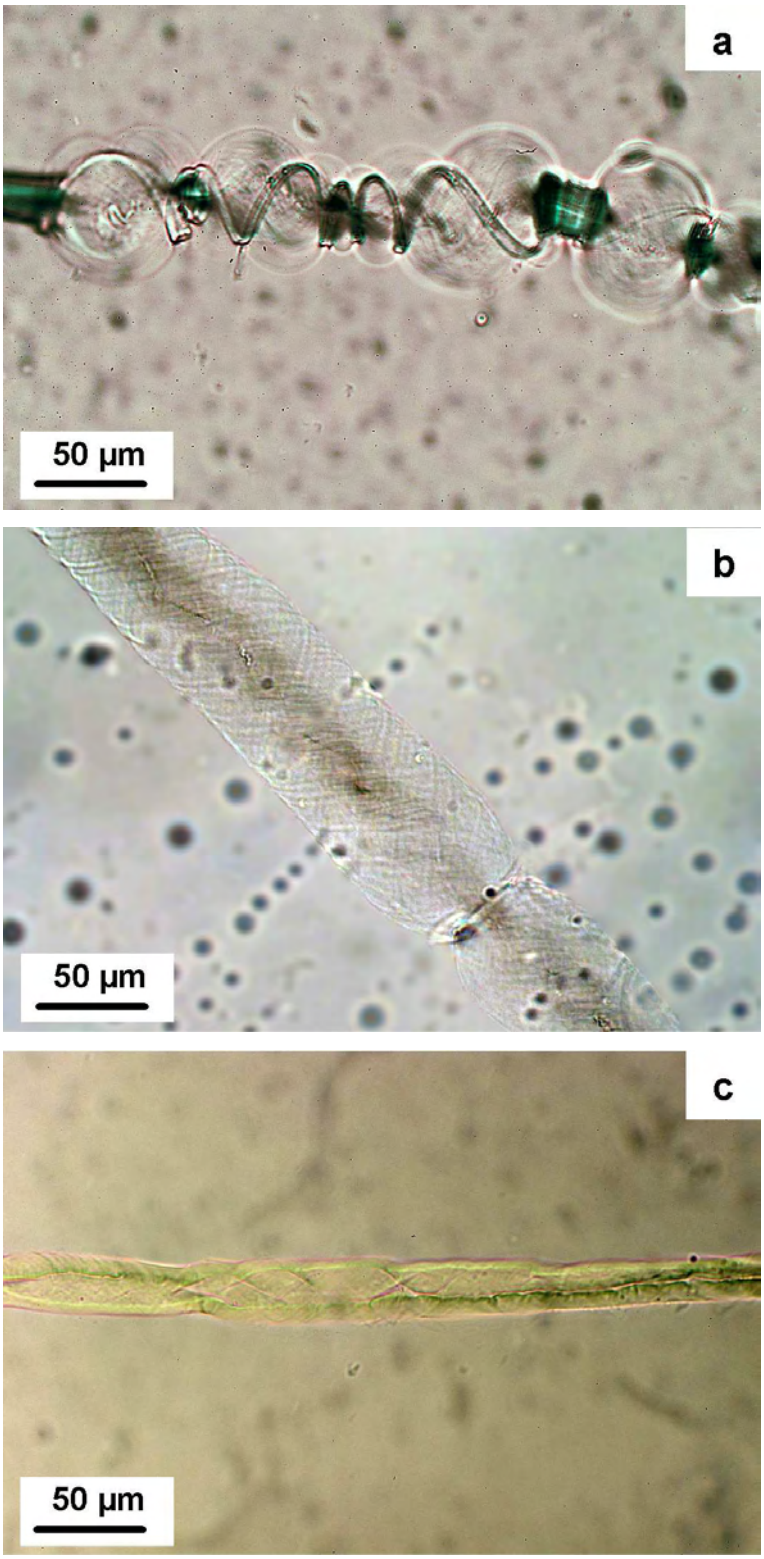

Figure 2. Swollen cotton hairs under varied conditions of tension. (a), Swelling by ballooning (430%) right before the dissolution, no tension was applied to the fibre. (b), Large homogeneous swelling (370%) and no dissolution, the fibre is under low tension. (c), Low homogeneous swelling (100%) and no dissolution, a higher tension was applied to the fibre.

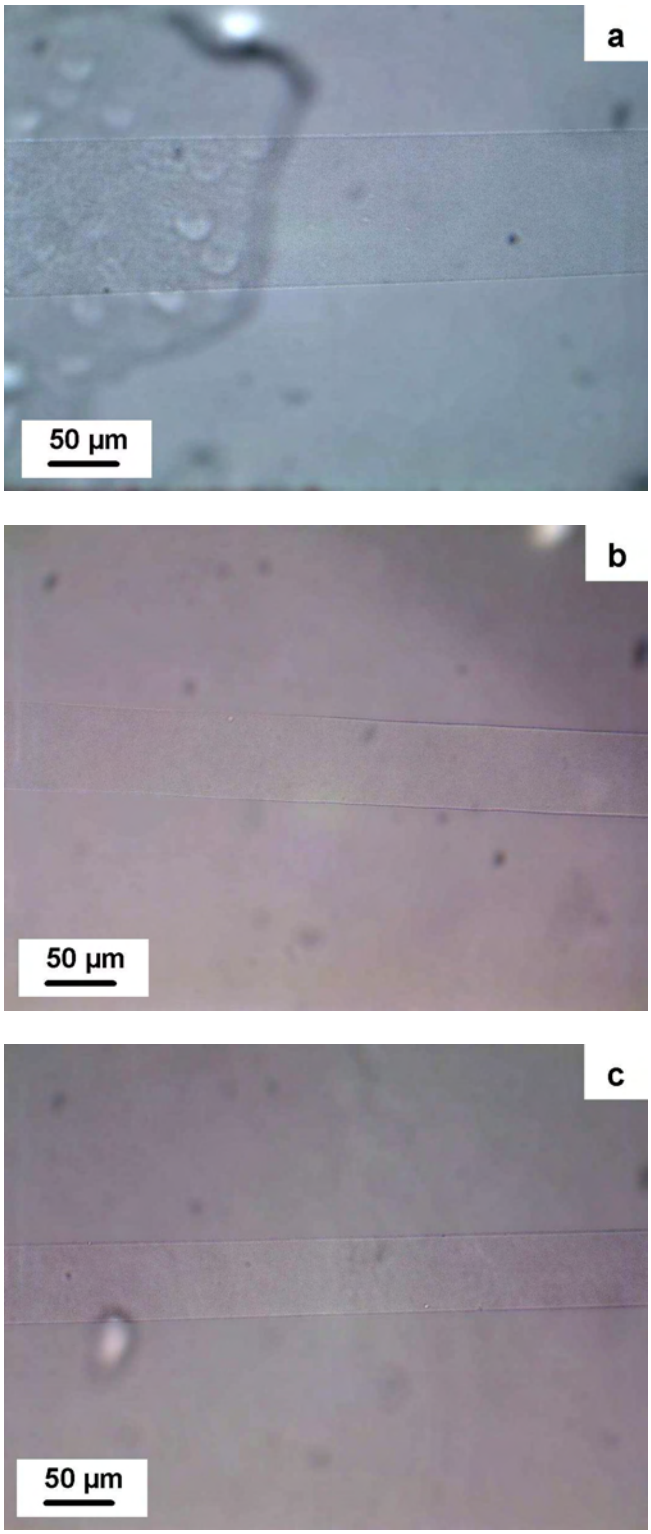

Figure 3. Swollen regenerated fibre under varied conditions of tension. (a) Very large homogeneous swelling (850%) right before the dissolution, no tension was applied to the fibre. (b), Lower homogeneous swelling (420%), the fibre is under low tension. (c), Lower homogeneous swelling (370%), a higher tension was applied to the fibre but the slippage of the fibre at the points of silicone grease leads to a large swelling.

Swelling and dissolution under low axial tension.

When placed in the water concentration range of 20 to 23 %, loosely attached cotton hairs swell homogeneously and contract, this bringing a low tension state with a maximum swelling of about 370% (Figure 2b), similar to the swelling of the balloons observed without tension right before their dissolution. Swelling starts at localized places along the fibre but contrary to the tension-free case where the rolling of the primary wall limits its extension by forming unswollen regions, swelling extends along large dimensions along the hair until all the swelling regions merge. In marked contrast with the case without tension, hairs under low tension have no balloon and they are not dissolving: they are staying homogeneously swollen. In this homogeneous swollen state, the fibre is thus only composed of older deposited secondary wall layers (S1 layer) enclosing dissolved cellulose from S2 layer. In the case of regenerated fibres, for a water concentration of 20 %, fibres swell homogeneously and contract to reach a maximum swelling of about 420 % (Figure 3b). This swelling depends of the initial length of fibre over the length between the two blocking points and can vary from 350 % to 450 %. The main observation is that regenerated fibres, as cotton hairs, stay in this large swollen state and do not dissolve, contrary to the case with no axial tension.

Swelling and dissolution under higher axial tension.

Between 20 and 23 % of water, cotton hairs swell homogeneously and do not dissolve, but their swelling decreases with increasing tension strength (Figure 2c). A very interesting point is that if tension is released suddenly as it occurs when the hairs broke due to a too high tension generated by the contraction, hairs are dissolving immediately. The same phenomena are observed with regenerated fibres. However, the contraction forces are so high that the fibres are often sliding at the points of silicone grease, decreasing thus the tension. The swelling can thus reach high values equivalent to the low tension case (Figure 3c).

Accessibility to the lumen.

Since the set-up leading to placing hairs under axial tension was preventing access of solvents to the lumen, we checked that cotton hairs without tension and without access to the lumen were still showing the same swelling and dissolution mechanisms as free hairs. Lack of lumen access is not the reason for the above-observed phenomena when hairs are placed under tension.

Dissolution of a semi-crystalline polymer in a solvent proceeds classically through the local swelling of the polymer at the polymer-solvent interface followed by its disentanglement and its diffusion into the solvent.[10] There is no need for the whole polymer part to be accessible to the solvent prior to dissolution. Due to the difficulties for dissolving or chemically treating cellulose, it has always been postulated, and taken for granted, that the whole cellulose part must be first brought accessible to the solvent by methods like (i) opening of the pores present in native or regenerated cellulose, (ii) swelling non-crystalline regions, (iii) breakage of the crystalline areas, (iv) weakening the hydrogen-bond array by chemical or physical treatments or (v) decreasing molecular weight by chemical or enzymatic treatments. It is implicitly assumed that the classical mechanisms of polymer dissolution acting from the cellulose object-solvent interface are not applicable to cellulose.

The main result of this work is the absence of dissolution when a cotton hair or a regenerated fibre, immersed into a moderate quality solvent, are put under tension and prevented to contract. The swelling reached under low tension is of similar magnitude as the swelling of balloons seen during the dissolution of hairs without tension. Similar swellings are also observed with and without tension for regenerated fibres. This shows that the opening of pores or the need for the cellulose chains to be close to the solvent are not the major reasons why cellulose is not dissolving in a solvent. The fact that a swollen cotton hair or a regenerated fibre under tension is immediately dissolving when the hair is breaking shows that the solvent was present around chains prior to hair breakage and was able to disrupt then the whole structure, solvating chains or chain aggregates. The accessibility is thus not the full story for explaining cellulose dissolution and treatments. This finding is also supported by a recent work showing that an inhibition of acetylation occurs when a regenerated cellulose fibre is placed under tension during chemical reaction, despite that the swelling reached under tension is high enough (around 800 %) to perform acetylation (work in preparation Spinu, M.; Heinze, T.; Navard, P.; 2008).

The fact that both cotton hairs and well oriented regenerated fibres are showing dissolution and reactivity inhibitions under tension indicates that the detailed structural morphology of the cellulose fibre is not involved. The common point is the fact that cellulose chains are oriented and interlinked into strong intermolecular hydrogen bond arrays.[11] Dissolution or chemical reaction impose that the reacting or solvating molecule approaches the cellulose chain and couples to it, inducing local conformational movements that depends on the reagent involves and to which site of the anhydroglucose unit it binds with.

With few exceptions like crankshaft motions, local movements impose the chain to rearrange its conformation along its axis. The lack of reactivity under tension, despite having reagent accessibility, shows that the local conformation necessary for solvatation are prevented. This can be understood if we consider that cellulose chains in cotton hairs and regenerated fibres are in straight, parallel conformation even in the non-crystalline regions[12] and that an hydrogen bond array is linking all chains together in the entire sample or at least in the S1 layer (case of cotton hairs at low tension), even with the large swelling involved. The fact that the solvent is not extremely good implies that not all the intra and inter molecular hydrogen bonds are broken, inhibiting thus local molecular movements needed for the disentanglement of the chains when the length of the hair or the fibre is fixed by tension. Without being able to disentangle, chains are not dissolving in the solvent. This phenomenon of non-dissolution under tension can only occur because chains are all in a straight conformation. It shows that there is no region with disordered amorphous organisations but that the "amorphous" zones are well aligned. It is known that it is the case for Lyocell regenerated fibres.[13] Our results show that it is also the case for cotton hair. The CSC thus produces chains that all keep a parallel straight conformation up to coagulating on the cell wall because of their stiffness, their high hydrogen bonding capacity[3,4] and also topological constraints due to the proximity of the many chains exiting from the CSC orifices.[14-17]

Conclusions

To be able to dissolve or to be chemically or enzymatically treated, cellulose chains must be allowed to perform local conformational movements requiring long range chain mobility, not possible when the chain is blocked within its hydrogen bond array. It is not enough for the chains to be close to the reagent or to be not crystalline. This result is suggesting that activation must concentrate on finding better ways to break the hydrogen bond array and prevent its reformation. This is a critical step in the field of cellulose solubility and degradation, necessary to develop biofuel directly from ligno-cellulosic substrates, prepare new cellulose-based materials able to substitute oil-based polymers and be a source of bio-mass based synthons.

References

(1) Paredez, A. R.; Somerville, C. R.; Ehrhardt, D. W. *Science* **2006**, 312, 1491–1495.

(2) Emons, A. M. C.; Höfte, H.; Mulder, B. M. *Trends Plant Sci.* **2007**, 12, 279–281.

(3) Krässig, H. A., In *Cellulose - Structure, Accessibility and Reactivity,* Polymer Monographs; ed. M.B. Huglin; Gordon and Breach Science Publishers, Amsterdam, 1993; Vol. 11, p 166.

(4) Klemm, D.; Philipp, B.; Heinze, T.; Heinze, U.; Wagenknecht, W. In *Comprehensive Cellulose Chemistry*; Wiley-VCH, Weinheim, 1998; Vol. 1, p 29.

(5) Isogai, A.; Atalla, R. H. *Cellulose* **1998**, 5, 309–319.

(6) Warwicker, J. O.; Jeffries R.; Colbran R. L.; Robinson R. N. In *A Review of the Literature on the Effect of Caustic Soda and Other Swelling Agents on the Fine Structure of Cotton,* Shirley Institute Pamphlet; St Ann's Press, England, 1966; Vol. 93, p 17.

(7) Abu Rous, M.; Ingolic, E.; Schuster, KC. *Cellulose* **2006**, 4, 411–419.

(8) Cuissinat, C.; Navard, P. *Macromol. Symp.* **2006**, 244, 1–18.

(9) Le Moigne, N.; Montes, E.; Pannetier, C.; Höfte, H.; Navard, P. *Macromol. Symp.* **2008**, 262, 65–71.

(10) Miller-chou, B. A.; Koenig, J. L. *Prog. Polym. Sci.* **2003**, 28, 1223–1270.

(11) Fengel, D.; Wegener, G. In *Wood: Chemistry, Ultrastructure, Reactions*, Walter de Gruyter; Berlin and New York, 1984.

(12) O'Sullivan, A. C. *Cellulose* **1997**, 4, 173–207.

(13) Stana-Kleinschek, K.; Kreze, T.; Ribitsch, V.; Strnad, S. *Colloids Surf., A* **2001**, 195, 275–284.

(14) Mueller, S. C.; R. M. Brown Jr. *J. Cell Biol.* **1980**, 84, 315–326.

(15) Emons, A. M. C. *Planta* **1985**, 163, 350–359.

(16) Bowling, A.; R. M. Brown Jr. *A new view of cellulose synthase*. http://www.botany.utexas.edu/lab/research_basic/bowling/default.htm, **2005**.

(17) Diotallevi, F.; Mulder, B. *Biophys. J.* **2007**, 92, 2666–2673.

Chapter IV

Dissolution mechanisms of wood cellulose fibres in NaOH-water.

Dissolution mechanisms of wood cellulose fibres in NaOH-water

Abstract Four wood pulps and a microcrystalline cellulose were dissolved in a NaOH 8% - water solution. The insoluble and soluble fractions were isolated by centrifugation and were observed by optical microscopy and Transmission Electron Microscopy. Molecular weight distribution, carbohydrate composition and cellulose II content were measured. The dissolution of wood cellulose fibres in NaOH 8%- water solutions occurs by successive dismantlement and fragmentation steps governed by the swelling and the shearing of the original structure. The insoluble and soluble fractions are both converted in cellulose II and the insoluble fractions contain more mannan than the soluble fractions. Besides, the molecular weight distributions of insoluble and soluble fractions reveal the existence of heterogeneities in dissolution capacity of the cellulose chains, independent to the degree of polymerization, which are related to the localization and the chemical environment of the chains within the fibre structure.

Introduction

The dissolution of cellulose is of great interest and it has been studied in numerous solvents for over a century. However, some of the mechanisms involved in the dissolution at the different structural levels of cellulose fibre are still not well understood and controlled. First evidences of the complex swelling and dissolution of cellulose fibres such as the ballooning phenomenon were observed and discussed long ago by Nägeli in 1864 [1] and were followed by several studies during the last century, e.g. Pennetier in 1883, [2] Fleming and Thaysen in 1919, [3] Marsh *et al*. in 1941, [4] Hock in 1950,[5] Tripp and Rollins in 1952 [6, 7] or Ott.[8] More recent studies of Chanzy *et al.* in 1983 [9] and Cuissinat and Navard in 2006 [10] have shown that the dissolution mechanisms of cellulose fibre are strongly dependent on the solvent quality. The last authors identified four main dissolution modes for wood and cotton fibres as a function of the quality of the solvent by using *N*-methylmorpholine-*N*-oxide (NMMO) with various amounts of water. The same mechanisms were also observed when using solvents as NaOH-water with or without additives,[11] ionic liquids [12] and other chemicals [13] for a wide range of plant fibres [14] and some cellulose derivatives that were prepared without dissolution.[15] From all these studies, it was shown that the key parameter in the dissolution mechanism is the morphology of the fibre: as long as the original wall structure of the native fibre is preserved,

the dissolution mechanisms are mostly similar for wood, cotton, other plant fibres and some cellulose derivatives. In a recent paper, [16] we demonstrated the existence of a centripetal radial gradient in the dissolution capacity within the fibre. The older was the deposition, the more difficult it is to dissolve it. These results can be related to age-dependent structural re-organisations in the cell wall layers and / or to the presence of non-cellulosic polysaccharide networks in outside walls.

All these features originate from the succession of polymer and product depositions and their deformation during the extension and thickening of the plant cell. The existence of the different successively deposited walls with different solubilities does not seem to be the only relevant parameters. Dissolution or chemical treatments of cotton and wood pulp are not easy. As far as dissolution is concerned, a lot of reports suggest that the classical thermodynamic parameters, i.e concentration and molecular weights, are not of primary importance (they are of course playing their usual thermodynamic role) and the same applies for the often reported culprit for bad solubility, crystallinity. At least at rather low molar mass and in situations where the structure is not hampering dissolution, crystalline and amorphous parts are dissolving in about the same way. As was suggesting by Isogaï and Atalla, [17] the origin of the difficulty of dissolving cellulose fibres should be searched in an unknown long range ordering or interaction that must be disrupted before being able to fully dissolve high molar mass pulp. This conclusion came after remarking that pulps that were not dissolving in a bad solvent (NaOH-water) were soluble after full dissolution in another solvent and regeneration. The hypothesis of a long range organisation to be removed to facilitate dissolution is in agreement with other works where it was showed that placing a cotton fibre or a regenerated fibre under tension is either preventing dissolution (see chapter III) or decreasing the efficiency of a chemical derivatization (work in preparation Spinu, M.; Heinze, T.; Navard, P.; 2008). In both cases, the solvent or the reaction agents are able to fully access the cellulose chains under tension, thus eliminating the classical “accessibility of the chain” reason for this lack of reactivity. The hypothesis brought by the authors is that, to dissolve, chains must perform conformational movements that are not allowed if the full polymer chain is blocked into a long range H-bond network that is fixed.

Activation is the usual term for describing treatments that increase cellulose reactivity. Aside obvious physical changes that are indeed helping reactivity, some activation treatments may include the destruction of these “long range interactions” that must be removed to have reactive cellulose fibres.

Another possibility for explaining the difficulty to dissolve cotton and wood pulp is that the insoluble areas would be composed of non-cellulosic chains and products. This is not a general rule since insoluble parts may contain a larger fraction of cellulose (measured by the glucose content) than the original product.[17]

Aside from the facts that some parts of pulp fibres are not dissolving well, it is interesting to look in a closer way at the areas in the fibre that may have different dissolving abilities. As already said, it was shown for example that in the case of cotton fibres, the younger cellulose chains are easier to dissolve.

In the present work, we dissolved five different cellulose samples in a bad solvent (NaOH-8%water), then separated, analysed and compared insoluble and soluble fractions. The resulting fractions were observed by optical microscopy and TEM. Molecular weight distribution, carbohydrate composition and cellulose II content were measured. The aim of this study was to better understand the dissolution mechanisms of wood fibres in NaOH-water systems and to better identified and characterized the regions in the fibres that have different dissolution capacities.

Experimental part

Sample and solution preparation. Five samples were studied: two dissolving wood pulps prepared by steam explosion and provided by Borregaard (Norway), a microcrystalline cellulose (MCC) provided by Sigma-Aldrich, a bleached sulphite pulp provided by Borregaard and a PH Kraft pulp provided by the vTI-Institute of Wood Technology and Wood Biology (Hamburg, Germany). The origin of the cellulose, the type of pre-treatment, the degree of polymerization (DP) given by the providers and the fibre / particle diameter are reported in Table 1.

Samples	*Origin*	*Pre-treatment*	*DP*	*Fibre / particle diameter*
SE DP 403	Spruce (Borregaard)	Sulphite + steam explosion (SE) 15 bars, 100 s	403	15 - 30 µm
SE DP 360	Spruce (Borregaard)	Sulphite + steam explosion (SE) 15 bars, 100 s	360	15 - 30 µm
Avicel PH 101	Wood origin unknown	Hydrolysis (MCC)	170	5 - 100 µm
Bleached Sulphite pulp	Spruce (Borregaard)	Sulphite	400	15 - 30 µm
PH Kraft pulp	Mixed hardwood	Pre-hydrolysed (PH) kraft	2000	15 - 30 µm

Table 1. Properties of the wood-based cellulose samples used for fractionation by centrifugation.

The different samples were dissolved in a NaOH 8% - water solution at the concentration of 1% cellulose by weight. The cellulose solutions were prepared as follows: 330 grams of NaOH 12% - water were stored in a freezer. 5 grams of cellulose sample were dried at 50°C overnight then added to 165 grams of distilled water and stored 1 hour at 4°C. Then, NaOH 12% - water and cellulose - water solutions were mixed together using a rotary overhead mixer during two hours at -6°C and 1000 rpm giving 500 grams of a solution of 1% cellulose in NaOH 8% - water. A supplementary solution of the SE DP 403 pulp was prepared in the same conditions without the mixing at 1000 rpm with only a gentle stirring applied at the beginning of the preparation to ensure a good dispersion of the fibres in the solution. Three solutions were prepared for each sample to check reproducibility of the experiments and measurements. These 1% cellulose solutions were centrifuged without further treatment by following the experimental protocol shown in Figure 1 and described in the next paragraph.

Fractionation by centrifugation. Centrifugation was performed on a HETTICH Universal 320RHK centrifuge equipped with a 1620A rotor and a JULABO cryostat. By increasing the centrifugation velocity, it is possible to isolate different fractions from the solutions (Figure 1). Protocols were adjusted following a preliminary study, not reported here. For the SE DP 403 and SE DP 360 pulp samples, a protocol in three steps was tailored to separate high, medium, low insoluble fractions (fractions 1, 2 and 3 respectively) and soluble fraction (fraction 4). The centrifuge tubes were refrigerated at 4°C before starting centrifugation. Three rotation speeds were successively applied: 2250 rpm (560 g), 4750 rpm (2520 g) and finally 9000 rpm (9050 g). Despite the cryostat was set at 0°C, the temperature inside the rotating sample varied between 8 and 12°C due to centrifugation heating and heat loss between the cryostat and the centrifuge. The centrifugation time for each step was 5 minutes. The low concentration of cellulose (1%), the low temperature (below 15°C) and the short time (5 min) prevent the gelation of the samples during centrifugation.[18]

In the case of Avicel PH 101, bleached sulphite pulp, PH Kraft pulp and non-agitated SE DP 403 samples, only one centrifugation step at maximum speed 9000 rpm (9400 g) was applied and two fractions were obtained, insoluble fraction (fraction 1) and soluble fraction (fraction 2).

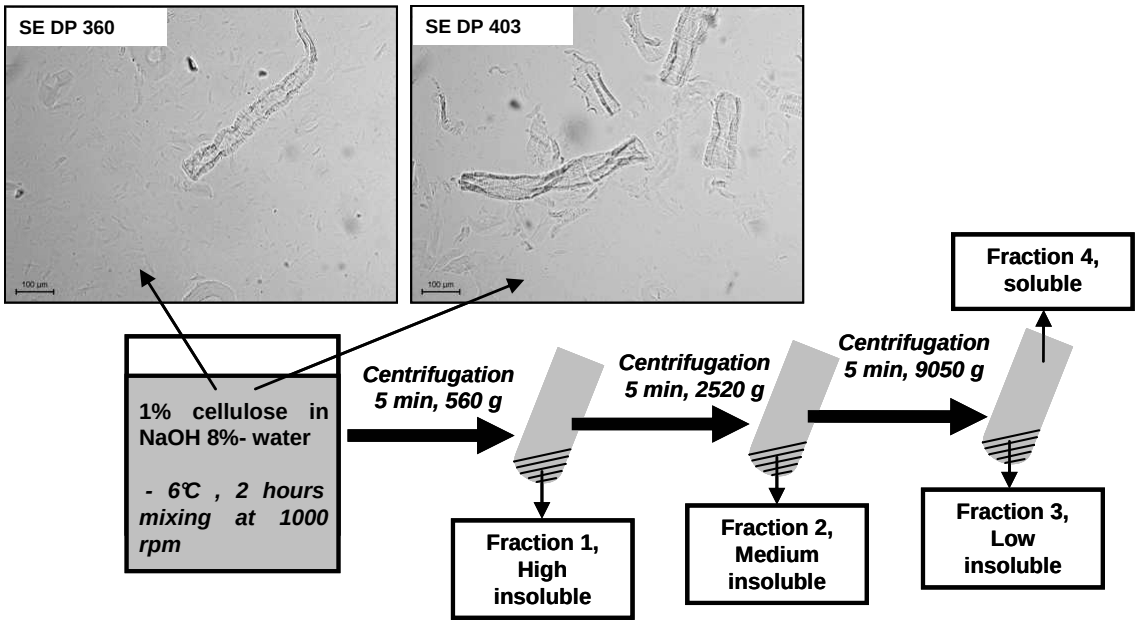

Figure 1. Centrifugation protocol in three steps for the SE DP 360 and SE DP 403 samples to fractionate insoluble fractions (fractions 1, 2, 3) and soluble fraction (fraction 4) in cellulose / NaOH 8% - water solutions.

Optical microscopy and TEM observations. After centrifugation, all fractions were placed between two glass plates and observed by optical microscopy in transmission mode with and without cross-polarizers with a Metallux 3 (Leitz) equipped with a high resolution 3-CCD camera JVC KY-F75U. Fraction 4 (soluble cellulose) was also observed by Transmission Electron Microscopy (TEM) with a CM12 TEM/STEM Philips. A drop of fraction 4 was deposited on a copper grid recovered by a Formvar resin and a carbon film. The grid was deposited on a blotting paper to remove the solvent and then on the TEM sample holder. The accelerating voltage was adjusted at 120 KV and the magnification was 8800 x.

Weighing of the fractions. The different fractions were regenerated in distilled water in several baths until the pH was neutral. The resulting products were dried overnight in an air oven at 50°C. Each fraction was weighed after total drying. The amount of insoluble fractions was defined as the weight ratio (dried insoluble fraction) / (dried sample introduced).

Molecular weight distribution, carbohydrate composition and cellulose II content. The molecular weight distribution of each dried fraction was investigated by underivatized size exclusion chromatography (SEC) (dissolution system DMAc / LiCl = mobile phase) with

refractive index detection coupled with static light scattering measurements ("MALLS" = multi angle laser light scattering). The carbohydrate composition was determined by HPLC (anion chromatography with pulsed amperometric detection "PAD") after a two step sulfuric acid hydrolysis. The cellulose II content was evaluated by a FTIR-ATR comparative method calibrated by WAXS and by ^{13}C-NMR.[19] The evaluation and correlation of IR-spectra from various samples fully characterized by WAXS and ^{13}C-NMR allows to obtain information on type of crystal lattice (cellulose I, II, ...). All the analyses were performed by Lenzing AG (Austria).

Results

Steam exploded (SE) wood pulps: observations of fraction 1, high insoluble (low rotation speed, 560 g)

The optical microscopy observations of fraction 1 of pulps reveal only very few completely undissolved fibres. Some of these fibres are as the original fibres, but some are swollen and shows a ballooning with diameters around 50-100 µm with unswollen sections and thick helices (Figure 2). The ballooning phenomenon is due to the swelling and dissolution of the secondary wall which induce the breaking of the primary wall, forming unswollen sections and thick helices. The observation of some ballooned fibres in fraction 1 indicates that the external walls, especially the primary wall, are still present on these fibres. However, most of the fibres present in fraction 1 are highly swollen (230-560% of swelling) with diameters of about 100 µm and their primary wall is not present anymore, i.e no unswollen sections and helices are observed. Only the secondary wall, including S1 wall and S2 wall, is present in these fibres, inducing a regular swelling all along the fibres. These observations show that the steam explosion pre-treatment of the pulps leads to heterogeneous effects on the fibres, some keeping their primary wall nearly intact, some loosing it but having their secondary walls not touched, while most of the fibres were destructured enough to loose their integrity during treatment with the solvent. These differences in efficiency of the steam explosion are due to heterogeneities in the structure and origin of the used fibres.

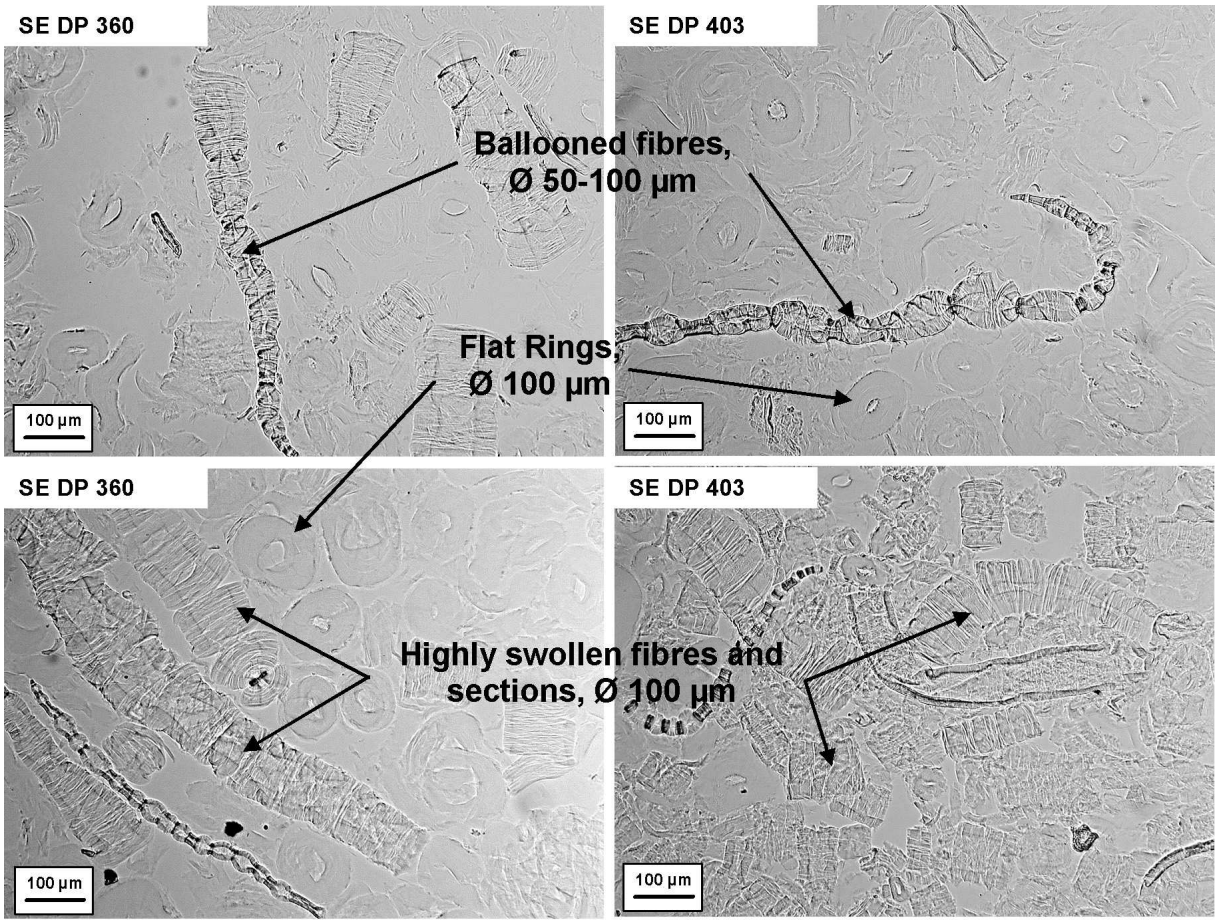

Figure 2. Fraction 1 of the SE DP 360 and the SE DP 403 samples observed by optical microscopy. Ballooned fibres, highly swollen fibres, highly swollen sections and flat rings are observed.

Sections of several hundred microns length, 100 µm diameters and numerous flat rings with external diameters of 100 µm, internal diameters of about 10 to 50 µm are also observed (Figure 2). Similar sections and flat rings were first described by Stawitz and Kage in 1959 [20] with the swelling of carboxymethyl cellulose (CMC). More recently, Jardeby *et al.* [21] have observed by optical microscopy undissolved residuals in CMC solutions and suggested that highly swollen sections and flat rings probably come from the ballooned fibres or from swelled pores. Considering the dimension and the shape of the sections and the rings, the hypothesis that they come from the cutting of the highly swollen fibres is the most probable. We will come to that point later.

Steam exploded (SE) wood pulps: observations of fraction 2, medium insoluble (higher centrifugation speed, 2520 g)

This fraction does not show any large pieces of undissolved fibre like in fraction 1. Only numerous flat rings were observed with diameters equivalent to those observed in fraction 1. Lots of fragments with various sizes and shapes from 50 to 100 µm were also observed. Looking at their shapes, we can deduce that these fragments come from the breaking of flat rings due to the shear stresses occurring during mixing (Figure 3). As can be seen, some fragments show a circular shape reminding those of the rings. However, it is also possible that fibres tear directly into fragments without going through the stage of flat rings.

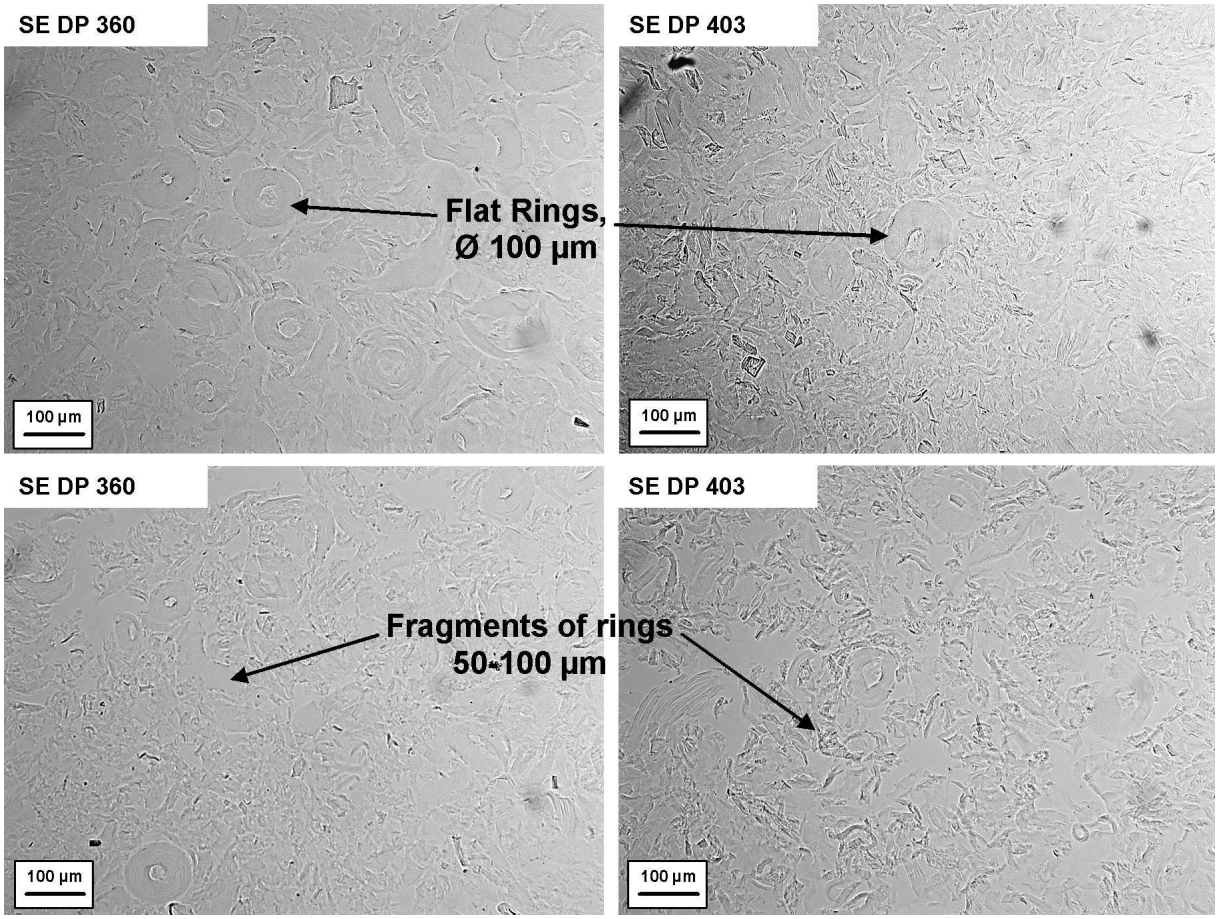

Figure 3. Fraction 2 of the SE DP 360 and the SE DP 403 samples observed by optical microscopy. Flat rings and fragments of rings are observed.

Steam exploded (SE) wood pulps: observations of fraction 3, low insoluble (high centrifugation speed, 9050 g)

After this last centrifugation stage, small fragments of about 10-50 µm were collected (Figure 4). These littler fragments are coming from the breaking of the fibres, the flat rings and their fragments. The mixing of solution during preparation decreases the size of insoluble parts due to shear stresses and the resulting solution is clearer. However, many light insoluble parts are still present in the solution showing that the reduction of their size is not the only parameter governing the dissolution of wood fibres in NaOH-water systems. To break insoluble parts in small pieces does not lead to complete dissolution. Structural and composition parameters must be considered as major factors influencing the dissolution of cellulose fibres.

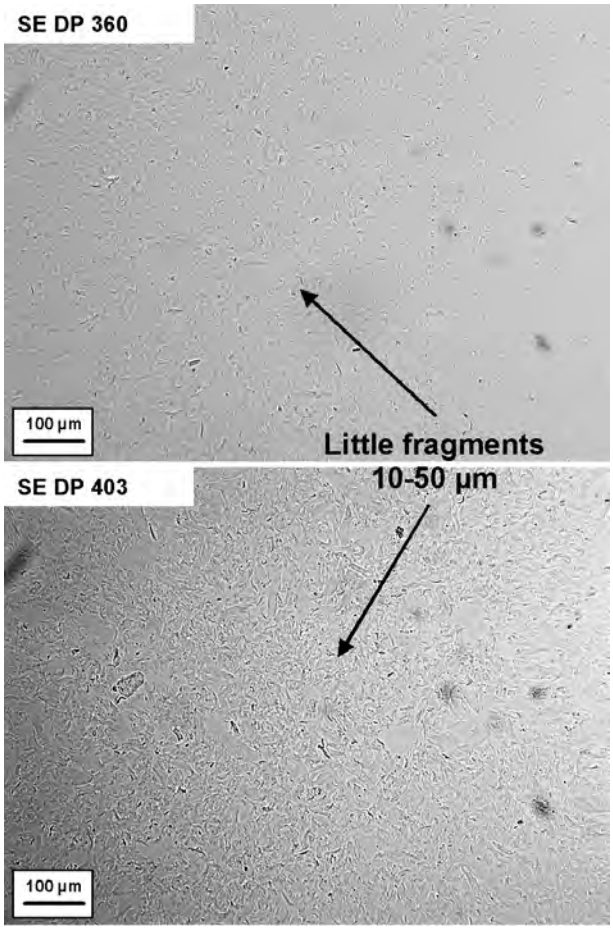

Figure 4. Fraction 3 of the SE DP 360 and the SE DP 403 samples observed by optical microscopy. Only small fragments 10-50 µm are observed.

Steam exploded (SE) wood pulps: observations of fraction 4, soluble fraction

This last fraction is an optically clear solution of cellulose (Figure 5 a and b). Some small insoluble parts with their largest dimension 2-3 µm were observed by Transmission Electron Microscopy (Figure 5c) showing that the fractionation by centrifugation was not fully effective for removing all undissolved material.

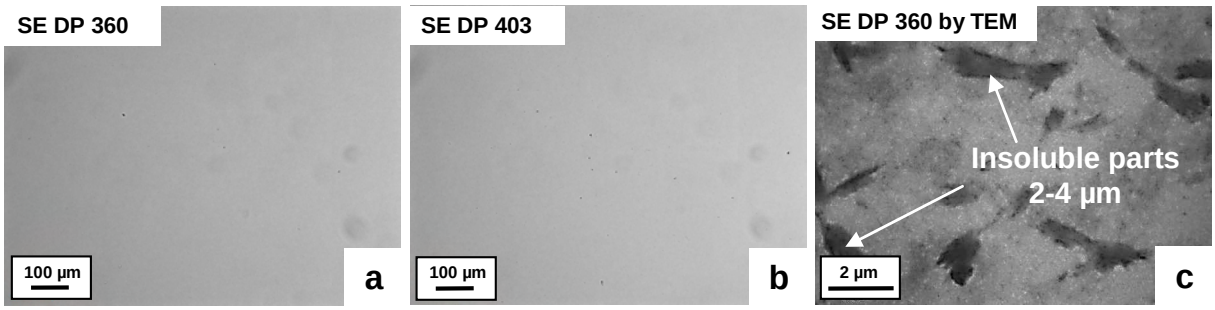

Figure 5. Fraction 4 observed by optical microscopy, (a) SE DP 360 and (b) SE DP 403 ; and by (TEM) Transmission Electron Microscopy (c) SE DP 360. Despite the optical microscopy does not show insoluble material due to their small size and lack of optical contrast because of their very high swelling, a few small insoluble parts can be seen by TEM.

Steam exploded (SE) wood pulps: influence of the mixing on the shapes of insoluble parts

The influence of the mixing process which occurs at 1000 rpm in a mechanical mixer for two hours was tested by preparing a solution of SE DP 403 with the same preparation protocol, but without agitation. As can be seen on Figure 6, highly swollen sections and flat rings are also present for this solution preparation without mechanical mixing. On one hand, it clearly indicates that the high degree of swelling of the fibres attained in this solvent is sufficient to dismantle the fibre in sections and rings. The shearing involved by the agitation is thus not the main parameter that governed the dismantlement in sections and rings. On the other hand, it confirms that a shearing is necessary for the breaking of the different entities in smaller and smaller fragments. Finally, the soluble fraction must be considered as a mixture mainly composed of cellulose aggregates [22] and in lower proportions of isolated chains, both coming from the dismantlement and the fragmentation of the fibres.

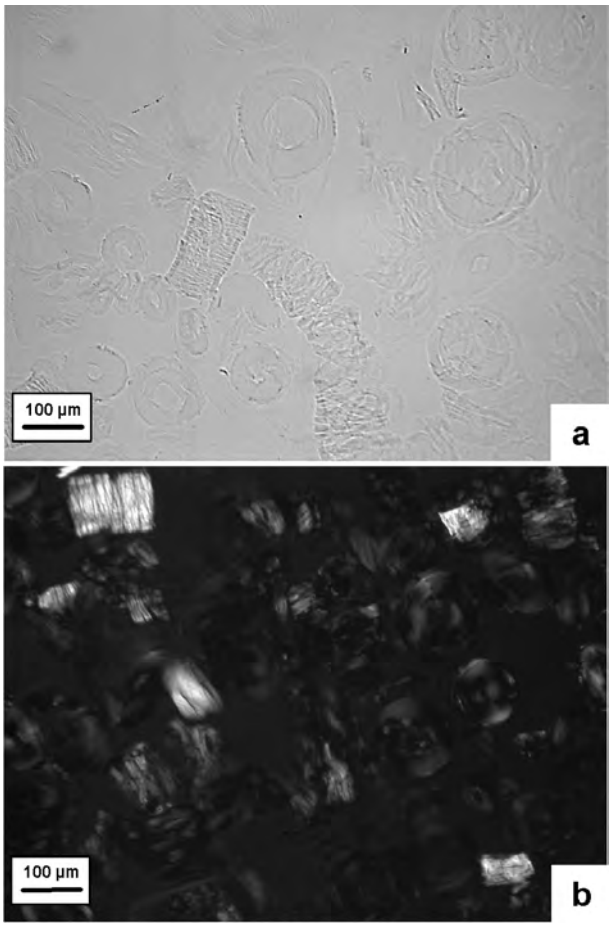

Figure 6. Highly swollen fibres, sections and flat rings observed in a non-agitated solution of SE DP 403 in NaOH 8%-water. (a) direct light transmission, (b) between cross-polarizer.

Wood pulps: Observations of insoluble parts in PH Kraft pulp and bleached sulphite pulp

The effect of the pre-treatments has been tested by studying the morphology of insoluble parts in other wood fibres, i.e. a bleached sulphite pulp and a PH Kraft pulp samples. Most of the fibres were only slightly swollen in the case of the PH Kraft pulp sample. However, as can be seen on Figure 7, highly swollen fibres, sections and flat rings are observable in both samples. It means that these flat rings are not due the steam explosion pre-treatment or differences of chemical action between the sulphate and the sulphite cooking. It has to be noticed that the flat rings show lower swelling and present a square shape in the case of the PH Kraft pulp sample which reminds the original shape of a non swollen wood fibre. This has to be related with the presence of the external walls, especially the primary wall, which prevents swelling in not too good solvents.

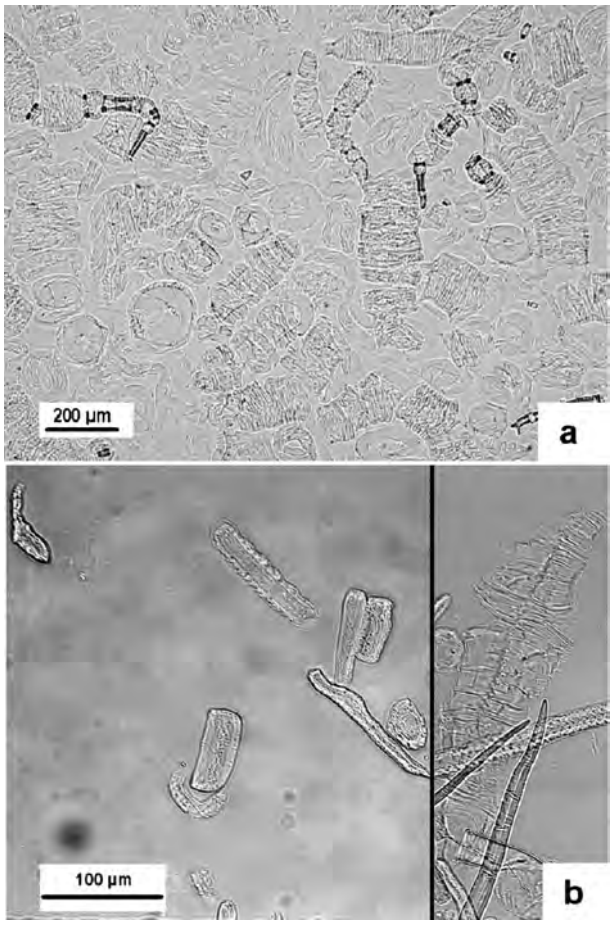

Figure 7. Highly swollen fibres, sections and flat rings observed for (a) bleached sulphite pulp and (b) PH Kraft pulp.

Microcrystalline cellulose: observations of the insoluble fraction

Avicel PH 101 (DP 170) is not fully dissolving in NaOH 8% - water. Centrifugation clearly produced a fraction with insoluble parts in. These insoluble parts, having their largest dimension of about 1 to 10 µm, can be observed even for a 1% MCC solution (Figure 8). These insoluble parts are fragment-like pieces as those observed in fraction 3 for wood pulp samples and observations between cross-polarizer indicate that these pieces are oriented. These insoluble particles can influence optical properties of the solution.

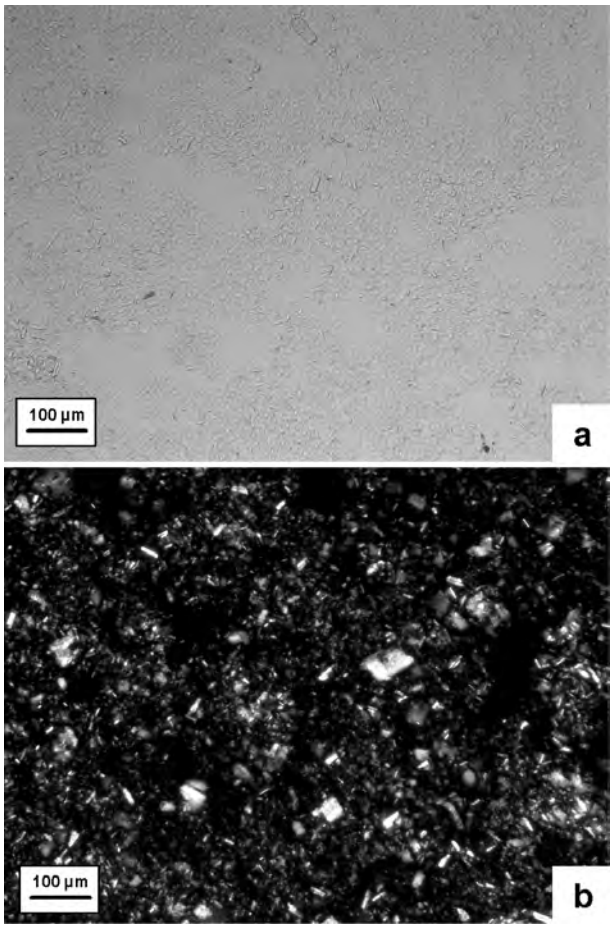

Figure 8. Insoluble parts (1-10 µm) in a solution of 1% MCC (Avicel PH 101) in NaOH 8% - water observed by optical microscopy (a) in transmission light and (b) between cross-polarizer.

Weighing of the insoluble and soluble fractions

After centrifugation, regeneration in distilled water and drying at 50°C overnight, the weight of the recovered solid material of each fraction was measured. The detailed weight fractions are reported in Table 2 for SE DP 360 and SE DP 403 samples (each value is an average of three measurements). About 28-30 % of the total product is lost due to the centrifugation protocol and the regeneration in several steps. However, most of the lost product should come from the soluble fraction which is the more difficult to recover. The total amount of insoluble products varied between 10-14% (assuming that the entire lost product is coming from the soluble fraction).

Samples	Fractions	Average amount %
SE DP 360	**1**, Highly insoluble	3.5
	2, Medium insoluble	6.4
	3, Low insoluble	3.8
	4, Soluble product	58.2
	Lost product	28.1
SE DP 403	**1**, Highly insoluble	4.7
	2, Medium insoluble	5.0
	3, Low insoluble	2.3
	4, Soluble product	58.5
	Lost product	29.6

Table 2. Amount of dried fractions 1, 2, 3 and 4 after centrifugation for the SE DP 360 and SE DP 403 samples.

As can be seen on Figure 9, the amount of insoluble material for the PH Kraft pulp sample is very high due its high degree of polymerisation (DP) and to the fact that the fibre has not been too much de-structured during treatments. The bleached sulphite treatment leads to a medium quantity of insoluble parts (42%) due to the decrease of DP and to the loosening of integrity of the original structure. Without agitation, the quantity of insoluble material for the SE DP 403 sample is increased by three showing the role of agitation on the dissolution process. The lowest insoluble material amount is reached with the Avicel PH 101 (2-4 %) sample which is the most destructurated. However, the presence of insoluble parts in this sample shows that the hydrolysis is not preventing to keep parts of the wall structure in the sample.

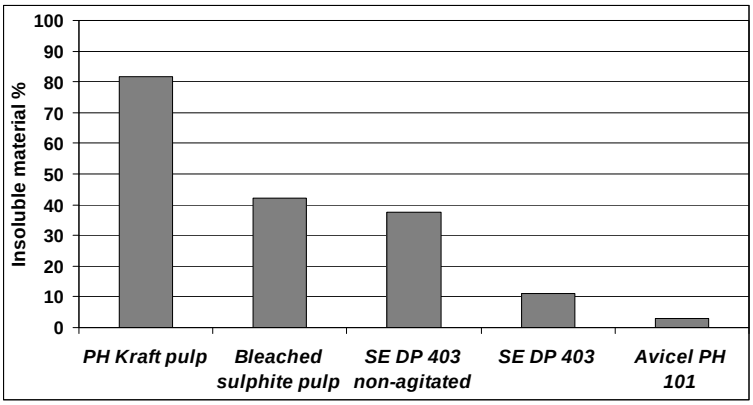

Figure 9. Amounts of insoluble material in NaOH 8% - water solutions of PH Kraft pulp, bleached sulphite pulp, SE DP 403 (steam exploded sulphite pulp), non-agitated SE DP 403 and Avicel PH 101.

Molecular weight distributions of the insoluble and soluble fractions

The molecular weight distributions of the various fractions show that insoluble fractions have higher mean molar masses (Figure 10) than the mean molar masses of the original samples. For the two steam exploded samples, SE DP 360 and SE DP 403, the average molecular weights Mw of the insoluble fractions are about two times higher than the one of the soluble fractions, i.e. 120 000-160 000 g/mol^{-1} versus 76 000 g/mol^{-1}. The average molecular weights Mn of insoluble fractions are also roughly 1.5 times higher than the soluble fractions, i.e. 59 000-65 000 g/mol^{-1} versus 39 000-43 000 g/mol^{-1}.

Molecular weight distributions of the two Avicel PH 101 fractions are similar. This can be due to the very low initial molar mass of the sample (DPn 170) and also to the fact that the original structure has been strongly degraded by the acidic hydrolysis pre-treatment. The effect of the fibre structure is thus not visible. However, fragments (2-4% by weight) having average DPn of about 220 remain insoluble although the original wall structure was supposed to be destroyed. The fine structure and the composition at the molecular level are thus very influent on the dissolution capacity.

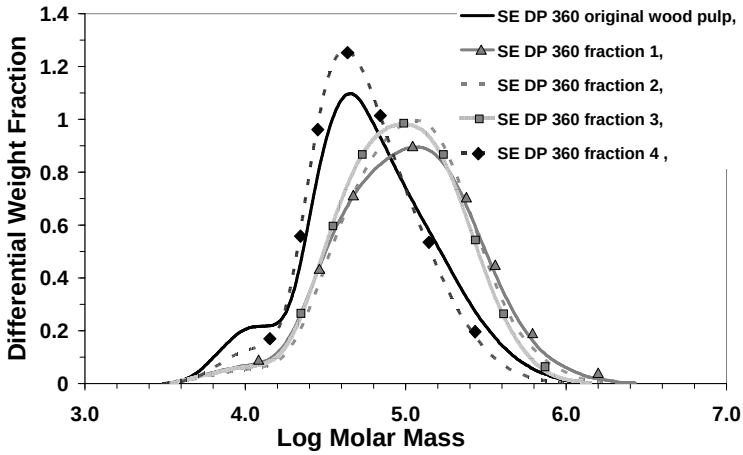

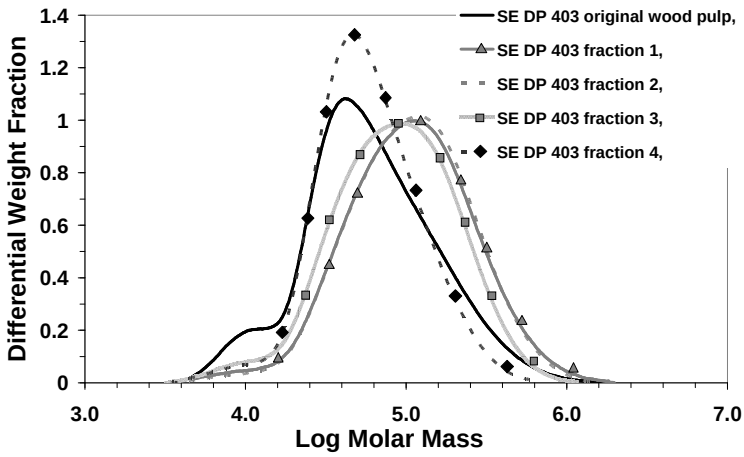

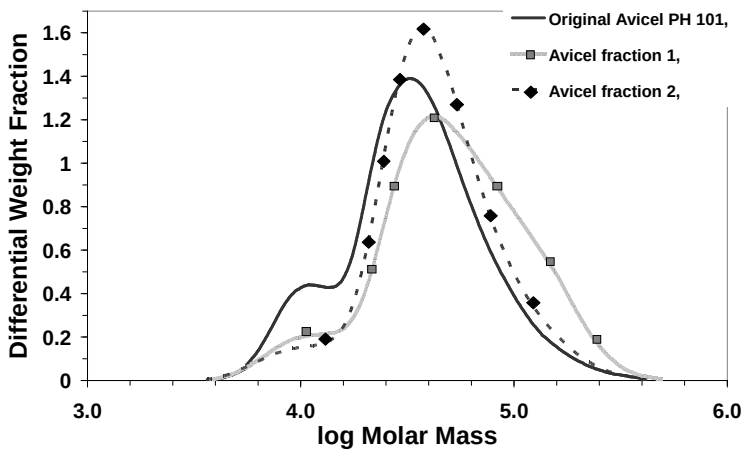

Figure 10. Molecular weight distributions of original samples, insoluble fractions (1, 2 and 3 for SE DP 360 and SE DP 403 wood pulps, 1 for Avicel PH 101) and soluble fractions (4 for SE DP 360 and SE DP 403 pulps, 2 for Avicel PH 101).

The polymolecularity index is higher for the insoluble fractions than for the soluble fractions, i.e. ≈ 2.35 and 1.8 respectively for SE DP 403 and 360 wood pulps, and 1.9 and 1.6 respectively for Avicel. Insoluble parts are thus containing small chains as in the original samples and in the soluble parts together with a large share of the long chains. The fact that these shorter cellulose chains did not dissolve while some others did, indicates that these chains were less accessible and embedded in regions difficult to dissolve. It is not simply long chains that are not dissolving but complex regions where these long chains are predominantly present. It shows that the dissolution capacity of cellulose chains, beyond thermodynamic considerations, is very dependant of their localization in the cell wall structure. The length of the chains is not the main parameter, since otherwise molecular weight distributions of insoluble fractions and soluble fractions would be clearly different.

Carbohydrate composition of the insoluble and soluble fractions

The carbohydrate composition shows that a part of xylan and mannan were removed during the dissolution (Table 3). However, insoluble fractions (fraction 1, 2 and 3) contain more mannan than the soluble fractions (0.6-0.8 % vs 0.2-0.3 % respectively) while the xylan content stays constant on all fractions (0.2-0.3 %). It is interesting to note that hemicelluloses are present in Avicel PH 101 MCC samples. The fact that hemicelluloses are present both in insoluble fractions and soluble fractions is illustrating the known strong interactions between cellulose and hemicelluloses. As was reported by Isogaï and Atalla, [17] these interactions are

supposed to be physical, in the sense of co-aggregation [23] or based on chemical linkages. [24] It was also suggested that glucomannans are more associated with cellulose while xylans are more associated with lignin. These results were supported by dynamic FT-IR spectroscopy investigations. [25] Isogaï and Atalla [17] assumed that the presence of hemicelluloses does not seem to prevent the dissolution because most of hemicelluloses fractions are soluble in the aqueous NaOH. However, the authors were only compared hemicelluloses content in original samples and insoluble fractions, no measurements were done on the soluble fractions. The differences in hemicelluloses contents between insoluble and soluble fractions are not very large and the influence of such variations on dissolution capacity remains to be demonstrated.

Several authors assume that the hemicelluloses are distributed in layers between the cellulose microfibrils and the elementary fibrils [26, 27, 28] meaning that a very fine dispersion of the hemicelluloses occurs around the cellulose microfibrils and elementary fibrils. Such fine dispersion and the strong interactions between cellulose and hemicelluloses should have an influence on the behaviour of cellulose chains towards dissolution, even if the concentration of hemicelluloses is low. The variations in dissolution capacity of cellulose chains shown by the above molecular weight distribution results might be related to the localization of the cellulose chains in the cellulose / hemicelluloses complex, i.e. cellulose chains are more or less embedded in a hemicellulose matrix.

Samples	Sugar composition (%)						
	Glucan	Xylan	Mannan	Arabinan	Rhamnan	Galactan	Total
Original SE DP 360 Wood pulp	96.0	1.4	0.9	0	0	0	98.3
SE DP 360 Fraction 1	98.1	0.3	0.5	0	0	0	98.9
SE DP 360 Fraction 2	98.7	0.2	0.6	0	0	0	99.6
SE DP 360 Fraction 3	99.2	0.2	0.6	0	0	0	100.0
SE DP 360 Fraction 4	99.1	0.2	0.3	0	0	0	99.6
Original SE DP 403 Wood pulp	97.4	1.4	0.9	0	0	0	99.6
SE DP 403 Fraction 1	96.4	0.2	0.6	0	0	0	97.3
SE DP 403 Fraction 2	97.9	0.1	0.6	0	0	0	98.6
SE DP 403 Fraction 3	97.7	0.2	0.6	0	0	0	98.6
SE DP 403 Fraction 4	97.0	0.2	0.3	0	0	0	97.4
Original Avicel PH 101	98.6	1.6	1.2	0	0	0	101.5
Avicel PH 101 Fraction 1	96.4	0.2	0.8	0	0	0	97.4
Avicel PH 101 Fraction 2	98.3	0.2	0.2	0	0	0	98.8

Table 3. Carbohydrate compositions of original samples, insoluble fractions (1, 2 and 3 for SE DP 360 and SE DP 403 pulps, 1 for Avicel PH 101) and soluble fractions (4 for SE DP 360 and SE DP 403 pulps, 2 for Avicel PH 101).

Cellulose II content of the insoluble and the soluble fractions

The cellulose II content in insoluble and soluble fractions was investigated by FTIR-ATR using a comparative method (Lenzing AG).[19] The deconvoluted OH regions (bands around 2720, 3278, 3344, 3422, 3450 and 3700 cm^{-1} with 2900 $cm^{-}1$ as reference band) of the samples spectra were compared with those of several cellulose I / cellulose II composition references prepared in NaOH-water at various concentration (Figure 11). The OH region area is larger for cellulose II than cellulose I and thus increases with the amount of cellulose I converted in cellulose II. The content of cellulose II is deducted from the calculated area of the OH region which is specific to a cellulose I / cellulose II composition. The cellulose I / cellulose II composition values of the references were calibrated by ^{13}C-NMR. The band 2900 cm^{-1}, assign to CH_2 stretching, is commonly used as reference because it is unaffected by changes in sample preparation, crystallinity or humidity and shows a constant intensity. [29]

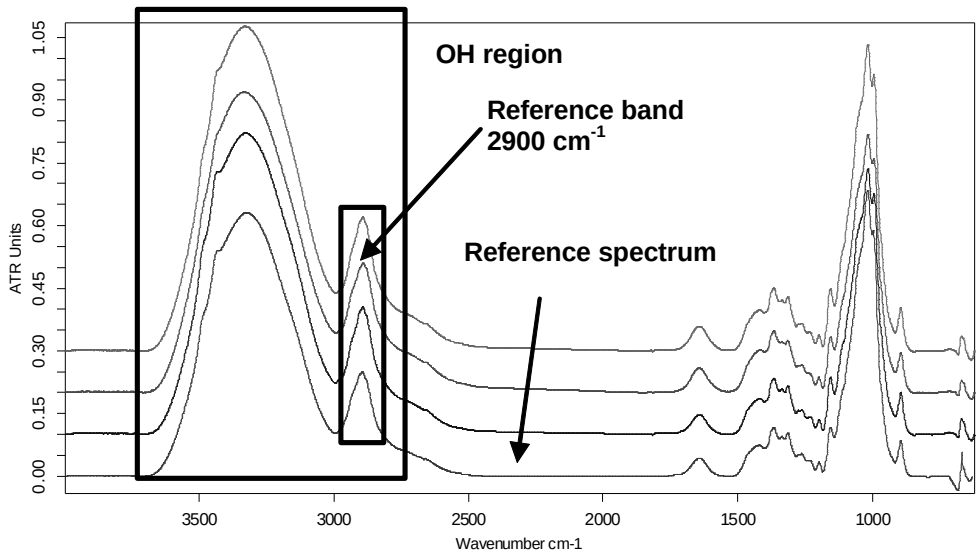

Figure 11. FTIR-ATR spectra of different fractions as compared to the most equivalent cellulose I / cellulose II composition reference spectrum.

Samples	% cellulose II
SE DP 360 wood pulp	0
SE DP 360 Fraction 1	92
SE DP 360 Fraction 2	88
SE DP 360 Fraction 3	92
SE DP 360 Fraction 4	94
SE403 Wood pulp	-4
SE403 Fraction 1	98
SE403 Fraction 2	96
SE403 Fraction 3	94
SE403 Fraction 4	97
Avicel PH101	-4
Avicel PH101 - Fraction 1	100
Avicel PH101 - Fraction 2	98

Table 4. Cellulose II content original samples, insoluble fractions (1, 2 and 3 for SE DP 360 and SE DP 403 pulps, 1 for Avicel PH 101) and soluble fractions (4 for SE DP 360 and SE DP 403 pulps, 1 for Avicel PH 101).

The results presented in Table 4 shows that most of the cellulose I was converted in cellulose II even for insoluble fractions. The crystal structure of highly swollen fibres, sections and flat rings after regeneration is thus cellulose II. Even if the cellulose parts in the fractions stay insoluble, the large swelling gives enough molecular mobility to convert cellulose I in cellulose II, as it is doing in the mercerisation process.

Discussion and Conclusions

The dissolution of wood fibres in NaOH-water is not very easy. Aside thermodynamic limitations due to the NaOH/AGU ratio needed to solubilize cellulose [30] and the fast gelation of the solutions, [18] the results reported here show that dissolution proceeds in a complex way that strongly depends on the location of cellulose inside the cell structure. We already showed that there is a gradient of dissolution capability inside the cell wall structure, the younger deposited layers being easier to dissolve than the oldest ones (i.e; cellulose embedded into the primary wall or into the secondary wall close to the primary wall is more difficult to dissolve than the one deep inside the secondary wall, close to the cell nucleus).[16]

The results reported here show that the dissolution picture is even more complicated. The dissolution capability of wood fibres must be considered at two levels, (i) the macrostructure that needs to be dismantled for increase dissolution, and (ii) the cellulose chain chemical environment.

Macrostructural level

Destructuration of the layer structure by steam explosion, agitation or acidic hydrolysis helps the dissolution. As for all polymer dissolution, agitation is removing concentrated solution away from the dissolving part and brings fresh solvent. With agitation, the quantity of insoluble material is decreased by three showing the role of agitation on the dissolution process (Figure 9). This is facilitated in wood cellulose by treatments like steam explosion. The steam explosion of the SE DP 403 sample acts as a destructuration treatment which facilitates the dismantlement and the fragmentation of the fibre in the NaOH 8%- water mixture and leads to a lower insoluble material amount (10-12 %).

Cellulose chain chemical environment

The fact that short cellulose chains did not dissolve while some others did, indicates that these chains were less accessible and embedded in regions difficult to dissolve. It shows that the dissolution capacity of cellulose chains, beyond thermodynamic considerations, is very dependant of their localization in the cell wall structure. These variations in dissolution capacity of cellulose chains might be related to the localization of the cellulose chains in the cellulose / hemicelluloses complex, i.e. cellulose chains are more or less embedded in a hemicelluloses matrix.

Origin of the flat rings

The reasons that lead to the particular “flat rings” geometry need to be more detailed. To what extent the cutting in flat rings is due to the original structure of the fibre, to the chemical pre-treatment or to the swelling and dissolution undergone by the fibres is an interesting question?

Dissolution produces different parts that correspond to successive morphologies during dissolution: the insoluble fraction containing the highly swollen fibres, the highly swollen sections, the flat rings, the fragments and the soluble fraction containing mostly the cellulose aggregates. This mechanism of dismantlement and fragmentation is mainly governed by the high swelling and in a lower extent by the shear stress involved during the solution preparation. The different steps of dissolution of wood cellulose fibres in NaOH 8%- water are schematically represented on Figure 12.

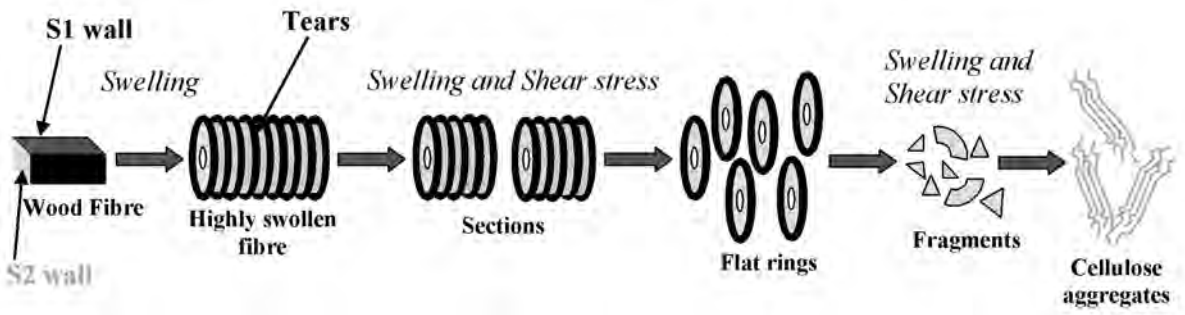

Figure 12. Schematic representation of the dissolution steps of wood fibres in NaOH 8%-water.

In the highly swollen fibres, we have shown previously that the primary wall is not present due to the absence of ballooning. Only the S1 wall and the S2 wall are thus present in these highly swollen fibres. Cellulose microfibrils in wood fibre generally have orientation angle of about 50-70° [31] or 70-90° [32] in S1 wall and 0-30° in S2 wall.[33] The large swelling of the fibre involves a regular tear of the outer layer, i.e. the S1 wall, every 10 µm which is clearly visible on Figure 2. Numerous tears transverse to the fibre axis (clearer lines) are observable along highly swollen fibres and sections. Considering the high radial swelling (230 to 560 %), the outer S1 wall must tear because its microfibrils are almost perpendicular to the fibre axis. The regular repetition of these tear every 10 µm still have to be explained but it has to be related with the deposition and the cohesion of the cellulose microfibrils in the S1 wall. These tearing zones can be considered as weak points where the fibre can break in sections and flat rings. This mechanism requires that the S2 wall is transversely cut while its microfibrils are almost parallel (0-30°) to the fibre axis. The loss of mechanical properties of the S2 wall is explained by the fact that the original compact cellulose structure is not preserved since the S2 wall is highly swollen (230-560%) and partially dissolved. A shear stress is thus not essential to cut the highly swollen fibres in sections and flat rings. It has to be noticed that the cutting of the highly swollen fibres in rings and not in disks shows that the wood fibres were not fully mature or that the inside tertiary wall and wart layer were removed by the pre-treatments or easily soluble in the NaOH 8% / water solution.

The flat rings observed with PH Kraft pulp show that a high degree of swelling is not necessary and, in this case, we must assume that shearing was the main factor of the cutting in flat rings. All these experiments show that wood fibres can dismantle in flat rings when putting in NaOH 8%-water, independent of their original cooking (steam explosion pre-treatment, sulphite or sulphate processes).

Limit of solubility

The limit of solubility of cellulose in NaOH 8% - water at -6°C in terms of DP can be approximated as the average DPn and DPw of the soluble fraction, 252 (Mn / 162 g/mol^{-1}) and 469 (Mw / 162 g/mol^{-1}) respectively. These values have to be considered as an average and the molecular weight distributions shows that longer chains are also dissolved. Values of DPn (107) and DPw (268) were recently reported after filtration of enzymatically treated samples dissolved in 7.8 wt.% NaOH and 0.84 wt.% ZnO at 3°C.[34] All these estimations may not be relevant of the solubility of pure cellulose. In wood samples, cellulose chains are embedded in a complex and compact layer structure. As an example, in 8.5 wt.% NaOH and 1 wt.% urea at -5°C, bacterial cellulose was shown to be dissolved so long as its DPw is below 560,[35] stressing the adverse influence of the wood cell wall structure and composition on dissolution capability.

References

(1) Nägeli, C. *Sitzber Bay. Akad. Wiss. Munchen*, **1864**, 1, 282-323, 2, 114–171.

(2) Pennetier, G. *Bull. Soc. Ind. Rouen*, **1883**, 11, 235–237.

(3) Flemming, N.; Thaysen, A. C. *Biochem. J.*, **1919**, 14, 1, 25–28.

(4) Marsh, J. T. In *The growth and structure of cotton, Mercerising*, Chapman & Hall Ltd, London, 1941.

(5) Hock, C. W. *Text. Res. J.*, **1950**, 20, 141–151.

(6) Tripp, V. W.; Rollins, M. L. *Anal. Chem.*, **1952**, 24, 11, 1721–1728.

(7) Rollins, M. L.; Tripp, V. W. *Text. Res. J.* **1954**, 24, 345–357.

(8) Ott, E.; Spurlin, H. M.; Grafflin, M. W. In *Cellulose and cellulose derivatives (Part 1)*, Interscience Publisher, New York, 1954, p 353.

(9) Chanzy, H.; Noe, P.; Paillet, M.; Smith, P.; *J. Appl. Polym. Sci.*, **1983**, 37, 239–259.

(10) Cuissinat, C.; Navard, P. *Macromol. Symp.*, **2006**, 244, 1, 1–15.

(11) Cuissinat, C.; Navard, P. *Macromol. Symp.*, **2006**, 244, 1, 19–30.

(12) Cuissinat, C. ; Heinze, T. ; Navard, P. *Carbohydr. Polymer*, **2008**, 72, 590–596.

(13) Cuissinat, C. *Swelling and dissolution mechanisms of native cellulose fibres*. Thèse de doctorat, Ecole des Mines de Paris, Sophia-Antipolis, 2006, http://pastel.paristech.org/2729/01/these-Cuissinat.pdf

(14) Cuissinat, C. ; Navard, P. *Cellulose*, **2008**, 15, 67–74.

(15) Cuissinat, C. ; Heinze, T. ; Navard, P. *Cellulose*, **2008**, 15, 75–80.

(16) Le Moigne, N.; Montes, E.; Pannetier, C.; Höfte, H.; Navard, P. *Macromol. Symp.*, **2008**, 262, 1, 65–71.

(17) Isogai, A.; Atalla, R. H. *Cellulose*, **1998**, 5, 309–319.

(18) Roy, C.; Budtova, T.; Navard, P. *Biomacromolecules*, **2003**, 4, 259–264.

(19) Baldinger, T.; Moosbauer, J.; Sixta, H. In *Supermolecular structure of cellulosic materials by fourier transform infrared spectroscopy (FT-IR) calibrated by WAXS and 13C NMR*, Internal report from LENZING AG, A- 4860 Lenzing, Austria, **2005**.

(20) Stawitz, J.; Kage, M.P. *Das Papier*, **1959**, 13, 567–572.

(21) Jardeby, K.; Germgård, U.; Kreutz, B.; Heinze, T.; Ute, H.; Lennholm, H. *Cellulose*, **2005**, 12, 167–175.

(22). Schulz, L.; Seger, B.; Burchard, W. *Macromol. Chem. Phys.*, **2000**, 201, 2008–2022.

(23) Hackney, J. M.; Atalla, R. H.; VanderHart, D. L. *Int. Biol. Macromol.*, **1994**, 16, 215–218.

(24) Isogai, A.; Ishizu, A.; Nakano, J. *Holtzforschung*, **1989**, 43, 333–338.

(25) Åkerholm, M.; Salmén, L. *Polymer*, **2001**, 42, 963–969.

(26) Fengel, D. *J. Polym. Sci.: part C*, **1971**, 9, 383–392.

(27). O'Sullivan, A. C. *Cellulose*, **1997**, 4, 173–207.

(28) Fahlén, J. *The cell wall ultrastructure of wood fibres: Effects of the chemical pulp fibre line*. Ph.D. Thesis, Fibre and Polymer Technology, KTH Royal Institute of Technology, Stockholm, **2005**, p 10, http://www.diva-portal.org/kth/theses/abstract.xsql?dbid=129

(29) Nelson, M. L.; O'Connor, R. T. *J. Appl. Polym. Sci.*, **1964**, 8, 1325–1341.

(30) Egal, M.; Budtova, T.; Navard, P. *Biomacromolecules*, **2007**, 8, 2282–2287.

(31) Roelofsen, P. A. In *The Plant Cell-Wall, Encyclopedia of plant anatomy*, Gebrüder Borntraeger, Berlin, 1959, p 213.

(32) Brändström, J.; Bardage, S. L.; Daniel, G.; Nilsson, T. *IAWA J.*, **2003**, 24, 27–40.

(33) Sahlberg, U.; Salmén, L.; Oscarsson, A. *Wood Sci. Technol.*, **1997**, 31, 77–86.

(34) Vehviläinen, M.; Kamppuri, T.; Rom, M.; Janicki, J.; Ciechańska, D.; Grönqvist, S.; Siika-Aho, M.; Christoffersson, K. E.; Nousiainen, P. *Cellulose* **2008**, 15, 671–680.

(35) Łaszkiewicz, B. *J. Appl. Polym. Sci.*, **1998**, 67, 1871–1876.

Chapter V

Structural changes and alkaline solubility of wood cellulose fibres after enzymatic peeling treatment.

Structural changes and alkaline solubility of wood cellulose fibres after enzymatic peeling treatment

Abstract Two dissolving sulphite wood pulps were treated by an enzymatic peeling protocol and the changes in terms of structure and alkaline solubility were analyzed. The enzymatic treatment leads to a fast and large decrease of degree of polymerization and of crystallinity, showing that the enzymes do not act simply on the fibre surface. The swelling and dissolution behaviour of the treated samples showed that the enzyme mixture used has two effects at short peeling times, (i) a digestion of the primary wall which is seen by the near absence of ballooning and (ii) a destructuration action in the inside of the fibre which is seen by the large decrease of the degree of polymerization. At long peeling times, the external walls are totally digested and the fibre structure is totally destructured, as seen by the absence of birefringence. The alkaline solubility of the different treated samples was investigated in a NaOH 8% - water solution. As expected from thermodynamic considerations, there is a direct correlation between the solubility and the degree of polymerization. However, aside thermodynamics, the removal of the external walls and the macrostructural destructuration of the fibres are key factors in the improvement of the dissolution of wood cellulose fibres. At constant intrinsic viscosities of the cellulose materials, the alkaline solubility is almost two times higher when the external walls are removed. The macrostructural destructuration of the fibre by the enzymes allows preserving a high degree of polymerization while keeping a good alkaline solubility.

Introduction

Cellulose fibres from wood and higher plants are very complex composite biomaterials. Their original structure is generally described at three length scales or levels, (i) the molecular level, (ii) the aggregated level and (iii) the macrostructural level.[1, 2] Except in raw wood, some plant fibres and cotton hairs, cellulose cannot be used without extraction. In case of uses other than paper and reinforcement fibers, cellulose must be dissolved since it cannot be melted. The goal that faced generations of scientists and numerous companies is to find a cheap, simple and non polluting dissolving process. The dissolution of cellulose has been investigated in many solvents over the last hundred years. However, some of the mechanisms

involved in the dissolution at the different structural levels of cellulose fibres are still not well understood. In parallel, several physical and chemical methods, called "activation", have been developed to ease the dissolution of cellulose by an increase accessibility of the solvent to the whole structure (e.g ball or vibration milling[1, 3], steam explosion[4], beam irradiation[5]). The challenge is to be able to disrupt the aggregated and the macro structure of cellulose while preserving the original molecular solid-state. However, aside improving the dissolution, these activations are always accompanied of strong degradations of the cellulose polymer leading to low degree of polymerisation (DP) values. In chapter III, it was shown that there is a restricted dissolution capacity when a cotton hair or a regenerated fibre immersed into a moderate quality solvent was put under tension and prevented to contract despite reaching sufficient swelling ratio for accessibility. This result showed that it is not enough for the cellulose chains to be close to the reagent or to be not crystalline. Chains must be allowed to perform local conformational movements requiring long range chain mobility. Such a long range disruption was already suggested by Isogaï and Attala when studying the dissolution of cellulose in aqueous NaOH solutions.[6]

The chemical environment of the cellulose chains is also playing a role in the dissolution capability (see chapter IV). Cellulose chains of similar molecular mass can be soluble or not depending on their location in the cell wall. In a recent paper, [7] the existence of a centripetal radial gradient in the dissolution capacity within the fibre was proposed. The older was the deposition, the more difficult it is to dissolve it. These results can be related to age-dependent structural re-organizations in the cell wall layers or more probably to the presence of non-cellulosic components around cellulose chains.

Since the presence of the primary wall is a handicap for dissolving cellulose fibres, it is important to investigate in details the influence of the removal of the external walls of wood pulp fibres on dissolution. This can be performed by an enzymatic peeling treatment. The hope is to remove only what impedes the dissolution of cellulose without degrading too much the rest of the fibre. The consequence of an enzymatic treatment on cellulose dissolution has been studied in several works. It was always suggested that the increase of solubility after an enzymatic treatment is due to a decrease of both DP and hydrogen bond density.[8, 9] However, no data on the influence of potential macrostructural changes like removal of external layer or deeper changes exists. The aim of the present study is to investigate the role that macrostructural changes occurring during an enzymatic peeling treatment play on dissolution

capacity of wood cellulose fibres, in addition to the classically evocated thermodynamic parameters.

Experimental

Cellulose samples. Three dissolving sulphite wood pulp samples were used named VHV-S, SA (Super Aceta) and LV-U (bleached sulphite pulp) all provided by Borregaard (Norway). The main characteristics of the pulps are reported in Table 1. VHV-S and SA pulps have high intrinsic viscosity values. However, the original structure of the fibre is supposed to be more preserved in the case of the VHV-S pulp since it was digested at a higher kappa number than the SA and LV-U pulps.

Pulp samples	Wood origin	Supplier	Intrinsic viscosity *	Glucan °	Xylan °	Mannan °	Crystallinity °
VHV-S	Norway spruce	Borregaard	1430 ml/g	90%	3.5%	1.8%	46%
SA	Norway spruce	Borregaard	880 ml/g	94.7%	1.9%	1.1%	49%
LV-U	Norway spruce	Borregaard	350 ml/g	-	-	-	-

* Measured by Borregaard according to ISO 5351/1B

° Measured by Lenzing AG as described in the materials and methods

Table 1. Main properties of the wood pulp samples used.

Enzymatic peeling protocol. A mixture of two commercial enzymes were used, Celluclast 1.5L (cellulase derived from *Trichoderma reesei*, sold by Novozymes, Denmark, used classically for the hydrolysis of lignocellulosic biomass feedstocks. This enzyme contains a broad spectrum of cellulolytic enzyme activities, like cellobiohydrolases and endo-1,4-glucanases) and Econase HC400 (highly concentrated liquid formulation of endo-1.4- beta-xylanase produced by *Trichoderma reesei* and standardised to minimum enzyme activity of 400,000 BXU/g as well as side activities like beta –glucanase, sold by AB enzymes, Finland).

The enzymatic peeling protocol was adapted from the work of Sjöberg *et al.*[10]. The treatments were performed only on SA and VHV-S pulps as follows: 50 g of pulp (wet, never dried with a pulp consistency of approximately 16%, i.e. 8 g of dried pulp) were mixed in 500 ml buffer solution for a few minutes before adding the enzymes mixture. Stirring was done with a large magnet stirrer (300 rpm). The peeling time was varied from 1 to 30 min. After the peeling reaction was finished, the pulp was filtered and washed on a filter paper circle (589/1, diameter 125 mm, ash free, black ribbon, Schleicher and Schuell MicroScience). The washing

proceeded until neutral pH of the filtrate was measured. The samples were then dried overnight at room temperature which leads to a standard pulp consistency of 95%.

Buffer and enzymes mixture. The buffer solution was prepared as follows: 9.92 g NaAc was dissolved in 3.5L deionised water. pH was adjusted to 4.0 with acetic acid. The solution was then diluted to 4L. The enzymes mixture was made of 8.35 ml of Celluclast 1.5L and 4.20 ml of Econase HC 400. A fresh enzymes mixture was used for each treatment.

Sample weight evolution during the enzymatic peeling. The weight of the samples was measured after the enzymatic treatment by a gravimetric method. The sample weight (%) is defined as the amount of fibres (w/w) which remains after the enzymatic treatment, e.g. 7 g of pulp after treatment (pulp consistency 95%, i.e. 6.65 g of dried pulp) correspond to a sample weight of 83% as regard to the initial 8 g of pulp introduced.

Intrinsic viscosity and degree of polymerization. The intrinsic viscosity was measured by Borregaard for each samples according to ISO 5351/1B (determination of the intrinsic viscosity of pulp in a dilute cupri-ethylenediamine (CuEn) solution). The intrinsic viscosity is almost linearly correlated with DP and can be calculated by the following formula[11]: $DP^{0.905} = 0.75\ [\eta]$ (ml/g).

Crystallinity and carbohydrate composition. The crystallinity was evaluated by a FTIR-ATR comparative method calibrated by WAXS and by ^{13}C-NMR.[12] The evaluation and correlation of IR-spectra from various samples fully characterized by WAXS and ^{13}C-NMR provide algorithms to determine the degree of crystallinity. The carbohydrate composition was determined by HPLC (anion chromatography with pulsed amperometric detection "PAD") after a two step sulfuric acid hydrolysis. All the analyses were performed by Lenzing AG.

Swelling and dissolution observations. The swelling and dissolution observations were performed in two solvent systems:

- *N*-methylmorpholine *N*-oxide (NMMO) with 22% of distilled water (w/w), i.e. NMMO-22% water : 0.78 g of NMMO with 0.22 g of distilled water for a 1 g mixture. The NMMO was provided by Sigma-Aldrich.

- 8% of NaOH in distilled water (w/w), i.e. NaOH 8% - water: 0.08 g of NaOH and 0.92 g of distilled water for a 1 g mixture. The NaOH was provided by Sigma-Aldrich.

Samples were observed between two glass plates by optical microscopy in transmission mode with a Metallux 3 (Leitz) equipped with a high resolution 3-CCD camera JVC KY-F75U and a Linkam TMS 91 stage settled at 90°C for the NMMO solvent system and at -6°C for the NaOH solvent system. The solvent contained in a pipette was injected by capillarity between the two glass plates. No agitation was applied to the system.

Pulp solution preparation. The different non-treated and treated pulps were dissolved in a NaOH 8%- water solution to test their alkaline solubility. The solutions were prepared as follows: 132 g of NaOH 12% - water were stored at -6°C. 2 g of pulp were added to 66 g of distilled water and stored 1 hour at 4°C. Then, NaOH 12% - water and cellulose - water solutions were mixed together during two hours at -6°C and 1000 rpm giving 200 g of a solution of 1% cellulose in NaOH 8% - water. These 1% cellulose solutions were directly centrifuged to isolate the insoluble fraction.

Isolation by centrifugation of the insoluble fractions. Centrifugation was performed on a HETTICH Universal 320RHK centrifuge equipped with a 1620A rotor and a JULABO cryostat. The centrifuge was settled at 9000 rpm (9050 g) and the centrifugation time was 5 minutes. The centrifuge tubes were refrigerated at 4°c before starting the centrifugation protocol. Despite the cryostat was set at 0°C, the temperature inside the rotating sample varied between 8 and 12°C due to centrifugation heating and heat loss between the cryostat and the centrifuge. The low concentration of cellulose (1%), the low temperature (below 15°C) and the short centrifugation time (5 min) prevent gelation of the samples during centrifugation.[13]

Optical microscopy observations of the insoluble fractions. After centrifugation, insoluble fractions were observed between two glass plates by optical microscopy in transmission mode with and without cross-polarizer with a Metallux 3 (Leitz) equipped with a high resolution 3-CCD camera JVC KY-F75U.

Amount of insoluble material and alkaline solubility. The insoluble fractions were washed in distilled water in several baths until the pH was neutral. The resulting products were dried overnight in an air oven at 50°C. Each fraction was weighed after total drying. The amount of insoluble fraction was defined as the following weight ratio: [Dried insoluble fraction] / [Initial dried sample introduced]. The alkaline solubility is thus defined as the inverse of the fraction of insoluble material amount. The measured pulp consistency of the samples introduced in the NaOH 8%- water solution was 96% (after drying in the same conditions as the insoluble fractions, i.e. 50°C in an air oven, overnight), i.e. the initial 2 g of sample introduced corresponds to 1.92 g of dried sample.

Results and discussion

Molecular structural changes after the enzymatic peeling treatment

The enzymes mixture is made of celluclast 1.5L and Econase HC 400. The Celluclast 1.5L contains a large spectrum of enzymes, most notably cellobiohydrolases (CBHs) and endo-1,4-β-glucanase (EGs).[14] These two enzymes are able to digest cellulose to give cellobiose and glucose. It is known that the EGs digest preferentially the easily available amorphous chains and that the CBHs are able to degrade crystalline zones.[15] In addition, CBHs are able to hydrolyze cellulose at both reducing and non-reducing ends by its two activities, CBHI and CBHII respectively.[14, 16, 17] The degradation of the amorphous zones by the EGs makes entrance points for the CBHs to attack crystalline cellulose.[18] This concerted action of CBHs with EGs is a synergism phenomenon that has been reported on both lignocellulosic substrates and pure cellulose substrates for varying cellulase systems.[14, 19-21] Amorphous zones were also shown to degrade much faster than crystalline zones.[18, 21] Crystallinity should thus increase during cellulose hydrolysis. However, due to varying and conflicting results on the change of crystallinity during hydrolysis, crystallinity is not considered as a determinant parameter to analyze the rate of enzymatic hydrolysis.[21] The Econase HC 400 is an endo-1,4-β-xylanase which attacks specifically xylan, i.e. arabinoglucoronoxylan, on interior portions of the chains to give xylose, arabinose and 4-O-MeGlcA.

Figure 1 shows that the sample weight decreases continuously for both VHV-S and SA pulps but much faster during the first 5 minutes. It means that the activity of the enzymes is effective but not constant all along the 30 minutes of peeling.

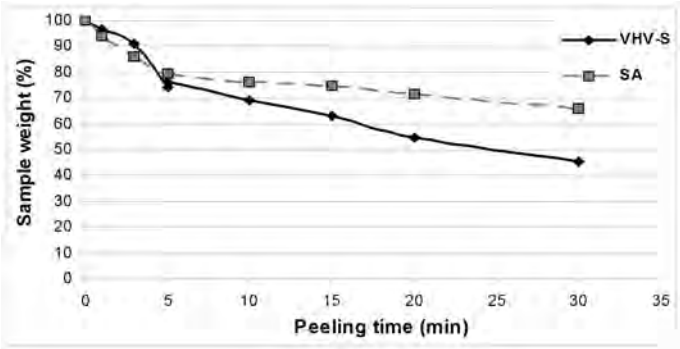

Figure 1. Evolution of the sample weight versus the peeling time for the VHV-S and SA pulps.

The evolution of the intrinsic viscosity (Figure 2), which can almost linearly correlated with the DP (see Experimental section), shows a large and fast decrease during the first 5 minutes before reaching a plateau at nearly 600 ml/g and 400 ml/g for VHV-S and SA respectively. The first fast decrease phase can be attributed to the action of the EGs which act on less ordered regions and interior portions of the chain and thus rapidly decrease the DP. Then, the CBHs, which act only on chain ends, decrease the DP only incrementally. These results are indeed supported by several studies which are reported in the well documented review of Zhang and Lynd.[21] In addition, Ramos *et al.*[22] and Pala *et al.*[23] showed that the Celluclast 1.5L has a more pronounced effect on the high molar masses.

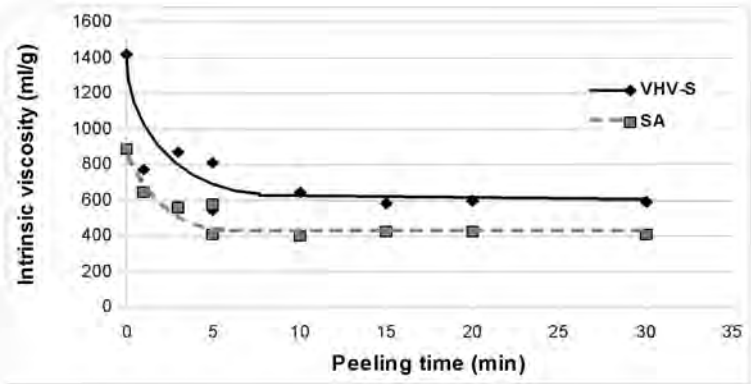

Figure 2. Evolution of the intrinsic viscosity versus the peeling time for the VHV-S and SA pulps.

This large decrease of DP should not be observed if the enzyme activity was localized only at the surface of the fibres. For a sample weight of 70%, i.e. 30% of the initial weight removed, the intrinsic viscosity represents only 45% of the initial intrinsic viscosity for both

SA and VHV-S pulp (Figure 3). The concept of peeling consisting that the enzymes digest the fibres layer by layer is thus not realistic. There is either a gradient of digestion inside the fibre or digestions deep inside the fibre. A gradient of digestion is understandable if the strong degradation of one layer is allowing enzymes to move more deeply inside cell walls, creating a degradation gradient. Another option is that enzymes are moving inside the wall through available pores and voids. In any case, the enzymes are active both in the outside and the inside of the fibres.

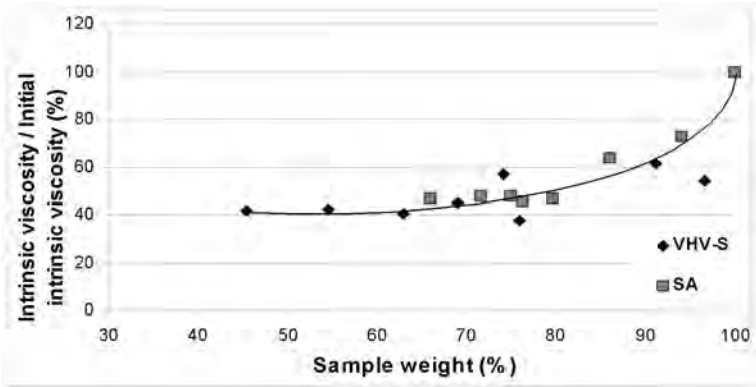

Figure 3. Intrinsic viscosity / Initial Intrinsic viscosity ratio versus the sample weight for the VHV-S and SA pulps.

Crystallinity follows the same evolution as the sample weight and the intrinsic viscosity. A large decrease of almost 50% of the initial crystallinity ratio is observed during the first 5 minutes, followed by a slow decrease (Figure 4).

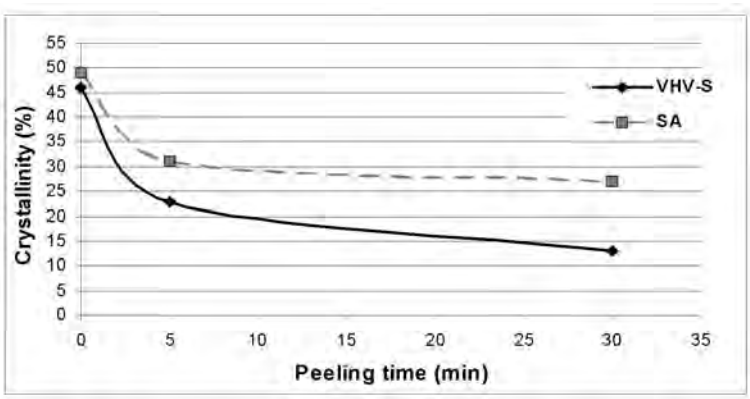

Figure 4. Evolution of the crystallinity versus the peeling time for the VHV-S and SA pulps.

The enzymatic peeling treatment is thus acting in two distinct phases. During the first 5 minutes, enzymes, especially EGs, attack randomly the cellulose chains and free cellulose blocks starting with the less ordered regions. This first phase has a strong effect of molecular destructuration on the fibre, and the DP and the crystallinity are nearly two times lower than in the original fibre. Then, the CBHs remove cellulose chains by chains. The sample weight and the crystallinity continuously decrease but only slowly. The overall DP is not affected and stays constant because some chains are not digested while others are totally digested. It has to be noticed that some side effect of the enzymatic hydrolysis could also have an influence on the lower activity of the enzymes after the first 5 minutes of treatment. In fact, an inhibition of the enzymes by the hydrolysis products, i.e. cellobiose and glucose, can happen depending of the accumulation of this product in the microenvironments in which hydrolysis occurs.[18]

Influence of the enzymatic peeling treatment on the macrostructural morphology

The trends of the intrinsic viscosity and the crystallinity have shown that the enzymes attack both the outside and the inside of the fibres. However, these results give no information about the effect of the enzymes on the fibre macrostructure. To evaluate in what extent the macrostructural morphology have been affected by the treatment, we have analyzed and compared the swelling and dissolution mechanisms of non-treated and treated samples between two glass plates without agitation. The solvent quality was adjusted to be in the zone where the ballooning phenomenon occurs, i.e. NMMO with 19 to 24 % of water and NaOH 8% - water.[24, 25]

In the ballooning zone, it is possible to clearly identify the behavior of the three main walls of wood and cotton fibres[9], i.e the primary wall, the S1 wall and the S2 wall. In NMMO-19 to 24% water, the inside of the fibre (S2 wall) fragments and dissolves, while the S1 wall swells significantly to form the membrane of the balloons and the primary wall breaks and rolls up to form unswollen sections and helices. Then, the S1 wall and the primary wall dissolve slowly. In NaOH-water system, no fragmentation of the S2 wall is observed but the large swelling of the secondary wall leads to the breaking of the primary wall which also forms helices and unswollen sections. Then, the fibres stay in this ballooned state if no agitation or shearing is applied to the system (see chapter IV).

If the external walls – the primary wall and the S1 wall – are removed, unswollen sections, helices and membranes should not be observed. Only fragmentation should be observed in the

case of NMMO-water system and only a large homogeneous swelling should be observed in the case of NaOH-water system. This hypothesis was checked. First non-treated fibres were observed. As can be seen on Figures 5a, 5d, 6a and 6d, non-treated pulps show a ballooning phenomenon meaning that the external walls were present, despite of the difference of sulphite treatment severity and intrinsic viscosity values (1430 ml/g for VHV-S and 880 ml/g for SA). The original wall structure is thus initially present in both VHV-S and SA samples.

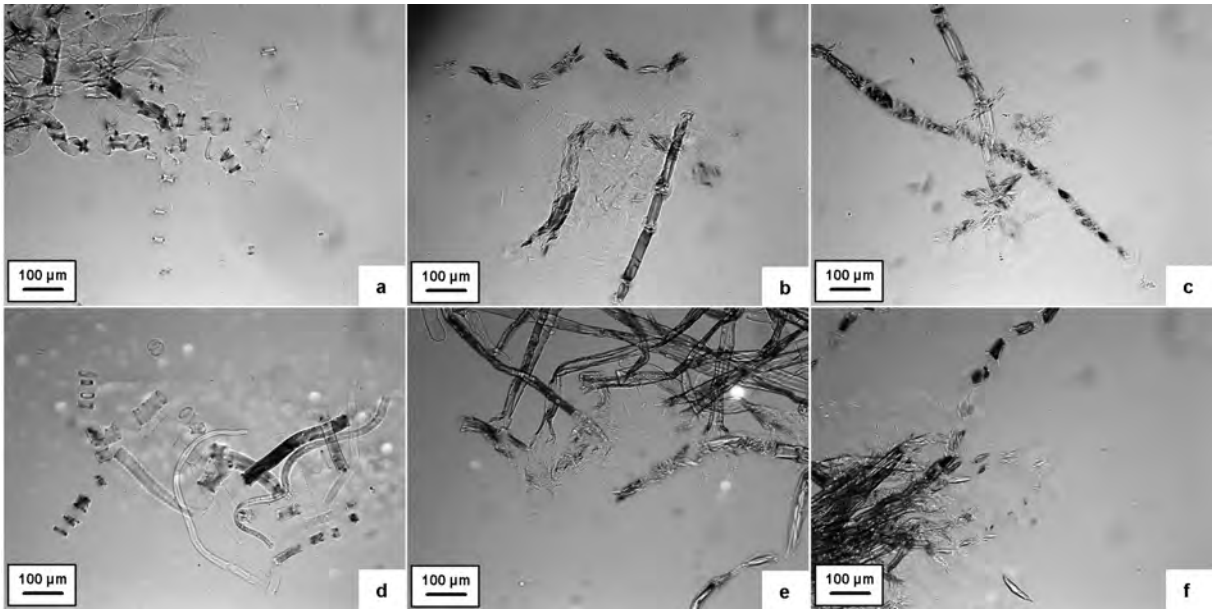

Figure 5. Swelling and dissolution behavior of VHV-S and SA pulp in NMMO- 22% water. (a) Non-treated VHV-S, (b) VHV-S after 3 min of enzymatic peeling and (c) VHV-S after 10 min of enzymatic peeling; (d) Non-treated SA, (e) SA after 3 min of enzymatic peeling and (f) SA after 10 min of enzymatic peeling.

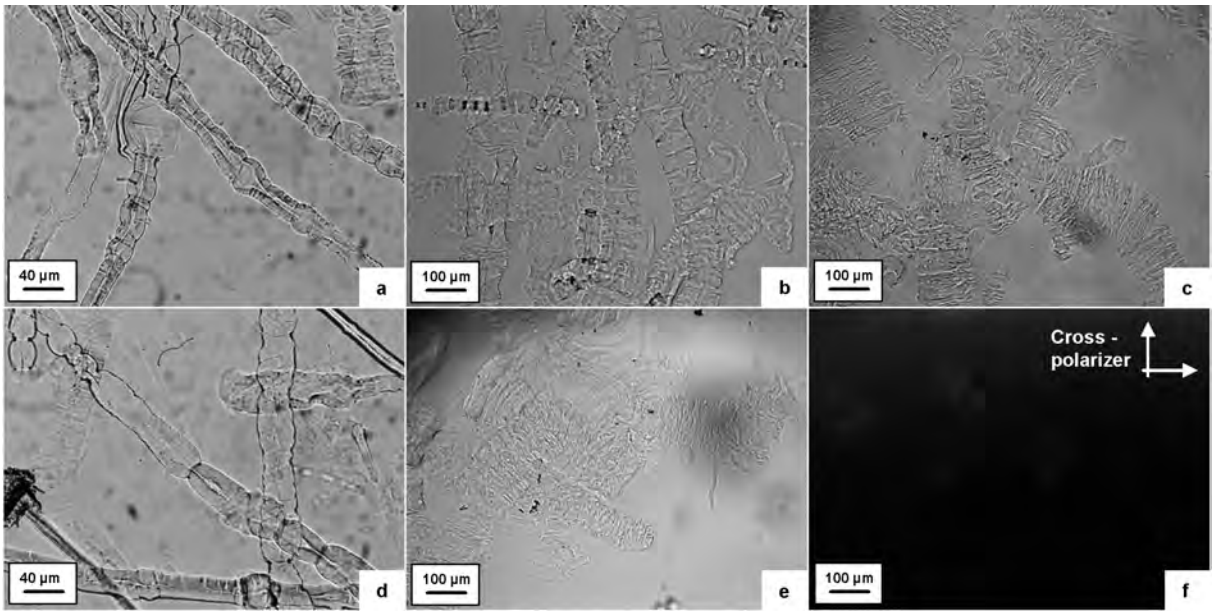

Figure 6. Swelling and dissolution behavior of VHV-S and SA pulp in NaOH 8%- water. (a) Non-treated VHV-S, (b) VHV-S after 3 min of enzymatic peeling and (c) VHV-S after 10 min of enzymatic peeling; (d) Non-treated SA, (e) SA after 10 min of enzymatic peeling and (f) SA after 10 min of enzymatic peeling observed between cross-polarizer.

After a short peeling time of around 3 min, the ballooning phenomenon almost completely disappears. Only fragmentation and some membrane parts are observable in NMMO- 22% water, as seen in Figures 5b and 5e. In NaOH 8%- water, fibres are largely swollen (100 µm in diameter) without helices and unswollen sections, as seen in Figure 6b. A few ballooned fibres are still observable (Figures 5b, 5e, 6b) showing that the enzymatic treatment was not fully homogeneous. The external walls, especially the primary wall, have thus been removed after a short peeling time which is in accordance with the results of Sjöberg obtained with the same enzymes mixture.[26]

At longer peeling time, fibres dissolve by fragmentation in NMMO - 22% water (Figures 5c and 5f) and swell dramatically (almost 200µm) in NaOH 8%- water (Figures 6c and 6e) meaning that the external walls have been totally removed and that the structure of the fibre has been very damaged by the enzymatic hydrolysis. Moreover, there is no visible birefringence of the highly swollen fibres and sections observed in NaOH 8%- water (Figure 6f) which indicates that the crystalline zones have entirely disappeared (or at least are of such small size that they do not generate a visible birefringence) and that all orientational order has disappeared.

The enzyme mixture used has thus two effects at short peeling times, (i) a digestion of the primary wall which is seen by the near absence of ballooning and (ii) a destructuration action in the inside of the fibre which is seen by the large decrease of DP. At long peeling time, the external walls are totally digested and the fibre structure is totally destructured, as seen by the absence of birefringence.

Observations and quantification of insoluble material in NaOH- water system

The different samples were dissolved in NaOH 8% - water as described in the Experimental section. The resulting solutions were centrifuged to isolate the insoluble material fractions. We showed in chapter IV that the dissolution of wood fibres in NaOH 8%- water solutions occurs by successive dismantlement and fragmentation mechanisms mainly governed by the high swelling and the shearing involved during the solution preparation. The different steps of dissolution leads to a soluble phase probably mainly composed of cellulose aggregates.[27]

The observation by optical microscopy of the insoluble material clearly shows the two effects of the enzymatic peeling treatment, i.e. the removal of the external walls and the destructuration of the fibre. Non-treated samples mostly stay in a low swelling or ballooned state even after two hours of mixing (Figures 7a and 7d). The SA sample contains fibres with high swelling ratio which can be related to the more severe digestion of the fibres during the original sulphite pre-treatment. Several fibres are cut in sections due to the shearing involved by the mixing and few fragments can also be observed. After 2 min of peeling, the shape of the insoluble parts is changing drastically. Only highly swollen sections and flat rings are observed (Figures 7b and 7e). The removal of the primary wall by the enzymatic peeling gives a large swelling of the fibres and a subsequent cutting in flat rings. This cutting in flat rings was observed when putting and submitting fibres to shearing in NaOH 8%- water, independently of the origin and the preparation mode of the wood pulp. With fibres without primary wall, the large swelling was shown to be sufficient to dismantle the fibres in highly swollen sections and flat rings (chapter IV). At longer peeling time, the insoluble material is made of small fragments implying that the fibres were totally destructured by the enzyme treatment (Figures 7c and 7f).

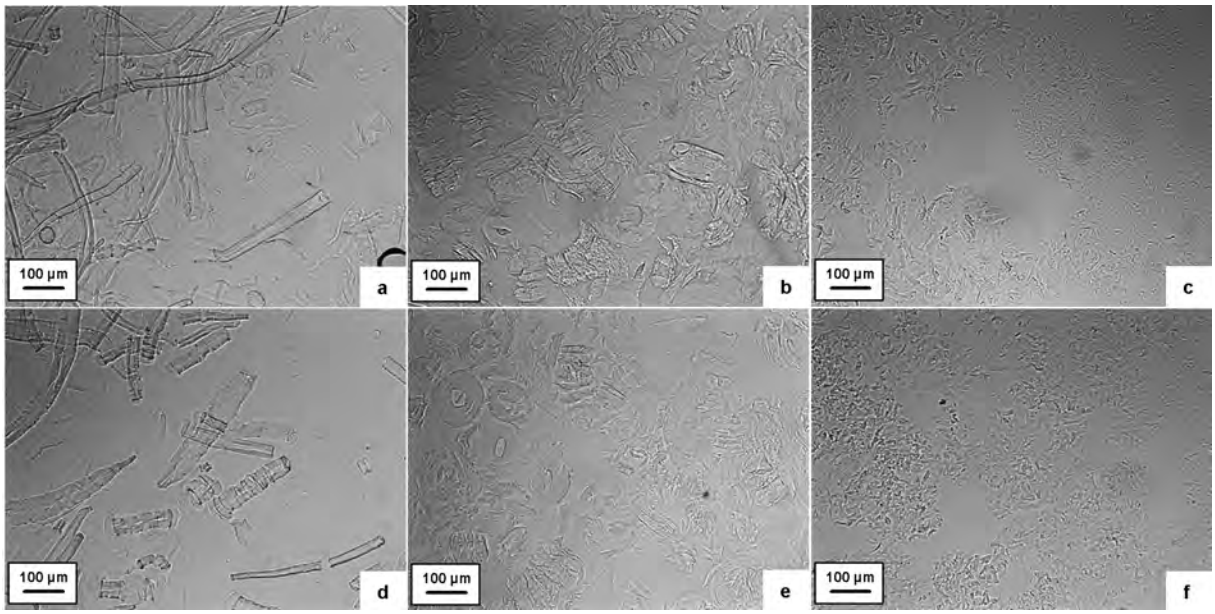

Figure 7. Observations by optical microscopy of the insoluble material in a NaOH 8% -water solution. (a) Non-treated VHV-S, (b) VHV-S after 2 min of enzymatic peeling and (c) VHV-S after 30 min of enzymatic peeling; (d) Non-treated SA, (e) SA after 2 min of enzymatic peeling and (f) SA after 30 min of enzymatic peeling.

The evolution of the amount of insoluble material as a function of peeling time is divided in two main phases (Figure 8). During the first minutes of treatment, the amount of insoluble material decreases quickly. Then it decreases very slowly and the alkaline solubility reaches a plateau. The evolution of the alkaline solubility is related with all the structural changes that occurred upon the enzymatic peeling treatment.

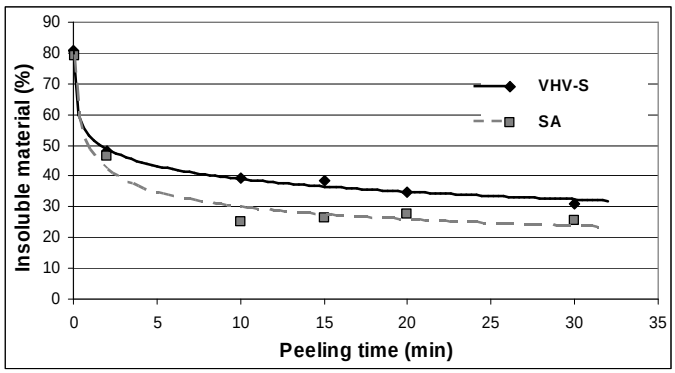

Figure 8. Evolution of the amount of insoluble material versus the peeling time for the VHV-S and SA pulps in NaOH - 8% water.

Relationship between the structural changes and the alkaline solubility

As can be seen on Figure 9, the amount of insoluble material follows a linear relationship as a function of intrinsic viscosity and crystallinity. A simple way to explain the evolution of the alkaline solubility after the enzymatic treatment is thus to associate the increase of solubility to the decrease of the DP and of the crystallinity. This interpretation is supported by several studies.[8, 9]

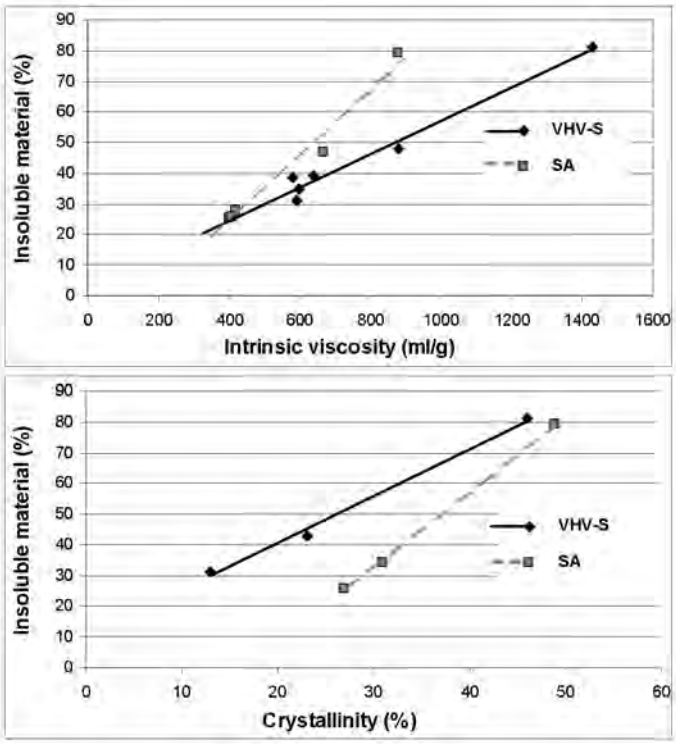

Figure 9. Relationship between the amount of insoluble material and the intrinsic viscosity (up), and the crystallinity (down) for the non-treated and treated VHV-S and SA pulps.

However, the morphological study of the insoluble parts gives a more comprehensive interpretation on the influence of the structural changes due to the enzymatic treatment on the alkaline solubility. Figure 10 gives the amount of insoluble material of the non-treated (A, B) and 2 min enzymatically treated (C, D) SA and VHV-S pulps and of the LV-U pulp (E). By following the dotted line number 1 of Figure 10, an interesting result is found. Despite the large difference of intrinsic viscosity of the two original SA and VHV-S pulps (880 ml/g and 1430 ml/g respectively), the amount of insoluble material is nearly the same. The DP is thus not the only parameter that governs the alkaline solubility after enzymatic treatment. This result was already found in chapter IV. The dotted line number 2 of Figure 10 shows that the amount of insoluble material of the treated VHV-S sample (D, black diamond) is nearly two

times lower than the original SA sample (A, grey square) while keeping the same intrinsic viscosity. This observation has to be related with the removal of the external walls that occur during the first minutes of treatment. The external walls are still present in the original SA sample (Figure 7d) while they have been removed in the 2 min treated VHV-S sample (Figure 7b). The removal of the external walls allows a higher swelling and thus eases the dismantlement and the fragmentation of the fibres during the solution preparation. The dotted line 3 shows that the LV-U sample (E) which was not enzymatically treated present similar amount of insoluble material as compared to the treated SA and VHV-S samples (C, D) while its intrinsic viscosity is more than two times lower. The enzyme destructuration allows to have a better solubility by favoring the fragmentation of the fibres during the dissolution.

The removal of the external walls and the macrostructural destructuration of the fibres must thus be considered as key factors in the dissolution of wood fibres in NaOH 8%- water.

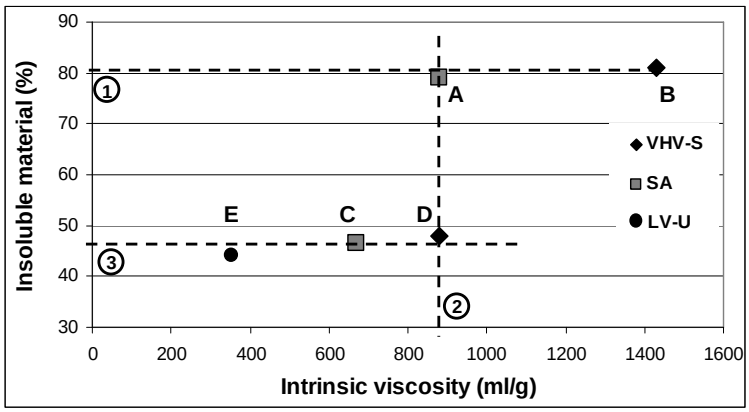

Figure 10. Final amount of insoluble material versus the intrinsic viscosity for the non-treated SA and VHV-S pulps (A, B), the 2 min treated SA and VHV-S pulps (C, D) and the non-treated LV-U pulp (E).

Conclusions

The enzymatic peeling treatment used in this study is giving important structural changes on the two treated wood pulps. Aside decreasing DP and crystallinity, the enzymes mixture is able to remove the external walls and to destructure the fibres at the macrostructural level. The action of the enzymes and the associated products after the dissolution of the treated samples in NaOH 8% - water are schematically represented in Figure 11.

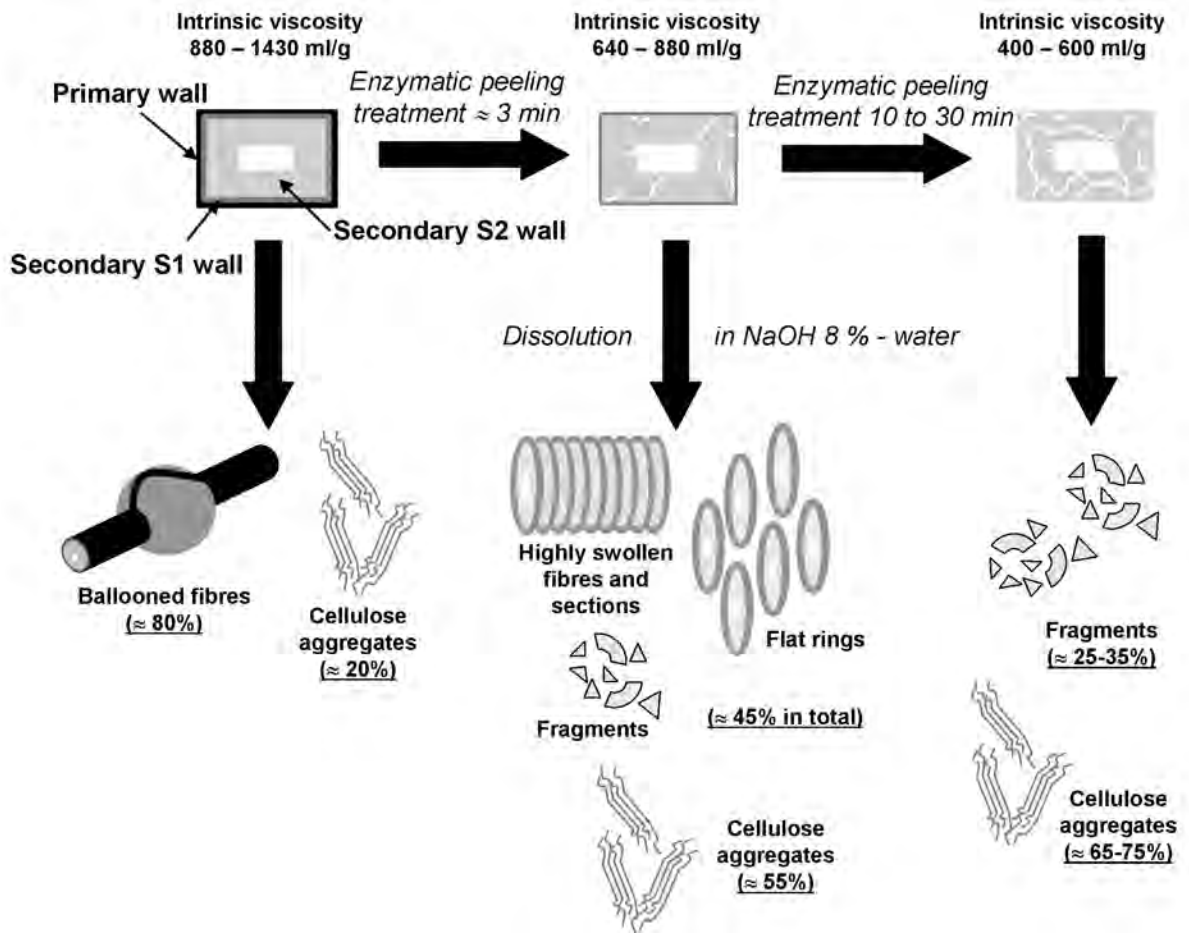

Figure 11. Schematic representation of the action of enzymes on the macrostructural morphology of the fibre and its associated dissolution products in NaOH - 8% water.

Beyond the classical thermodynamic considerations evocated for the increase of solubility after enzymatic treatment, we have shown that the removal of the external walls and the macrostructural destructuration of the fibre are key factors in the dissolution capacity of wood cellulose fibres. In fact, these morphological changes ease the swelling and the breaking of the fibres into fragments in NaOH 8% - water solutions and thus favor dissolution. These results are supported by the chapter IV where it is shown that the macrostructural destructuration involved by steam explosion or acidic hydrolysis also leads to the same dissolution mechanisms. The microenvironment around the cellulose chains, e.g. the hemicelluloses complex, is also an important parameter to consider for the dissolution of cellulose fibre since the insoluble material contain more hemicelluloses than the soluble fraction.

References

(1) Klemm, D.; Philipp, B.; Heinze, T.; Heinze, U.; Wagenknecht, W. In *Comprehensive Cellulose Chemistry*, 1, Wiley-VCH, Weinheim, 1998.

(2) Krässig, H. A. In *Cellulose - Structure, Accessibility and Reactivity*, Polymer Monographs 11, ed. M.B. Huglin, Gordon and Breach Science Publishers, Amsterdam, 1993.

(3) Wormald, P.; Wickholm, K.; Larsson, P. T.; Iversen, T. *Cellulose*, **1996**, 3, 141–152.

(4) Yamashiki, T.; Matsui, T.; Saitoh, M.; Okajima, K.; Kamide, K.; Sawada, T. *Brit. Polym. J.*, **1990**, 22, 73–83.

(5) Fischer, K.; Goldberg, W.; Wilke, M. *Lenzinger Ber.*, **1985** , 85, 32–39.

(6) Isogai, A.; Atalla, R. H. *Cellulose*, **1998**, 5, 309–319.

(7) Le Moigne, N.; Montes, E.; Pannetier, C.; Höfte, H.; Navard, P. *Macromol. Symp.*, **2008**, 262, 1, 65–71.

(8) Cao, Y.; Huimin, T. *Appl. Microbiol. Biotechnol.*, **2006**, 70, 176–182.

(9) Rahkamo, L.; Siika-Aho, M.; Vehviläinen, M.; Dolk, M.; Viikari, L.; Pertti, N.; Buchert, J. *Cellulose*, **1996**, 3, 153–163.

(10) Sjöberg, J.; Potthast, A.; Rosenau, T.; Kosma, P.; Sixta, H. *Biomacromolecules*, **2005**, 6, 3146–3151.

(11) Brown, W., Wikstrom, R. *Eur. Polym. J.*, **1965**, 1, 1–10.

(12) Baldinger, T.; Moosbauer, J.; Sixta, H. In *Supermolecular structure of cellulosic materials by fourier transform infrared spectroscopy (FT-IR) calibrated by WAXS and 13C NMR*, Internal report from LENZING AG, A- 4860 Lenzing, Austria, 2005.

(13) Roy, C.; Budtova, T.; Navard, P. *Biomacromolecules*, **2003**, 4, 259–264.

(14) Rosgaard, L.; Pedersen, S.; Langston, J.; Akerhielm, D.; Cherry, J. R., Meyer, A. S. *Biotechnol. Prog.*, **2007**, 23, 1270–1276.

(15) Henrissat, B.; Driguez, H.; Viet, C.; Schülein, M. *Nature Biotechnol.*, **1985**, 3, 722–726.

(16) Rouvinen, J.; Bergfors, T.; Teeri, T.; Knowles, J. K.; Jones, T. A. *Science*, **1990**, 249, 380–386.

(17) Divne, C.; Ståhlberg, J.; Reinikainen, T.; Ruohonen, L.; Pettersson, G.; Knowles, J. K.; Teeri, T.T.; Jones, T. A. *Science*, **1994**, 265, 524–528.

(18) Lynd, L. R.; Weimer, P. J.; Van Zyl, W. H.; Pretorius, I. S. *Microbiol. Mol. Biol. Rev.*, **2002**, 66, 506–577.

(19) Gusakov, A. V.; Salanovich, T. N.; Antonov, A. I.; Ustinov, B. B.; Okunev, O. N.; Burlingame, R.; Emalfarb, M.; Baez, M.; Sinitsyn, A. P. *Biotechnol. Bioeng.*, **2007**, 97, 1028–1038.

(20) Mansfield, S. D.; Meder, R. *Cellulose*, **2003**, 10, 159–169.

(21) Zhang, Y-H. P.; Lynd, L. R. *Biotechnol. Bioeng.*, **2004**, 88, 797–824.

(22) Ramos, L. P.; Zandoná Filho, A.; Deschamps, F. C., Saddler J. N. *Enzyme Microb. Technol.*, **1999**, 24, 371–380.

(23) Pala, H.; Manuel, M. ; Gama, F. M. *Carbohydr. Polym.*, **2007**, 68, 101–108.

(24) Cuissinat, C.; Navard, P. *Macromol. Symp.*, **2006**, 244, 1–18.

(25) Cuissinat, C.; Navard, P. *Macromol. Symp.*, **2006**, 244, 19–30.

(26) Sjöberg, J. In *Characterization of chemical pulp fibre surfaces with an emphasis on the hemicelluloses*. Ph.D. Thesis, Fibre and Polymer Technology, Stockholm : KTH Royal Institute of Technology, **2002**, p 40, http://www.diva-portal.org/kth/abstract.xsql?dbid=3462.

(27) Schulz, L.; Seger, B.; Burchard, W. *Macromol. Chem. Phys.*, **2000**, 201, 2008–2022.

Chapter VI

Contraction and rotation of natural and regenerated cellulose fibres during swelling and dissolution.

Contraction and rotation of natural and regenerated cellulose fibres during swelling and dissolution

Abstract Upon swelling and dissolving, native cellulose fibres such as cotton of wood are rotating and contracting. Regenerated fibres like Lyocell are only contracting. Cotton has two rotation mechanisms, a macroscopic one due to the untwisting of the twisted fibre initially induced by the drying and a microscopic rotation that is also seen in wood fibres. The microscopic rotation is thought to be due to the elongation phase of the cell that is bringing the deposed helical orientation of the cellulose chain out of equilibrium, leading to internal stress unbalance that is released during swelling. Contraction originates from the fact that the cellulose chains are in an extended conformational state due to the spinning process for the regenerated fibres and to the bio-deposition process for native fibres. The contraction is related to the change of the mean conformation of cellulose chains from an extended state to a more condensed state.

Introduction

Swelling and dissolution of cellulose have been investigated in many solvents over the last century. For several important industrial applications like making fibres, films, sponges or derivatives, cellulose must be dissolved since it cannot be melted as common synthetic polymers. When placed in a swelling agent or a solvent, natural cellulose fibres can show a non regular swelling along the fibre. The most spectacular effect of this non regular swelling is the ballooning phenomenon where swelling takes place in some selected zones along the fibre. The ballooning has been observed long ago, first by Nägeli in 1864 [1], then by several authors [2,6] (Numerous other studies are also reported in reference [7]).

More recent studies of Chanzy *et al.* in 1983 [8] and Cuissinat and Navard in 2006 [9] showed that the dissolution mechanisms of cellulose fibres are strongly depended of the solvent quality. The last authors identified five main dissolution modes for wood and cotton fibres as a function of the quality of the solvent in *N*-methylmorpholine-*N*-oxide (NMMO) - water with various amounts of water (the lower the amount of water is, the better the solvent is): fast dissolution by fragmentation under 17% water, large swelling by ballooning, then dissolution between 19 to 23.5 % water, large swelling by ballooning, but no complete dissolution between 25 to 30 % water, homogeneous swelling and no dissolution between 35 to 40 %

water, and very low swelling above 40 % water. Similar mechanisms were also observed when using solvents as NaOH-water with or without additives,[10] ionic liquids[11] and other chemicals[12] for a wide range of plant fibres[13] and some cellulose derivatives that were prepared without dissolution.[14] These studies showed that the main parameter that governs the dissolution mechanisms, jointly with the solvent quality, is the morphology of the fibre. If the original wall structure of the native fibre is preserved, the general dissolution mechanisms are mostly similar for wood, cotton, other plant fibres and some cellulose derivatives.

In a recent paper,[15] the existence of a centripetal radial gradient in the dissolution capacity within cotton fibres was demonstrated. The older was the cellulose deposition, the more difficult it is to dissolve it. These results can be related to age-dependent structural re-organisations in the cell wall layers or more probably to the presence of non-cellulosic polysaccharide networks in the outside walls. The behaviour in swelling and dissolution of cellulose fibres is thus highly dependent of the chemical and the morphological structure of the successive deposited layers.

It has always been observed that the swelling and dissolution of fibres are also accompanied by several macroscopic movements, especially in moderate quality solvent, either or both rotation and contraction of the fibre. If the solvent is very good, the fast dissolution by fragmentation does not allow to observe such movements. If the solvent is very bad, i.e. being only a weak swelling agent, only untwisting rotation is observed in the case of cotton hairs.[7, 16]

The focus of this paper is to investigate the contraction and the rotation movements that occur during swelling and dissolution in moderate quality solvent, their influence on swollen morphologies and their origins for various cellulose fibre sources.

Experimental

Materials and solvents. Three very different cellulose samples were used: cotton hairs, *Gossypium barbadence*, with a fibre diameter of 15 µm provided by INRA (France), a sulphite spruce wood pulp, BBUE, with a fibre diameter of 20-30 µm provided by Borregaard (Norway) and Lyocell regenerated fibres, Tencel®, with a fibre diameter of 11 µm provided by Lenzing AG (Austria). The BBUE wood fibre presents a high intrinsic viscosity value (1700 ml/g) and its original wall structure is supposed to be almost preserved.

The swelling and dissolution treatments were performed in mixtures of *N*-methylmorpholine *N*-oxide (NMMO) and water at 90°C. The water content was varied from 20 to 23% w/w such as being able to dissolve (i) cotton hairs and wood fibres after the production of balloons and (ii) regenerated fibres after a large swelling (between 20 and 23 % of water, the NMMO - water mixture is considered as a moderately good solvent for cellulose [9, 15]).

Experimental Protocol. The experiments were performed by mixing the fibres and the solvent in a container made of two glass plates separated with double-sided tape. The solvent, previously heated at 90°C and contained in a pipette, was introduced by capillary forces between the two plates. Fibres were freely floating in the solvent and no agitation was applied to the mixture.

Observations method. The swelling and dissolution of fibres were observed by optical microscopy with a Metallux 3 (Leitz) equipped with a Linkam TMS 91 hot stage. The samples were investigated in transmission mode, at 90°C. To obtain high resolution pictures, the microscope was equipped with a high resolution numerical reflex camera (3000*2000 pixels) CANON D100 (Figure 1, 3, 4a, 6) and a high resolution 3-CCD camera (1360*1024 pixels) JVC KY-F75U (Figure 4b, 5). An enhancement of the contrast and the exposure was performed with Photoshop® software to obtain a better visualization of the fibres when needed. Fibres were also observed by scanning electron microscope (SEM) used in environmental mode with the following parameters: 5.5 mbar, 15 keV, relative humidity 30% (Figure 1b, 2). In this case, the dissolution process was stopped by a sudden addition of water and the fibre was extracted from the two glass plates and deposited on the SEM sample holder.

Results and discussion

First stage of ballooning for cotton hairs and wood fibres- rolling up of the primary wall

One classical explanation for the ballooning phenomenon is that the swelling of the cellulose present in the secondary wall is causing the primary wall to extend and burst. According to this view, the expanding swollen cellulose pushes its way through the tears in the primary

wall, the latter rolls up in such a way as to form helices and collars which restrict the uniform expansion of the fibre and forms balloons as described by Ott.[17]

As it was recently demonstrated, the secondary wall is the easiest to dissolve as compared to the external walls which contain larger amount of non-cellulosic components.[15] The solvent thus goes inside the fibre through the primary wall which is permeable to the solvent but not easy to dissolve and not extensible (Figure 1a). It was shown that the S2 wall dissolves by fragmentation[15] and the consequence is that the S1 wall swells transversely. The optical observations shows that the primary wall breaks (Figure 1b) in one or more places under the pressure of the S1 wall and then rolls up, forming threads and collars.

This rolling-up is clearly due to a stress release, in the same way as bi-component structures.[18, 19] This implies that there is a gradient of polymer organisation from the outside to the inside of the primary wall. One explanation can be the fact that the primary wall is built and at the same time elongated. This should induce a much larger deformation of the layer deposited first than the layer deposited when the cell is at almost its maximum size.[16] The high elongation of the external parts is released when the primary wall is detached from the fibre due to the swelling of the balloon, this implying a rolling up of the wall. This phenomenon is similar to what happens when a polymer part, having frozen stresses due to non equilibrium conformation of polymer chains induced by a fast cooling, is cut in small slices. The level of rolling is linked to the difference of released stress between the two sides of the layer.[20]

The primary wall thus forms threads and collars. Threads are formed when the primary wall rolls perpendicular to the fibre axis. Collars are formed when the rolling occurs in the fibre direction. The choice between these two directions is depending on the way the primary wall is broken (i.e. depends of the shape of the cut). The collars block the swelling of the regions where they are located, forming what has been called the unswollen sections (usually a region between two balloons). When the S2 wall is fully dissolved, the swelling of the balloons reaches its maximum (around 450 %). The balloon is formed of the dissolved S2 wall cellulose inside an undissolved membrane composed of the swollen S1 wall and surrounded by one or more threads of the primary wall (Figure 1c).

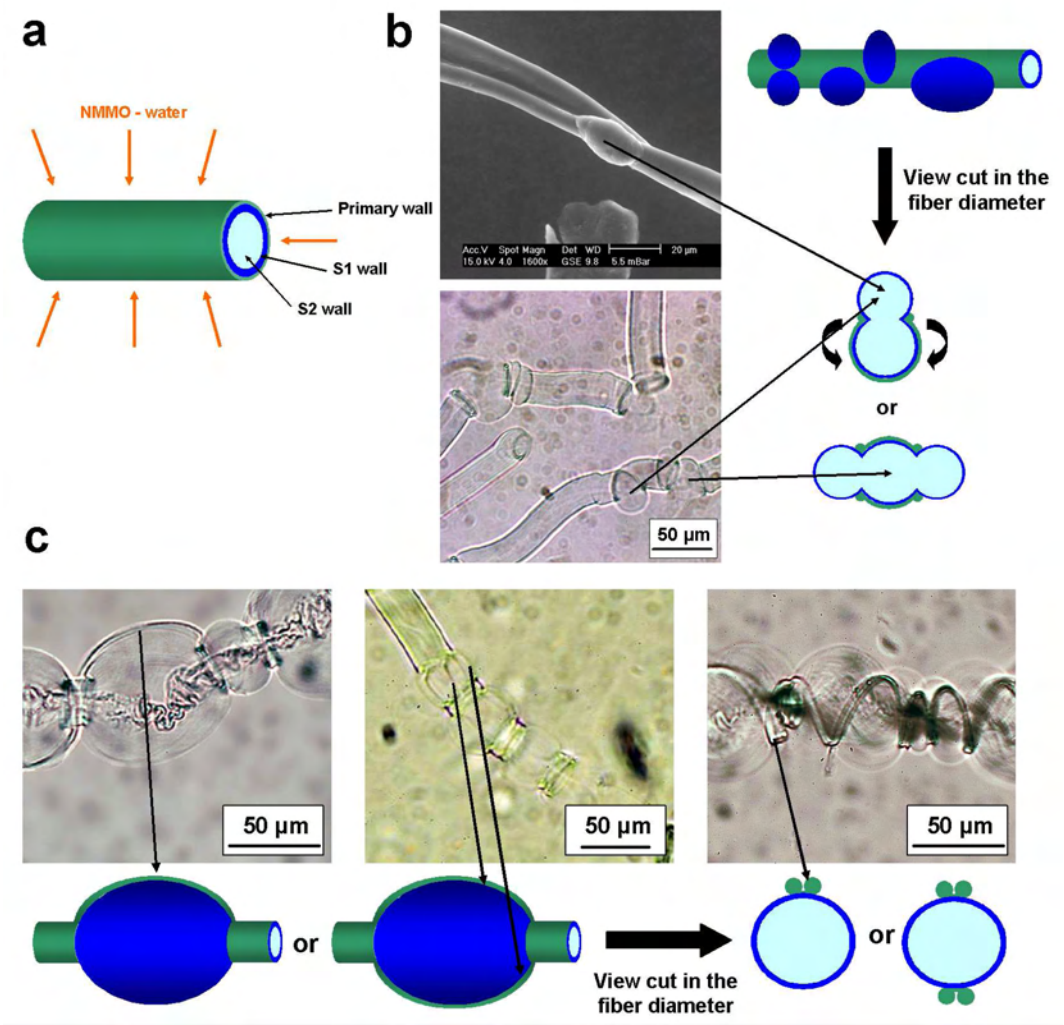

Figure 1. (a) First stage of ballooning: access of the solvent inside the fibre through the primary wall; (b) Second stage: birth of the balloons, swelling of the S1 wall due to the dissolution of the S2 wall, breakage and rolling up of the primary wall; (c) Third stage: shaping of the balloons, the S2 wall is fully dissolved, and hold by the S1 wall which forms the membrane of the balloons. The primary wall forms threads and collars which surrounds the balloons. As soon as it is broken, the primary wall rolls perpendicular to the fibre direction around the balloon, over the two opposite directions (each for each lip of the cut), forming a thread made of two cylinders, clearly seen on the picture.

Rotation in cotton hairs, wood fibres and regenerated fibres

Cotton hairs: for cotton hairs, two rotations are playing a role. One is a macroscopic rotation of the hair due to an untwisting upon re-wetting.[7] It is not related to the dissolution and can be observed with a slight swelling in water. Dried hairs received after harvesting are

highly twisted. The formation of these twists (Figure 2) occurs during the first drying of the cotton hairs in the boll, called the dehydration or desiccation step. Twists are attributed to localized overlaps of the S and Z reversals among concentric cellulose layers which create stresses and thus mechanical unbalances.[16]

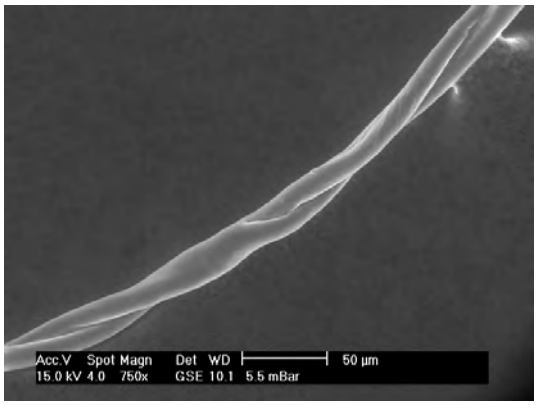

Figure 2. Twists of a *Gossypium barbadence* cotton hair observed by SEM.

A second rotation occurs, that we will call "microscopic rotation", when the cotton hairs are swelling and dissolving. This rotation induces the formation of helices from the broken primary wall threads around the balloon (Figure 3). Depending of the way the primary wall broke, leading to one or more rolled primary wall threads, one or more helices can be observed.

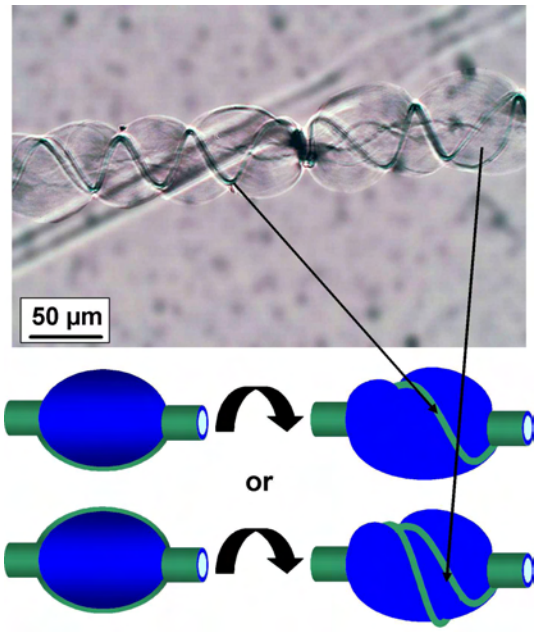

Figure 3. Formation of helices, due to the "microscopic rotation" that occurs during the swelling and dissolution of a *Gossypium barbadence* cotton hair.

Wood fibres: there is no "macroscopic rotation" (dried wood fibres have no pronounced, regular twisting). The "microscopic rotation" phenomenon is present but not so well defined. The threads can stay at the edge of the balloons as shown on Figure 4 a, after having rolled in the fibre direction. However, more pronounced helices were sometimes observed with wood fibres. This was attributed to the way the primary wall bursts during the first stage of ballooning which can creates helices without necessarily undergoing rotation.

Regenerated fibres: the regenerated lyocell fibres do not show any rotation and as was reported in chapter III, the final swollen morphology before total dissolution is a large homogeneous swelling (Figure 4 b). This is clearly due to the lack of complex morphologies. Regenerated Lyocell fibres have a simple, well oriented along fibre axis morphology without walls.[21] even if a weak skin-core morphology exist due to the sudden dripping of the spun fibre in the regenerated bath, with a very thin skin.[22]

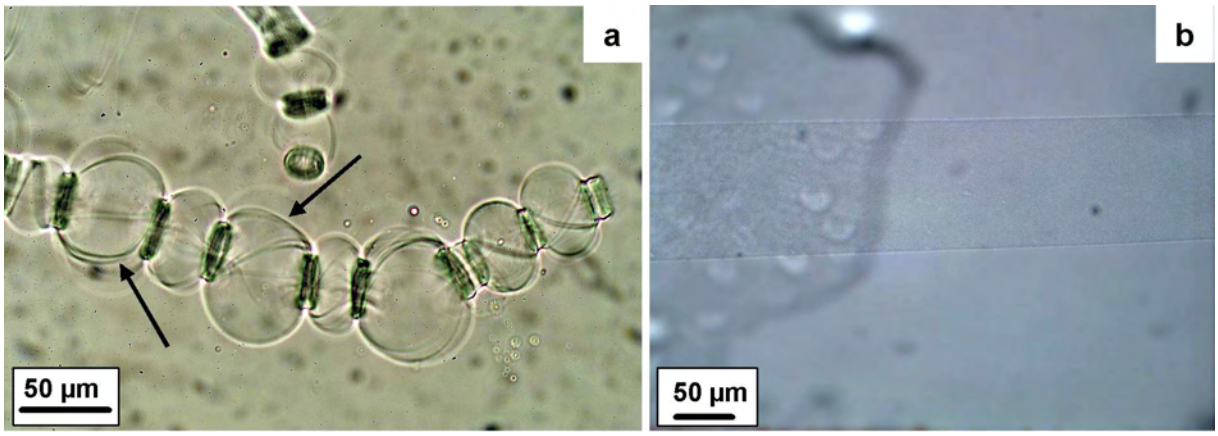

Figure 4. (a) Helices in the case of a BBUE wood fibre. The threads can stay at the edge of the balloons (black arrows); (b) Large homogeneous swelling in the case of a regenerated Lyocell fibre. There is no detachment of any part, and thus no helices or collars.

Microscopic rotation: the microscopic rotation is the one that is shown both for cotton hair and wood fibres as a consequence of the large swelling and dissolution of the S2 layer. There is a rotation of fibres when they are swelling because some frozen stress is released. The fact that regenerated fibres are not showing any rotation suggests that the origin of this untwisting rotation lies in the deposition structure and kinetics of the S1 and/or S2 layers of cotton and wood cells. A first morphological parameter is the angles the cellulose microfibrils are making towards the wood fibre or cotton hair axis. Cellulose microfibrils in wood fibre

generally have orientation angle of about 50-70° [23] or 70-90° [24] in S1 wall and 0-30° in S2 wall. [25] In cotton hairs, these angles are 20-30° and 35-45° for S1 and S2 wall, respectively.[7] The cellulose chain are thus deposited about at these angle by biosynthesis mechanism and the Cellulose Synthase Complexes (CSC) are moving along the wall with same angles, as was beautifully visualised recently.[26] When performing this deposition, there should be no associated unbalance of stress and there should be no untwisting during swelling since the equilibrium state is the helical one.

One possible origin of the microscopic rotation is the fact that the S1 layer is deposited while the fibres are still growing. The deposition angle is thus higher than the one obtained at the beginning of the elongation phase. This is creating a compression stress that is released during swelling and dissolution, when the fibres can be more mobile. The microscopic rotation may also originate from differences in mechanical properties inside the fibre due to the S and Z reversals that creates mechanical properties unbalances in the diameter of the fibre and consequently a rotation effect during swelling and dissolution due to the increased mobility of the fibres.

Contraction in cotton hairs, wood fibres and regenerated fibres

In addition, to the rotation phenomenon described above, a contraction of the fibres is observed during swelling and dissolution. We reported in chapter III that the contraction forces occurring during swelling and dissolution are so high that they can break the fibre when maintained at its two ends. As shown on Figure 5, ballooned wood fibres undergo large contraction of nearly 40 %. Contraction is also observed for cotton hairs (around 45%) and regenerated fibres (around 50 %).

Such large contractions are clearly due to the mechanism of cellulose chain deposition in cell walls (for native fibres) and to the spinning process for regenerated fibres. In both cases, cellulose chains are strongly oriented. In the case of regenerated fibres, the cellulose solution dope is very viscous and passes through a spinneret where shear forces orient the cellulose chains in the spinning direction. The cellulose solution fibre is then strongly elongated in an air gap before being suddenly regenerated in a water bath. Cellulose chains are frozen in a strongly extended conformation, out of equilibrium. The result is the well-known highly oriented morphology of lyocell fibres where both the crystalline and non-crystalline phases have their cellulose chains strongly oriented in the fibre direction. For different physical reasons, but somewhat for similar processing reasons, cellulose chains in cotton or wood cell are also in an extended conformational state, out of equilibrium. Here, the reason is due to the

deposition mechanism, where the cellulose synthase complex extrudes chains that are condensing into a crystalline microfibril, thus in an extended conformational state.

Upon partial dissolution or swelling, molecular mobility allows cellulose chains to try returning to an equilibrium conformation, with a much smaller end-to-end distance. The equilibrium end-to-end distance value depends on the swelling or dissolving agent. The strong network of hydrogen bonds among all chains brings the whole cellulose fibre to contract due to the return to conformational equilibrium of the individual chains. This is most probably a non linear process, some chains being able to contract without contracting the whole fibre.

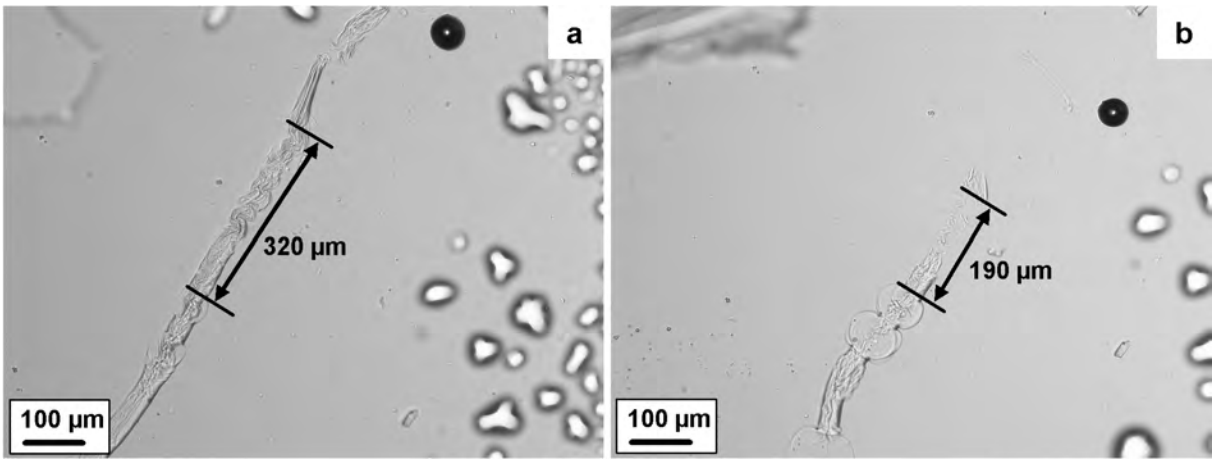

Figure 5. (From a to b) Contraction during the swelling and dissolution of a BBUE wood fibre.

Conclusions

The rotation and contraction of cellulose fibres that occur during swelling and dissolution are strongly dependent of the morphological structure of the cellulose fibres. The rotation phenomenon occurs only for native fibres like cotton or wood. It originates from mechanical properties unbalances due to the elongation phase of the cells. Contraction upon swelling is seen for both native and regenerated fibres. It is due to the fact that the cellulose chains are in an extended conformational state due to the spinning process for the regenerated fibres and to the bio-deposition process for native fibres. The contraction is related to the change of the mean conformation of cellulose chains from an extended state to a more condensed state. We showed in chapter III that when these movements are prevented by fixing the fibre at its two ends under tension, the dissolution capacity of cellulose fibres is restricted.

References

(1) Nägeli, C. *Sitzber. Bay. Akad. Wiss. München*, **1864**, 1, 282–323, 2, 114–171.

(2) Pennetier, G. *Bull. Soc. Ind. Rouen*, **1883**, 11, 235–237.

(3) Flemming, N.; Thaysen, A. C. *Biochem. J.*, **1919**, 14, 25–29, **1921**, 14, 407–415.

(4) Marsh, J. T. *The growth and structure of cotton, Mercerising*. Chapman & Hall Ltd, London, 1941.

(5) Hock, C. W. *Text. Res. J.*, **1950**, 20, 3, 141–151.

(6) Tripp, V. W.; Rollins, M. L. *Anal. Chem.*, **1952**, 24, 1721–1728.

(7) Warwicker, J. O.; Jeffries R.; Colbran R. L.; Robinson R. N. In *A Review of the Literature on the Effect of Caustic Soda and Other Swelling Agents on the Fine Structure of Cotton,* Shirley Institute Pamphlet; St Ann's Press, England, 1966; Vol. 93, p 17.

(8) Chanzy, H.; Noe, P.; Paillet, M.; Smith, P. *J. Appl. Polym. Sci.*, **1983**, 37, 239–259.

(9) Cuissinat, C.; Navard P. *Macromol. Symp.*, **2006**, 244, 1–18.

(10) Cuissinat, C.; Navard P. *Macromol. Symp.*, **2006**, 244, 19–30.

(11) Cuissinat, C.; Navard, P.; Heinze, T. *Carbohydr. Polym.*, **2008**, 72, 590–596.

(12) Cuissinat, C. *Swelling and dissolution mechanisms of native cellulose fibres*. Thèse de doctorat, Ecole des Mines de Paris, Sophia-Antipolis, 2006, http://pastel.paristech.org/2729/01/these-Cuissinat.pdf

(13) Cuissinat, C.; Navard, P. *Cellulose*, **2008**, 15, 67–74.

(14) Cuissinat, C.; Navard, P.; Heinze, T. *Cellulose*, **2008**, 15, 75–80.

(15) Le Moigne, N.; Montes, E.; Pannetier, C.; Höfte, H.; Navard, P. *Macromol. Symp.*, **2008**, 262, 1, 65–71.

(16) Basra, A. S. In Cotton Fibers: Developmental Biology, Quality Improvement and Textile Processing, ed. Basra A. S., Food Products Press/Haworth Press, New York, 1999.

(17) Ott, E.; Spurlin, H. M.; Grafflin, M. W. *Cellulose and cellulose derivatives (Part 1)*, Interscience Publisher, New York, 1954.

(18) Paris, A. *Influence des conditions de filage sur les propriétés physiques et mécaniques de fibres de polypropylène*, Thèse de doctorat, Ecole des Mines de Paris, Sophia-Antipolis, 1992.

(19) El-Shiekh, A.; Bogdan, J.F.; Gupta, R.K. *Text. Res. J.*, **1971**, 41, 281–297.

(20) Giroud, T.; Vincent, M. *Mec. Ind.*, **2004**, 5, 481–487.

(21) Abu-Rous, M.; Ingolic, E.; Schuster, K.C. *Cellulose*, **2006**, 4, 411–419.

(22) Jianchin, Z.; Meiwu, S.; Zhu, H.; Kan, L. *Chem. Fibers Int.*, **1999**, 49, 496–500.

(23) Roelofsen, P. A. *The Plant Cell-Wall, Encyclopedia of plant anatomy*, Gebrüder Borntraeger, Berlin, 1959, p 213.

(24) Brändström, J.; Bardage, S. L.; Daniel, G.; Nilsson, T. *IAWA J.*, **2003**, 24, 27–40.

(25) Sahlberg, U.; Salmén, L.; Oscarsson, A. *Wood Sci. Technol.*, **1997**, 31, 77–86.

(26) Paredez, A. R.; Somerville, C. R.; Ehrhardt, D. W. *Science*, **2006**, 312, 1491–1495.

Chapter VII

Kinetics of dissolution of cellulose and cellulose derivatives under shear.

Kinetics of dissolution of cellulose and cellulose derivatives under shear

Abstract The kinetics of dissolution of cellulose is a relevant parameter in cellulose processing. In this study, we used a rheo-optics tool to investigate the kinetics of dissolution of cellulose fibres and cellulose derivatives. The contra-rotating rheometer used allows a direct microscopic observation of the dissolution for a wide range of solvent types and temperature conditions. The main advantage as compared to a conventional microscopic observation is the possibility to control the convection around the studied cellulose particles while keeping it in the field of observation. This provides a better homogenisation of the cellulose / solvent system. The contra-rotating rheometer thus allows a better prediction of the real dissolution conditions of cellulose and cellulose derivatives.

Introduction

Dissolution of a solid material in a solvent is a process of utmost importance in many fields, like pharmacy (where it is one of the main objectives of galenics) or food. Dissolution is controlled by two different factors, thermodynamics and kinetics. If thermodynamics is usually easy to master and understand through the building of phase diagrams, kinetics is more complicated, being controlled by a set of several interconnected physical and chemical phenomena in which flow convection plays an important role. The kinetics of dissolution of a solid polymer pellet has been widely investigated in the pharmaceutical field. When a solid (under Tg), compact, non crystalline polymer piece is placed in contact with a fluid solvent, the solvent will swell the outer part of the polymer piece, bringing it above its glass transition. Further penetration of solvent is thus eased and the polymer goes then in a disentangled state that allows chains to move out of the polymer into the solvent. It is this last part that is usually very dependent on the solvent convection around the swelling and dissolving polymer. Convection acts first by removing polymer chains out of the vicinity of the dissolving polymer piece, and bringing new solvent close by. It has a second effect which is to avoid the formation of a viscous polymer cake around the dissolving polymer, which is usually blocking fresh solvent access to the polymer piece. All these effects are well known, since stirring is nearly always associated with dissolution.

Native cellulose is a solid polymer that should follow the above described rules when placed in contact with a solvent. It has been shown that it is not the case, due to both a complex structure[1] and the existence of a strong hydrogen bond array (chapter III). As for many polymers, dissolution is an important process parameter for cellulose. Cellulose and cellulose derivatives are used in the form of fibres, films or products which preparation and processing usually involve a stage of dissolution.

All the studies performed so far on the swelling and dissolution mechanisms were performed visually without convection, or at least without a controlled convection of the solvent or by rheological methods where there is convection, but without visualizing the dissolution process. For example, Kosan *et al.* [2] and Michels and Kosan [3] studied the rheological behaviour of the cellulose / solvent mixture and showed that it is possible to distinguish the suspension phase, when fibres are dispersed in the solvent from the dissolved phase, the latter being much more viscous. Other studies on cellulose dissolution used the measurement of the rate of decrystallization by X-ray scattering. [4, 5] All these methods do not allow observing the dissolution mechanisms while measuring the dissolution kinetics.

There is thus the need to observe the dissolution by optical means while controlling the solvent convection. This can be done by using rheo-optical tools, where the flowing cell is transparent to light. The focus of this study is to illustrate the interest of using rheo-optical tools to study cellulose dissolution. The kinetics of dissolution of cellulose and cellulose derivatives will be investigated with such a technique in order to separate the influence of the intrinsic dissolution parameters from the possible formation of cellulose gels or highly viscous layers around the dissolving cellulose and cellulose derivative parts. The contra-rotating rheo-optical technique will allow visualizing a cellulose or cellulose derivative object up the end of dissolution, while keeping it in a controlled simple shear.

Materials and methods

Cellulose samples and solvents. The investigations had been carried out using cotton hairs, *Gossypium Barbadence*, provided by INRA (France), a wood pulp, MoDo-pulp 488, provided by TITK (Germany) and two cellulose derivatives, xanthate (61% CS_2) provided by Spontex (France) and methylhydroxyethylcellulose (MHEC), provided by Dow Wolff cellulosics (Germany).

The dissolution of cotton hairs was studied in mixtures of *N*-methylmorpholine *N*-oxide (NMMO) with 20 % of water (w/w) at 95°C. MoDo-pulp 488 wood pulp fibres were pre-dissolved at a w/w concentration of 9 % / in NMMO-monohydrate (13.3% water w/w). The MHEC was dissolved in tap water at 20°C. The cellulose xanthate was dissolved in NaOH 8% - water at three temperatures: 0°C, 10°C and 20°C.

Protocol for static dissolution observations. To investigate the dissolution in static conditions, i.e. without convection, we observed the dissolution of cotton hairs in NMMO-20% water at 95°C and the dissolution of MHEC in tap water by optical microscopy with a Metallux 3 (Leitz) equipped with a Linkam TMS 91 hot stage. The experiments were performed by placing a small amount of material (< 0.3% w/w) in a large excess of solvent in a container made of two thin glass plates separated with double-sided tape. The solvent, contained in a pipette, was introduced by capillary forces between the two glass plates. The samples were investigated in transmission mode and the data were recorded with a high resolution 3-CCD camera (1360*1024 pixels) JVC KY-F75U.

Precipitation of cellulose during the dissolution. Several droplets of water were added between the two glass plates during the dissolution of cotton hairs. The additional water dilutes the solvent and precipitates the dissolved cellulose which can be easily observed as will be described in the results and discussion section.

Contra-rotating rheometer devices. The first contra-rotating rheometer used is placed on a Metallux 3 (Leitz) optical microscope. The device consists of two glass plates which run in opposite directions (Figure 1). The rotation of the two glass plates is ensured by two potentiometers which can be manually controlled. The light source goes through the two glass plates and the sample is observed by optical microscopy in transmission mode linked to a recording system, i.e. an analogical camera JVC TK-C1481EG which provides 25 frames per second and a DVD recorder Sony RDR-HX710. A monitor allows a direct visualization during the experiments. A frame code generator (Sony FCG-700) displays the number of frames which allows to measure precisely the dissolution time, i.e. dissolution time in second equals to the number of frames divided by 25.

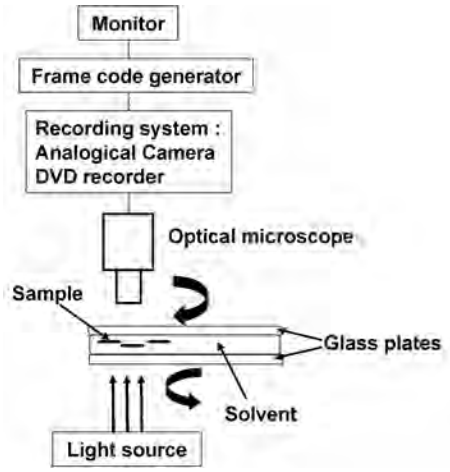

Figure 1. Contra-rotating rheometer device

The shearing $\dot{\gamma}$ applied to one particle is given by the following formula:

$$\dot{\gamma} = \frac{(Va + Vb) \times R}{H},$$

where Va and Vb are the rotation speeds of the two glass plates in rad/s, R is the radial position of the particle towards the rotation axis in mm, and H is the gap between the two glass plates in mm.

When the glass plates are running in opposite directions at similar speeds, it is possible to keep the studied particle in the field of observation. The glass plates can be heated or cooled by means of an external thermostating bath from 0°C to 50°C.

The experiments at higher temperature (95°C) were made with another contra-rotating rheometer, based on the same geometry but equipped with an oven able to heat the glass plates up to 200°C.

Protocol for dynamic dissolution observations. A little amount of sample (roughly 0.1-0.3% w/w as regard to the solvent in large excess) was placed between the two glass plates of the contra-rotating rheometer which was previously placed at the test temperature. The solvent is also heated to the test temperature. About 1.5 ml of solvent (or cellulose / NMMO solution in the case of wood pulp) was deposited between the two plates with a pipette. The gap was then adjusted at 700 µm so that the solvent forms a meniscus between the two plates. Consequently, the sample was put in contact with the solvent. That time was considered as the beginning of the dissolution experiment and the frame code generator was switched on. A

shearing was subsequently applied with the two running plates to ensure a good convection around the studied particles. The shearing varied from 0 to 10 s^{-1} for experiments with tap water and 10 to 25 s^{-1} for experiments with NaOH 8% - water and cellulose / NMMO-monohydrate solution.

Results and discussion

Static observations of the dissolution

The dissolution of cotton hairs in NMMO - 20% water occurred by ballooning as was reported by Cuissinat and Navard.[6] We know that during this stage, cellulose is dissolved inside the balloon, but nothing is known if cellulose chains are leaving the swollen fibre. One way to observe this is to send a regenerating medium like water during this dissolution and to see if regenerated cellulose can be seen. The precipitation of the dissolved cellulose during the dissolution by the addition of water shows the creation of tiny cellulose gel droplets of nearly spherical shape with diameter ranging from 1 to 10 µm (see insert in Figure 2). It was not possible to establish by which mechanism the phase separation occurred, either spinodal decomposition or nucleation and growth. The fact that neighbouring droplets are of the same size, aligned along strings and sometimes attached suggests that the mechanism is a spinodal decomposition.

The precipitation of dissolved cellulose allows observing its distribution around the dissolving cotton hair. As can be seen on Figure 2, the concentration of precipitated cellulose is very high in balloon regions (zones 1 and 2) and much smaller around the unswollen fibre parts (zones 3 and 4).

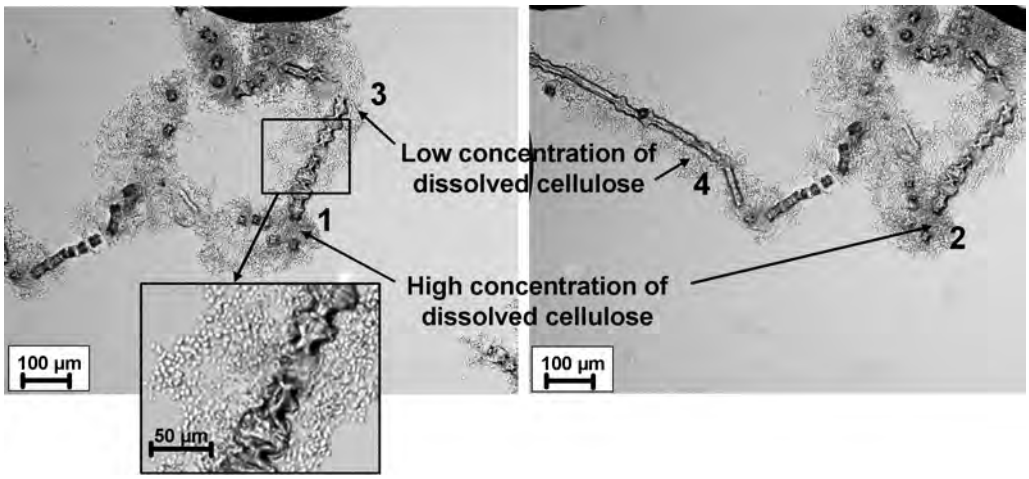

Figure 2. Precipitation of the dissolved cellulose during the dissolution of a cotton hair in NMMO- 20 % water.

These observations show that cellulose dissolving and leaving the cellulose fibre is staying close to the fibre in static conditions. It creates a zone with a very high cellulose concentration, forming a barrier. The diffusion of the solvent molecules is decreased as the dissolution is progressing, thus decreasing the kinetics of dissolution. This classical phenomenon is here well illustrated since the regenerated cellulose is easily visible.

The same phenomenon is seen when observing the dissolution of MHEC under static conditions. When tap water is introduced, some particles dissolve in few minutes, i.e. 3 to 5 minutes. However, some other particles dissolve slowly and are still visible after 10 minutes (Figure 3). As will be seen in the next section, the dissolution times are more homogeneous when putting the sample under convection.

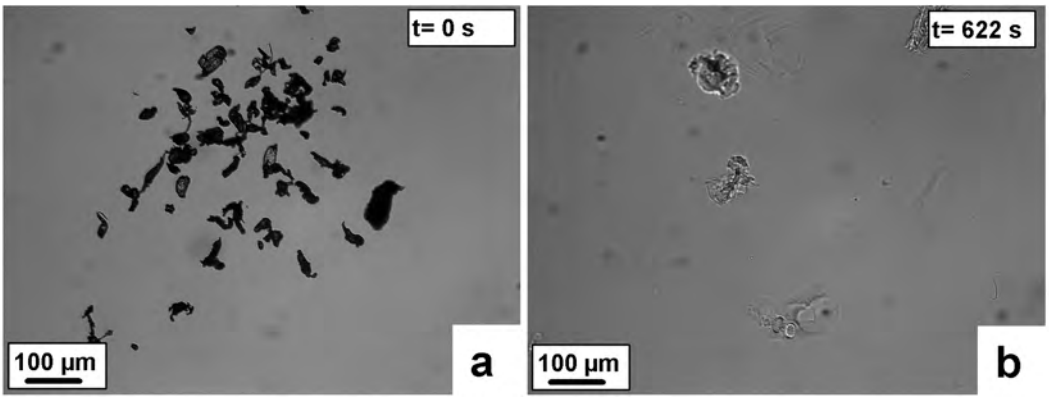

Figure 3. Dissolution of MHEC in static conditions observed by optical microscopy. (a) initial state; (b) several particles are still visible after 10 minutes.

Dynamic observations of the dissolution

The contra-rotating rheometer allows applying a controlled shear to the cellulose / solvent system while keeping the studied particles under the field of view of the microscope. The dispersion is thus improved and the particles do not stay agglomerated.

Dissolution of cellulose wood fibres: The dissolution of MoDo-pulp 488 was studied from a pre-doped solution of 9 % cellulose / NMMO monohydrate. As shown on Figure 4, two dissolution mechanisms were observed. Several fibres are dissolving quickly by fragmentation (Figure 4a), in about 1 or 2 minutes, but some are dissolving very slowly by ballooning (Figure 4b), in more than 15 minutes. These observations indicate that either the fibres are not all the same (many reasons can explain a fibre property variation, from the

wood itself to various treatment intensities) or that the NMMO concentration is varying in the solution.

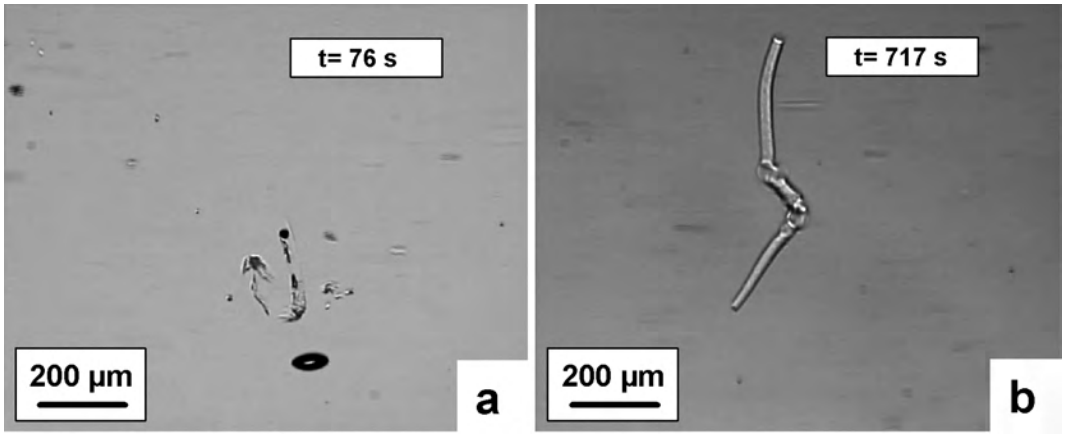

Figure 4. Dissolution of MoDo-pulp 488 in dynamic conditions observed with the contra-rotating rheometer. (a) fast dissolution by fragmentation, (b) slow dissolution by ballooning.

The use of a contra-rotating transparent rheometer shows that it is easy to well discriminate several dissolution behaviour avoiding making a concentrated layer around the dissolving particle, which could bring difficulties in interpreting kinetics results.

An additional observation is that fibres are aligned in the vorticity direction under shear, a feature associated with the flow of more or less rigid elongated object in a visco-elastic medium. It has to be noticed that fibres are not easy to keep in the field of observation due to their shape which involve a lot of flow disturbances under shear.

Dissolution of cellulose xanthate: The dissolution of cellulose xanthate was studied in NaOH 8% - water at 0°C, 10°C and 20°C. Cellulose xanthate forms a concentrated highly viscous phase around the dissolving part (Figure 5). Under shear, the viscous phase makes continuous filaments that are extracted from the particle. If the particle is well centred between the two plates, two filaments must be observed. However, the viscous phase was often causing the particle to stick on one plate. The convection was thus applied only in one direction involving the formation of only one filament.

The convection associated with shear is distributed the concentrated viscous phase into the solvent, increasing the homogeneisation of the mixture and increasing dissolution kinetics. Figure 5 shows clearly the solid particles dissolving into the highly viscous phase. The highest is the shear rate, the fastest the dissolution and the dispersion are. The dissolution time

was not influenced by the temperature and varied from 5 to 7 minutes depending of the initial particle size and the shearing.

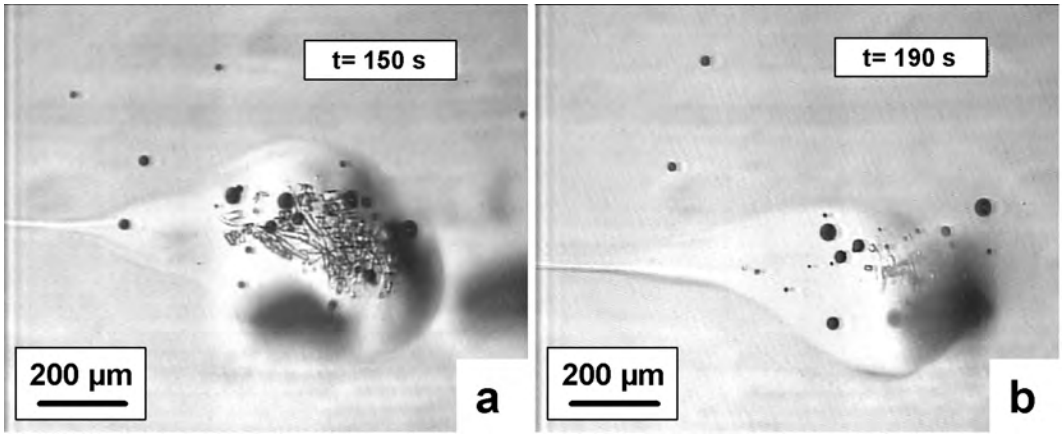

Figure 5. Dissolution of cellulose xanthate in dynamic conditions observed with the contra-rotating rheometer at two dissolution times.

Dissolution of MHEC: The dissolution of MHEC was studied in tap water. Most of the MHEC particules are swelling and dissolving under shear in about 3 to 5 minutes depending of their initial size (Figure 6), compared to more than 10mn in static conditions for some particles. Convection is bringing a better homogenisation of the MHEC/solvent system leading to a narrow distribution of dissolution times.

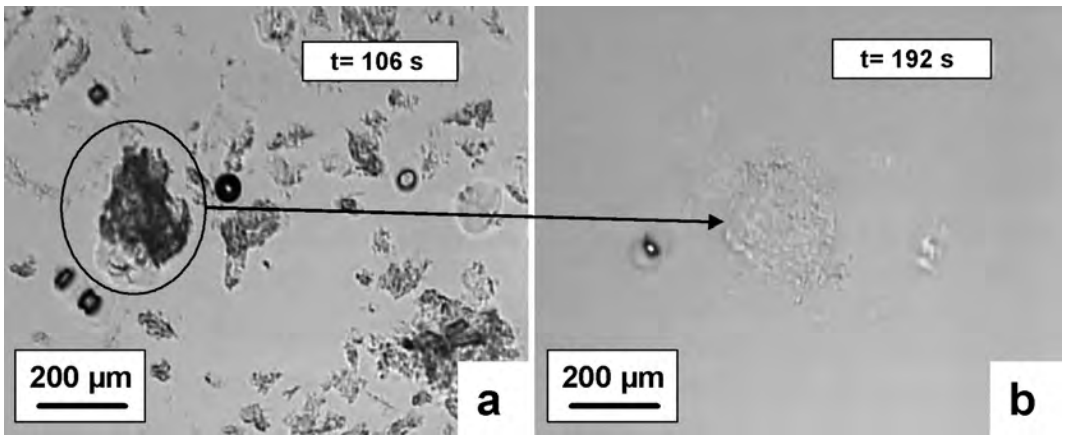

Figure 6. Dissolution of MHEC observed with the contra-rotating rheometer at two dissolution times from. (a) Beginning of the dissolution (106 s), no convection is applied, particles are partially swollen and stay agglomerated; (b) Intermediate time (192 s), convection is applied, the particle is highly swollen and almost dissolved.

Conclusions

The investigation of the kinetics of dissolution by using a contra-rotating rheometer allows coupling microscopic observations with flow. Such a system can be used with a wide variety of solvents and cellulose samples, in a large temperature range. Cellulose or cellulose derivatives particles can be observed in conditions where the formation of a highly concentrated polymer zone around the dissolving particle is avoided, a situation closer to real mixing processes. It can show peculiar mechanisms like the one occurring for cellulose xanthate, or better stress differences between cellulose fibre properties, as show for the wood pulp. All the experiments were performed with a large excess of solvent. Higher concentrations of cellulose should increase the difference between the kinetics of dissolution in static and dynamic conditions.

References

(1) Le Moigne, N.; Montes, E.; Pannetier, C.; Höfte, H.; Navard, P. *Macromol. Symp.*, **2008**, 262, 65–71.

(2) Kosan, B.; Michels, C.; Meister, F. *Cellulose*, **2008**, 15, 59–66.

(3) Michels, C.H.; Kosan, B. *Lenziger Berichte*, **2005**, 84, 62–70.

(4) Marson, G.A.; El Seoud, O.A. *J. Polym. Sci., A*, **2000**, 37, 3738–3744.

(5) Wang, Y.; Deng, Y. *Biotechnol. Bioeng.*, **2008** published online Oct, 3.

(6) Cuissinat, C.; Navard, P. *Macromol. Symp.*, **2006**, 244, 1–18.

Conclusions

Conclusions

The focus of this work was to study the swelling and dissolution of cellulose fibres by varying the quality of the solvent (NMMO with various amount of water, NaOH 8% - water), the dissolution conditions, as the tension, and the fibres sources (cotton, wood pulps, regenerated fibres and cellulose derivatives). The swelling and dissolution mechanisms were investigated by high resolution microscopic observations. A selective separation of insoluble and soluble fractions was performed by a centrifugation method. Molar mass distribution, crystallinity, sugar composition, allomorphy and amount of material of each fraction were analysed. From all these investigations, we were able to better describe the swelling and dissolution mechanisms of cellulose fibres and to identify the main parameters involved in the dissolution.

The dissolution capacity of cellulose fibres must be considered at the different levels of the fibre structure, (i) the molecular level, (ii) the aggregated level and (iii) the macrostructural level, as described in chapter I.

From the macrostructural to the aggregated level.

We showed that there is a gradient in dissolution capacity of the successively deposited cell wall layers within the cotton fibres. The older was the cellulose deposition, the most difficult it was to dissolve (Chapter II), meaning that the large amount of non-cellulosic materials present in the outside walls of the fibre may impede the dissolution of cellulose. We further demonstrated that the removal of the external walls by enzymatic peeling treatment (Chapter V) and the macrostructural destructuration of the layer structure by steam explosion, acidic hydrolysis or enzymatic treatments (Chapter IV and V) can improve the dissolution capacity of cellulose fibres as well as the usually thermodynamic reasons evocated. The rotation and the contraction movements of the fibre and the convection of the solvent around the fibre must also be favoured during the dissolution process (Chapter VI and VII). However, several fractions still remain insoluble and their dissolution capacity must be investigated at closer level of the structure. One interesting result was the presence of higher amount of hemicelluloses in these insoluble fractions as compared to the soluble one meaning that cellulose, in these fractions, may be more embedded in the hemicelluloses matrix (Chapter IV).

From the aggregated level to the molecular level.

In addition to the classical thermodynamic parameters (entropic and enthalpic effects) and to the effect of crystallinity, we showed that a significant fraction of cellulose chains, similar in length, can be either solubilized or not (Chapter IV). This result was related to the chemical environment of the chains in the insoluble fractions which contains larger amount of hemicelluloses. On the other hand, an interesting phenomenon was obtained by varying the fibre tension conditions during the dissolution. We showed that there is a restricted dissolution capacity of cellulose fibres under an axial elongational stress (Chapter III). In fact, besides the accessibility of the solvent to the cellulose chains, we found that the dissolution of cellulose fibres is mainly controlled by the possibility for the chains to perform conformational movements that are requiring long range chain mobility and thus chain ends to be free. When putting the strong H-bonds network of cellulose fibres under tension, the access of solvent to chain is not the only condition for dissolution, since conformational mobility is impeded.

Main parameters governing cellulose dissolution

The above results thus suggest that structural and molecular characteristics of cellulose fibres as well as process parameters must be better controlled to improve the dissolution:

(i) Process parameters are linked to the solvent convection and the possibility of movements of cellulose fibres in the solvent bath.

(ii) Structural parameters are linked with the removal of the external walls, the destructuration of the layer structure and the selective removal of the hemicelluloses.

(iii) Molecular parameters are dealing with the thermodynamic, as the chain length, the crystallinity, but also the enhancement of the conformational mobility of the chains.

The activation treatments prior to dissolution must thus concentrate on a more selective fibre destructuration and on the removal of the hemicelluloses which might be a strong factor of non solubility. In this sense, enzymatic treatments are good candidates since their action is local and can be very specific as compared to the classical steam explosion, grinding or derivatization methods which involve a strong degradation of the cellulose chains. However, one of the critical point is the possibility for the enzymes to penetrate in the complex fibre

structure in order to remove selective components. Activation must also concentrate in the enhancement of the chains mobility by breaking the hydrogen bond array and preventing its reformation and by better dismantling the hemicelluloses network. These actions might be either controlled before or during the dissolution process.

Despite advance knowledge in the chemical modification and dissolution of cellulose fibres, the cellulose swelling and dissolution still remains a complex scientific field and a breakthrough should be made by the understanding of the biosynthesis processes. In fact, it would allow to better control and/or modify the natural cellulose sources for their integration in varied industrial applications.

Articles and Communications

Articles

Le Moigne, N.; Montes, E.; Pannetier, C.; Höfte, H.; Navard, P. Gradient in dissolution capacity of successively deposited cell wall layers in cotton fibres. *Macromolecular Symposia*, **2008**, 262, 1, 65–71.

Oral communications

National ACS meeting. Spinu, M.; Le Moigne, N.; Navard, P. *Dissolution swelling transition in cellulose fibres : the influence of water*, New Orleans, April, 6-10, 2008.

3rd workshop on cellulose, regenerated cellulose and cellulose derivatives. Le Moigne, N.; Montes, E.; Pannetier, C.; Höfte, H.; Navard, P. S*welling and dissolution mechanisms of natural cellulose fibres*, prize for the best paper presented, Karlstad, Sueden, November, 13-14, 2007.

8th French-Romanian congress on polymers. Le Moigne, N.; Montes, E.; Pannetier, C.; Höfte, H.; Navard, P. *Swelling and dissolution mechanisms of natural cellulose fibres*, Grenoble, France, August, 26-30, 2007.

Zellcheming-Expo. Navard, P.; Le Moigne, N. *Swelling and Dissolution of Cellulose Fibres under Tension*, Wiesbaden, Germany, June, 25-28, 2007.

2nd EPNOE Workshop of PhD Students. Le Moigne, N.; Navard, P. S*welling and dissolution mechanisms of natural cellulose fibres*, Jena, Germany, April, 2-4, 2007.

National ACS meeting. Navard, P.; Cuissinat, C.; Le Moigne, N. *The dissolution of native cellulose fibers and its derivatives*, San Francisco, USA, September, 10-14, 2006.

Poster communication

European Polymer Congress (EPF). Navard, P.; Le Moigne, N. *Swelling and dissolution of cotton fibres. Influence of the tension of the fibre*, Portorož, Slovenia, July, 2-6, 2007.

Remerciements

Ce travail a été réalisé au Centre de Mise en Forme des Matériaux, laboratoire de l'Ecole des Mines de Paris, au sein du groupe « Physico-chimie des Polymères » et sponsorisé par Borregaard (Norvège), Dow Wolff Cellulosics GmbH (Allemagne), Lenzing AG (Autriche) et Spontex (France).

Je tiens en premier lieu à remercier mon directeur de thèse, Patrick Navard, pour m'avoir fait partager son goût pour la recherche et m'avoir guidé dans ma démarche scientifique tout au long de ces trois ans. J'adresse aussi mes remerciements à nos partenaires industriels, Kristina Jardeby et Torgeir Hjerde (Borregaard), Jürgen Engelhardt (Dow Wolff Cellulosics GmbH), Christoph Schrempf et Haio Harms (Lenzing AG), Michel Pierre (Spontex) pour leurs conseils et leurs expertises aussi bien techniques que scientifiques. Je remercie Herman Höfte, Martine Gonneau et Emilie Montes de l'Institut National de Recherche Agronomique (INRA) et Catherine Pannetier, Bruno Bachelier et Gérard Gawrysiak du Centre de coopération Internationale en Recherche Agronomique pour le Développement (CIRAD) avec qui les discussions et les collaborations furent riches et fructueuses.

Je remercie les membres du Jury Pedro Fardim, Herman Höfte et Jürgen Puls, d'avoir accepté d'évaluer mes travaux et d'y avoir apporté leurs commentaires et leurs suggestions.

Mes remerciements sont aussi adressés aux personnes du groupe « Physico-Chimie des Polymères »: Tatiana Budtova, Edith Peuvrel-Disdier et Roland Hainault pour leur soutien et leurs conseils ainsi qu'à toutes les personnes du laboratoire pour leur sympathie et leur disponibilité. Je pense aussi à tous mes collègues thésards et en particulier à mes collègues de bureau avec par ordre d'apparition dans mes bureaux successifs : Melinda Desse, Emmanuelle Relot et Céline Roux puis Bruno Dratz, Rachid El Khaoulani, Marie-Cécile Robin, Florian Deme et Jean-François Zaragoci. Je n'oublie évidemment pas mes collègues « cellulose », Monica Spinu et Romain Sescousse.

Mes remerciements vont enfin à ma famille qui a su me soutenir quand la cellulose ne voulait pas me livrer ses secrets, et à France Inter ainsi qu'à toutes les musiques qui m'ont accompagnés sur la (trop longue !!!) route du travail au cours de ces trois années.

Abstract

The focus of this work was to study the swelling and dissolution of cellulose fibres by varying the quality of the solvent (*N*-methylmorpholine-*N*-oxide with various amount of water, NaOH 8% - water), the dissolution conditions, as the tension, and the fibres sources (cotton, wood pulps, regenerated fibres and cellulose derivatives). The swelling and dissolution mechanisms were investigated by high resolution microscopic observations. A selective separation of insoluble and soluble fractions was performed by a centrifugation method. Molar mass distribution, crystallinity, sugar composition, allomorphy and amount of material of each fraction were analysed. From all these investigations, we were able to better describe the swelling and dissolution mechanisms of cellulose fibres and to identify the main parameters involved in the dissolution. Our results show that structural and molecular characteristics of cellulose fibres as well as process parameters must be better controlled to improve the dissolution, (i) process parameters are linked to the solvent convection and the possibility of movements of cellulose fibres in the solvent bath. (ii) Structural parameters are linked with the removal of the external walls, the destructuration of the layer structure and the selective removal of the hemicelluloses. (iii) Molecular parameters are dealing with thermodynamic, as the chain length, the crystallinity, but also the enhancement of the conformational mobility of the chains.

Keywords: cellulose, swelling, dissolution, solvent, structure, walls, enzymes, cotton, wood, regenerated fibres, *N*-methylmorpholine-*N*-oxide, NaOH.

Résumé

Le but de ces travaux était d'étudier les mécanismes de gonflement et de dissolution des fibres de cellulose en faisant varier la qualité du solvant (*N*-methylmorpholine-*N*-oxide avec différentes quantités d'eau et solutions aqueuses de NaOH à 8%), les conditions de dissolution, comme la tension, et l'origine des fibres (coton, bois, fibres régénérées ou dérivées). Les mécanismes de gonflement et de dissolution ont été étudiés par des observations microscopiques à haute résolution. Une séparation sélective des fractions solubles et insolubles a été réalisée par centrifugation. La distribution de masse molaire, la cristallinité, la composition en sucre, l'allomorphie et la quantité de chaque fraction ont été analysées. A partir de ces résultats, nous avons pu mieux décrire les mécanismes de gonflement et de dissolution des fibres de cellulose et ainsi identifier les principaux paramètres gouvernant la dissolution. Nos résultats montrent que les caractéristiques structurales et moléculaires des fibres de cellulose ainsi que les paramètres de procédés doivent être mieux contrôlés afin d'améliorer la dissolution. (i) Les paramètres de procédés concernent la convection du solvant et la possibilité de mouvements des fibres dans le solvant, (ii) les paramètres structuraux concernent la suppression des parois externes, la déstructuration des parois internes et la suppression sélectives des hémicelluloses, (iii) les paramètres moléculaires concernent la thermodynamique, comme la longueur des chaînes, la cristallinité mais aussi l'amélioration de la mobilité conformationelle des chaînes.

Mots clés: cellulose, gonflement, dissolution, solvant, structure, parois, enzymes, coton, bois, fibres régénérées, *N*-methylmorpholine-*N*-oxide, NaOH.